DOCTORAL DISSERTATION

Mechanisms of Resistance to $TPCS_{2a}$-Photodynamic Therapy: Implication for Photochemical Internalization

CATHRINE ELISABETH OLSEN

2017

Department of Radiation Biology
Institute for Cancer Research - The Norwegian Radium Hospital
Oslo University Hospital

Submitted to the Faculty of Mathematics and Natural Sciences at the University of Oslo for the degree of Dr. Philos.

Series of dissertations submitted to the
Faculty of Mathematics and Natural Sciences, University of Oslo
No. 1904

ISSN 1501-7710

Cover: Hanne Baadsgaard Utigard.
Print production: Reprosentralen, University of Oslo.

Acknowledgements

The work included in this thesis was undertaken from 2012 to 2017 in Prof. Kristian Berg's research group at the Institute for Cancer Research, and financially supported by the South-Eastern Norway Regional Health Authority, the Norwegian Radium Hospital Research Foundation (RadForsk) and the Norwegian Research Council (SFI-CAST).

I would first like to express my gratitude to Dr. Anette Weyergang, who encouraged me to embark on this journey that has become a big part of my life. Thank you for pushing me. I would also like to give a huge thank to Dr. Pål Kristian Selbo for your great enthusiasm and motivation throughout all this time. Thank you for all the discussions and for bringing fun and humour to the group. Special thanks to Prof. Kristian Berg for giving me the opportunity to be a part of this exciting research environment, and for always keeping your door open for discussions.

My time in the research group would not have been the same without the collaboration with Monica Bostad, Dr. Simen Sellevold, Dr. Kaja Lund and Dr. Theodossis Theodossiou. You are all important reasons for my motivation and joy of this work, and you have all contributed to my understanding of the research field. I wish you all the best of luck with your current and future research.

I would also like to thank all other co-authors and contributors for their experiments and discussions, especially Dr. Sebastian Patzke regarding microscopy, Idun Dale Rein, Dr. Kirsti Landsverk and Dr. Trond Stokke at the Core Facility for Flow Cytometry for your generous guidance and discussions.

I also wish to express my thankfulness to Ane Sofie Viset Fremstedal and Kari-Anne Frikstad for your encouragement and support, and to the master students for trusting me to co-supervise.

In 2015 the journey went to Prof. Michael Rosenblum's research lab at MD Anderson Cancer Center in Houston, Texas. I am grateful for your hospitality and for giving me the opportunity to work in your exciting field of recombinant technology. A special thank to Dr. Lawrence H. Cheung for your will to share your knowledge. I also thank Ass. Prof. Khalid Mohamedali and Dr. Ana Alvarez de Cienfuegos Suarez for your kindness and discussions in the lab. My greatest gratitude goes to Robert, Sarah, Daniel, Zachary and Bailey for your friendship and for making my stay in Houston so joyful.

Also, a special thank to Marius Strømbo Eng, Marte Jonsson and Lise Ellefsen Sandquist who have been my traveller companions on this research journey. I am happy I shared my time with you, and want to thank you for all academic and non-academic discussions.

Last, but not least, I would like to thank my husband, parents and sister. You always encouraged me and expressed your pride of me. This thesis is for you.

Contents

List of Publications and Manuscripts

(I) Olsen C.E., Weyergang A., Edwards W.T., Berg K., Brech A., Weisheit S., Høgset A. and Selbo P.K. Development of resistance to photodynamic therapy (PDT) in human breast cancer cells is photosensitizer-dependent: Possible mechanisms and approaches for overcoming PDT-resistance. Submitted manuscript (2017)

(II) Olsen C.E., Selbo P.K., Berg K. and Weyergang A. Circumvention of resistance to photodynamic therapy in doxorubicin-resistant sarcoma by photochemical internalization of gelonin. Free Radical Biology and Medicine 65 (2013) 1300-1309

(III) Lund K., Olsen C.E., Wong J.J.W., Olsen P.A., Høgset A., Krauss S. and Selbo P.K. 5-FU resistant EMT-like pancreatic cancer cells are hypersensitive to photochemical internalization of the novel endoglin-targeting immunotoxin CD105-saporin. Manuscript (2017)

(IV) Olsen C.E., Sellevold S., Theodossiou T., Patzke S. and Berg K. Impact of genotypic and phenotypic differences in sarcoma models on the outcome of photochemical internalization (PCI) of bleomycin. Submitted manuscript (2017)

(V) Bostad M., Olsen C.E., Peng Q., Berg K., Høgset A. and Selbo P.K. Light-controlled endosomal escape of the novel CD133-targeting immunotoxin AC133-saporin by photochemical internalization - A minimally invasive cancer stem cell-targeting strategy. Journal of Controlled Release 206 (2016) 37-48

(VI) Olsen C.E., Cheung L., Weyergang A., Berg K., Vallera D., Rosenblum M. and Selbo P.K. Design, characterization and evaluation of a novel CD133-targeting recombinant immunotoxin scFvCD133/rGelonin for use in combination with the endosomal escape method photochemical internalization. Manuscript (2017)

Aims of Study

Photochemical internalization (PCI) is a novel drug delivery method currently evaluated for clinical use in cancer therapy. It is based on the highly potent reactive oxygen species (ROS)-induction from $TPCS_{2a}$-PDT. PCI, hence, mediates the release of drugs sequestered in endocytic vesicles including endosomes and lysosomes. The method has so far been showing promising results circumventing cancer drug resistance both *in vitro* and *in vivo*, and in patients. Little is, however, known about $TPCS_{2a}$'s own susceptibility to resistance, and how it applies in PDT and PCI.

The work presented in this thesis therefore had the following objectives:

- Study $TPCS_{2a}$-PDT sensitivity
  - Study intrinsic and acquired resistance mechanisms
  - Impact of repeated chemotherapy
- Investigate PCI sensitivity
  - PCI in $TPCS_{2a}$-PDT-resistant cells
  - The role of ROS scavengers
  - Utilization of resistance-induced markers
- Target PCI towards CD133 expression on therapy-resistant cancer stem cells
  - A proof-of-principle study of a CD133 targeted immunotoxin with a chemical linker
  - Produce and characterize a recombinant CD133-targeted immunotoxin, and investigate its potential with PCI

Introduction

Chapter 1

Cancer and Adaption to New Conditions

Normal cells follow regulations for growth and survival in order to maintain normal tissue homoeostasis. They exhibit several checkpoints and control systems that ensure a normal cell survival and death balance. Cancers, however, arise from violations of these regulations (Alberts et al., 2004), which may allow them to continue their uncontrolled division, metastasize to other tissue and resisting treatment. In a world wide perspective, most common are cancers of the lung (1.69 million deaths world wide), liver (788 000), colorectal (774 000), stomach (754 000) and breast (571 000) (*WHO, Cancer Fact sheet, February 2017*). This makes cancer the second leading cause of death, after heart diseases, worldwide (2015).

Hanahan and Weinberg proposed six hallmarks that are associated with the transformation of normal cells to cancer cells; *The Hallmarks of Cancer* (Hanahan et al., 2000). They include the overriding of growth and proliferation signals, invasion and metastasis to other tissue, unlimited replication, developing blood vessels and resisting cell death. In addition, a deregulated metabolism and the ability to evade the immune system have subsequently been included as emerging hallmarks (Hanahan et al., 2011). These are important characteristics for the cancer cells to adapt to different conditions and become resistant to treatment. Acquisition of the hallmarks highly depend on alterations in the genome of the cells. Genomic instability can, hence, be considered superior to the hallmarks of cancer (Fig. 1.1).

Surgery, chemo- and radiotherapy are currently the three most important options for treatment of cancer (https://www.cancer.gov/about-cancer/treatment/types Date entered: 26. April 2017). Together with immunotherapy, which with recent advances (Snook et al., 2013) is emerging as a pillar in cancer therapy for melanoma (Sanlorenzo et al., 2014) and lung cancer (Anagnostou et al., 2015), they constitute the cornerstones in cancer therapy. Chemo- and radiotherapy are usually given at cycles, giving healthy cells time to recover from adverse effects. The aim is to minimize adverse effects while yet induce sufficient damage to the cancer. A consequence of the widely applied repetitive treatments, is the development of drug resistance, which comprises one of the biggest challenges in cancer therapy. Additionally, about one half of cancers are intrinsically resistant to treatment (Pinedo, 2007). Efforts are therefore put into developing treatment strategies that more precisely identify and target cancer cells. Strategies have included hormonal or targeted therapy, acting on *e.g.* intracellular signal pathways or gene expression modulators for blocking or turning off growth signals or angiogenesis, cell death pathways or the delivery of toxins to the cancer cells. Drug groups used in targeted therapy include *e.g.* monoclonal antibodies (mAbs), small molecular inhibitors (like tyrosine kinase inhibitor (TKI)s) (https://www.cancer.gov/about-cancer/treatm

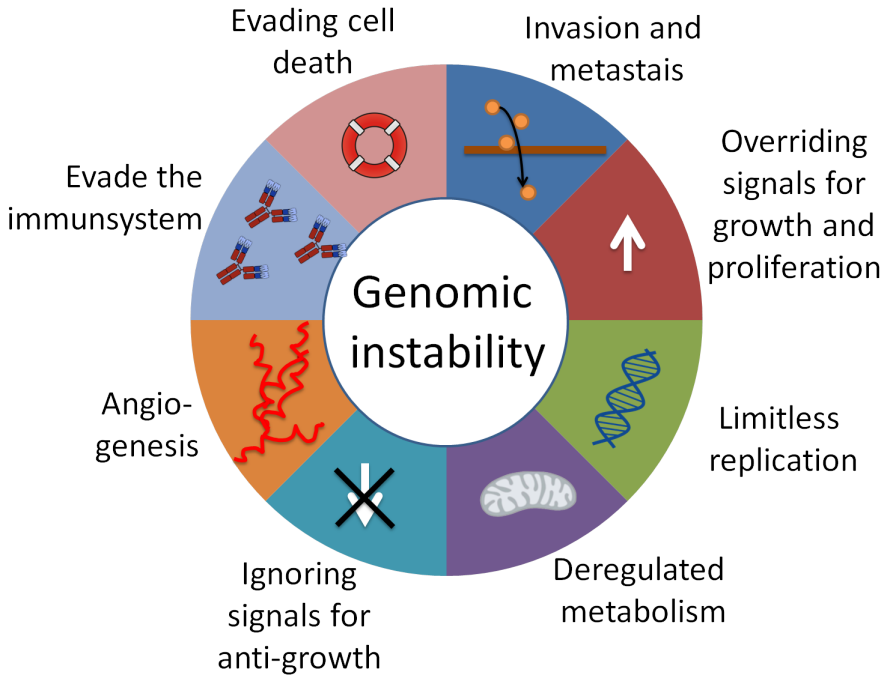

FIGURE 1.1: **The Hallmarks of Cancer**

Properties associated with transformation of normal cells to cancer cells based on the reviews from (Hanahan et al., 2000) and (Hanahan et al., 2011).

ent/types/targeted-therapies/), and antibody-drug-conjugate (ADC)s and immunotoxin (IT)s.

Despite these advances in cancer therapy, several challenges remain. For example, targeted therapy requires identification of molecular targets which are mainly expressed or mainly active in cancer cells so that healthy tissue is not affected. Moreover, a more controlled immune response is endeavoured in immunotherapy, as runaway responses still may cause autoimmune damage to normal tissue (https://www.cancer.gov/research/areas/treatment/#challenges Date entered: 28. April 2017). There is, therefore, a need for clinically relevant strategies to which cancer cells cannot adapt.

Chapter 2

Photochemical Internalization for Treatment of Cancer

2.1 Photochemical Internalization (PCI)

Berg and co-workers proposed in 1999 an idea of using photochemical treatment for tissue-specific transfer of drugs into drug-resistant cells (Berg et al., 1999). The method, reported to as PCI, is based on photosensitizers that are activated specifically in the membrane of endo-/lysosomes. The photochemical treatment leads to peroxidation of lipids and other biomolecules damaging these membranes so that the vesicle content may leak out to the cell cytosol (Fig. 2.1) (Berg et al., 2011). This opened the possibility to enhance the effect of several types of drugs that were otherwise sequestered and degraded in lysosomes (Berg et al., 2005; Selbo et al., 2006; Weyergang et al., 2006; Berg et al., 2010; Berstad et al., 2012; Weyergang et al., 2015). The principle depends on the endocytic trafficking pathways of drugs and the action of photochemical treatment, the latter also being used separately in PDT for treatment of non-malignant and malignant conditions.

2.1.1 Intracellular Trafficking Dynamics

Endocytosis is an active process in all nucleated cells, and is based on membrane invagination for the transport and degradation of molecules into the cell (Grant et al., 2009). The process involves the formation of vesicles that fuse with specific compartments (early endosomes) within the cell, forming multivesicular bodies (late endosomes). The late endosomes may route endocytosed material to the lysosomes which then break it down to new building material by means of hydrolytic enzymes.

Endocytosis can be subdivided into several modes of internalization. These include clathrin-mediated and clathrin-independent endocytosis, caveolae, macropinocytosis and phagocytosis (Maxfield et al., 2004). Clathrin- and caveolin-mediated endocytosis involve the receptor-binding of a ligand in clathrin- and caveolin-rich pits of the cell membrane. The pits are associated with receptor-mediated endocytosis of different growth factors and antibodies, and form vesicles with a size of <200 nm (clathrin-rich vesicles) and 60-80 nm (caveolin-rich vesicles) in diameter (McMahon et al., 2011; Parton et al., 2013). Macropinocytosis involves formation of larger vesicles (0.2-5 μm in diameter (Lim et al., 2011)) and does not require receptor binding. The process is, hence, non-specific. Phagocytosis resembles in many ways the process of macropinocytosis, but internalize particles larger than 0.5 μm in diameter (Freeman et al., 2014).

Early endosomes receive vesicles for the recycle of receptors to the surface, and sorting of endocytosed material to the late endosomes. The endosomes are slightly acidic

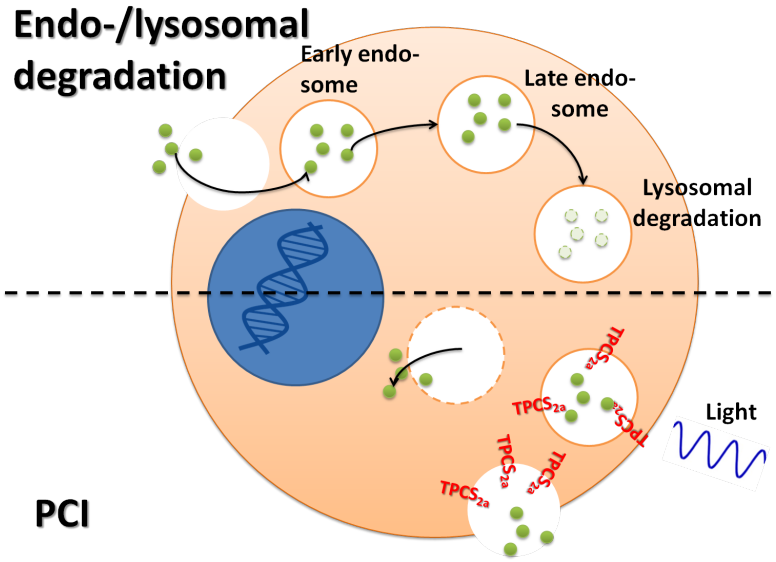

FIGURE 2.1: **Mechanism of Photochemical Internalization**

Endo-/lysosomal degradation: A drug is taken up by endocytosis and is transported to a lysosome for degradation. PCI: A drug is taken up by endocytosis and accumulates in endo-/lysosomal vesicles together with the amphiphilic photosensitizer. Activation of the photosensitizer by light induces generation of reactive oxygen species disrupting the endo-/lysosomal membranes. This leads to the release of the sequestered drug so that it can reach its intracellular target.

(pH 5-6) (Mellman et al., 1986), and are believed to mediate the final delivery of material to the lysosomes (Grant et al., 2009). The main function of the lysosomes is to break down material into simple compounds that can be used as new building-material, in addition to cell signaling, energy metabolism and plasma membrane repair (Settembre et al., 2013). The important degradation enzymes function optimally in the acidic milieu (pH 4.6-5.0) (Mellman et al., 1986).

2.1.2 Photodynamic Therapy (PDT)

For the release of drugs that are entrapped in endo-/lysosomes, the PCI technology utilizes photochemical toxicity based on the principle of PDT. PDT involves three individual non-toxic components; a photosensitizer, oxygen and light. A photosensitizer is a chemical compound that can be promoted to an excited state upon absorption of light, and transfer its energy to oxygen or another substrate, forming ROS, of which singlet oxygen is the most important (Agostinis et al., 2011).

PDT is a selective treatment for cancer, not only due to the confined light exposure of the target area, but also due to the preferential accumulation of the photosensitizer in tumor tissue (Bossu et al., 1997; Berg et al., 2011). Although this mechanism is not fully understood, some properties including leaky vasculature, poor lymphatic drainage (Bugelski et al., 1981) and the photosensitizers' affinity for LDL and subsequent delivery to LDL receptors in tumor tissue (Kessel, 1986) may contribute to this selection.

Photochemical treatment is recognized as non-invasive and minimally toxic because of the localized effect initiated by light, and can be dated back to 1400 BC, where the plant *Psoralea corylifolia* was used for treatment of the skin-condition vitiligo (Moan et al., 2003). The first attempts to apply PDT on tumors was performed in the early 1900 by von Tappeiner *et al.* who recognized that oxygen was required for the photodynamic effect (von Tappeiner, 1904). The investigation of photochemical treatment in clinical oncology trials was provided by Dougherty in 1978 (Dougherty et al., 1978), and today PDT is approved worldwide as a treatment of several conditions, including cancers of the skin (non-melanoma), bladder, brain, esophagus, lung, bile duct and ovary (Agostinis et al., 2011). PDT is additionally under clinical evaluation for the treatment of cancers of liver, colon, pancreas, prostate, sarcoma, cutaneous T-cell lymphoma and breast.

Photosensitizers for PCI

The first photosensitizers investigated for PCI included $TPPS_{2a}$, $TPPS_4$ and $AlPcS_{2a}$ (Berg et al., 1991; Berg et al., 1989). These are amphiphilic ($TPPS_{2a}$ and $AlPcS_{2a}$) or anionic ($TPPS_4$) non-patented structures with adjacent SO_3 groups (pKa = 3.9 (Lilletvedt et al., 2011)) kept deprotonated on the intra-luminal side of the endo-/lysosomes. This let them retain their position in the endo/lysosomal membrane while being activated by visible light. The blue light absorption and very low red light absorption properties of $TPPS_{2a}$ and $TPPS_4$ restrict, however, their activation only to thin-layer tissues, while $AlPcS_{2a}$ in general is limited by batch to batch production variations holding back their clinical potentials (Berg et al., 1989).

$TPCS_{2a}$ was specifically developed for deep tissue light-activation by modifying the porphyrin-structure of $TPPS_{2a}$ (Berg et al., 2011). The reduction of one of the double

bonds in the aromatic ring system yielded the chlorin-structure exhibiting a slightly different conformation not being aromatic throughout the ring-system. This resulted in increased light absorption in the red region of the visible spectrum allowing photosensitizer activation down to the sub-cutaneous tissue level (Agostinis et al., 2011).

Photosensitizer Reactions and Reactive Oxygen Species

The most active photosensitizers for clinical use include the porphyrins and their tetrapyrrolic analogues, which are activated by red light (600-800 nm) (Rapozzi et al., 2015). Although longer wavelengths can penetrate deeper, wavelengths exceeding 800 nm provide low excited state energy and will, hence, not be able to excite oxygen to its singlet state.

Photosensitizer activation can happen by two different mechanisms; type I or type II reactions as shown in Fig. 2.2, which can lead to changes of membrane fluidity, permeability and protein functionality (Broekgaarden et al., 2015). A photosensitizer's susceptibility to a type I or II reaction is dependent on the type of photosensitizer, the available substrate and oxygen (Castano et al., 2004), while the degree of damage mainly depends on photosensitizer localization, dose and oxygen availability (Dougherty et al., 1998). In a type II reaction, the excited triplet state photosensitizer transfers energy directly to oxygen, forming singlet oxygen ($^1O_2$). The formation of singlet oxygen is considered the most important reaction in PDT and PCI as it may react very efficiently with unsaturated carbon double bonds and may form organic hydroperoxides. Amino acids, fatty acids and cholesterol are, hence, readily affected. The lifetime of $^1O_2$ has been estimated to be <0.04 μs, resulting in an action-radius of <0.02 (Moan et al., 1991). Other reports indicate, however, that the lifetime and action-radius may be longer (Skovsen et al., 2005; Baier et al., 2005).

Type I reactions can produce different kinds of ROS by transferring a proton or an electron to bio-substrates forming a radical anion or radical cation. In the presence of oxygen, the oxidized form of the photosensitizer or the substrate add to oxygen. In this process, superoxide radical anion ($O_2^{\cdot -}$) can be generated. $O_2^{\cdot -}$ is not very active in biological systems (Castano et al., 2004), but may further react directly with other substrates or act as the precursor for other ROS, *e.g.* hydrogen peroxide (H_2O_2 by the process of "dismutation" by superoxide dismutase (SOD)) or hydroxyl radical ($OH^{\cdot}$ by a Fenton reaction) (Castano et al., 2004). $OH^{\cdot}$ can initiate a chain reaction with the subsequent damage to fatty acids and other lipids forming *e.g.* lipid peroxides (Castano et al., 2004). Lipid peroxides exhibit longer half lives than $^1O_2$ (Girotti, 1998), and may, hence, contribute in mediating secondary damage (Broekgaarden et al., 2015).

Photochemically Induced Toxicity

Due to the short half-life of singlet oxygen, the primary localization of photosensitizers determines the initial subcellular damage upon their activation (Moan et al., 1991). It is the physicochemical properties of photosensitizers that mainly affect their localization in cells; hydrophobic photosensitizers may diffuse across plasma membranes and relocate to other intracellular membranes, while photosensitizers that are positively charged and hydrophobic can localize in the mitochondria (Rapozzi et al., 2015). Photosensitizers relevant for PCI, that are less hydrophobic with up to two negative charges (amphiphilic) that are not protonated, are taken up by endocytosis. In addition to the toxicity mediated by the different drugs being released by PCI, activated photosensitizers may in general mediate their toxicity through direct damage to different vital

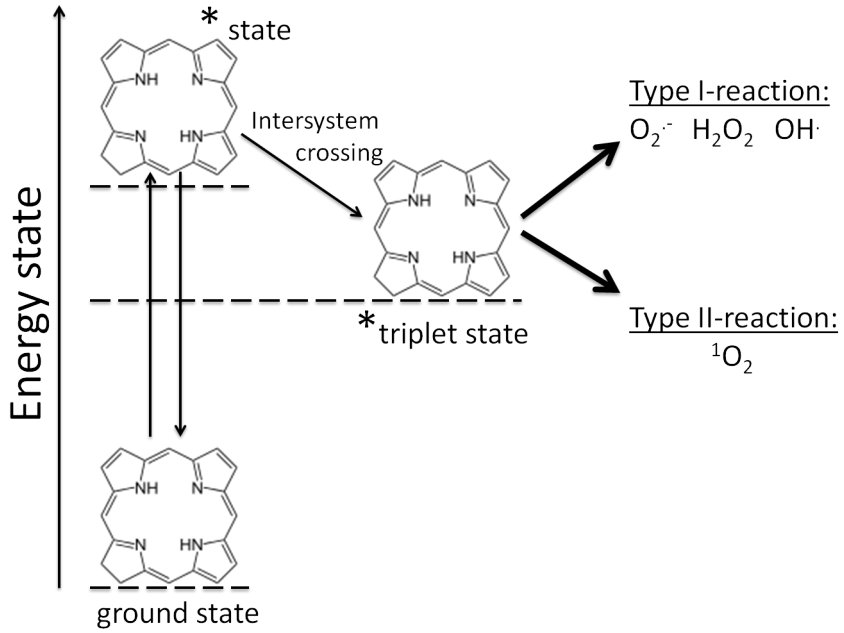

FIGURE 2.2: **Jablonski Diagram**

Light is absorbed by the photosensitizer and moves electrons from a low energy-state to a high energy-state. Energy can either be emitted by heat or fluorescence, or by inter-system crossing give the excited triplet state. From here the photosensitizer may either emit phosphorescence or react through a type I or II reaction subsequently damaging biomolecules.

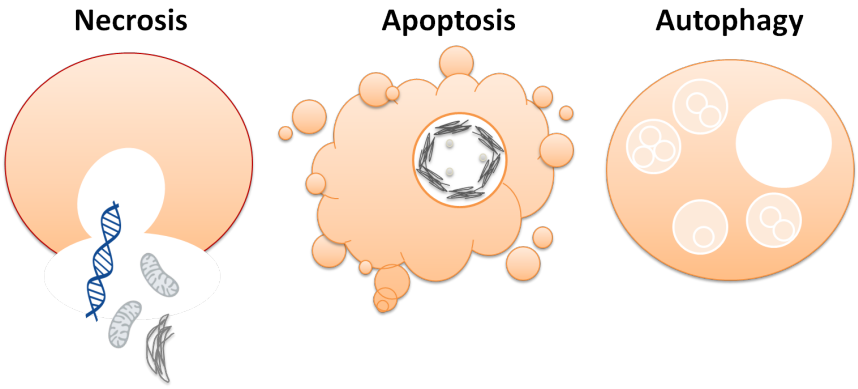

FIGURE 2.3: **Cell Death Types**

Phenotypic characterizations of a cell undergoing apoptosis, necrosis or autophagy-associated cell death, characterized by plasma membrane blebbing and chromatin condensation, nucleic membrane dilatation and cell membrane perforation, and vacuolization, respectively, as described in (Agostinis et al., 2011).

components of the cancer cells, initiating different cell death pathways such as necrosis, apoptosis and autophagy (Moor, 2000; Piette et al., 2003; Kessel et al., 2010; Broekgaarden et al., 2015; Agostinis et al., 2011; Bacellar et al., 2015). In addition to direct tumor cell damage, PDT can also mediate its effect by targeting the tumor associated vasculature (Chen et al., 2006). Due to increased photosensitizer uptake in endothelial cells, PCI has been suggested as a vascular damaging technology for cancer eradication (Vikdal et al., 2013).

Apoptosis, Necrosis and Autophagy Apoptosis may be triggered by both extracellular and intracellular stress signals. Photosensitizers localizing to mitochondria are, hence, examples of initiators of the apoptotic cell death pathway upon light exposure (Hamblin et al., 2008). Although PDT using photosensitizers that localize to endosomes and lysosomes may initiate apoptosis by cathepsin and cytochrome c release (Berg et al., 1994; Reiners et al., 2002), high PDT doses tend, in general, to shift the balance towards a necrotic cell death (Kessel et al., 2007; Hamblin et al., 2013). Likewise, excessive ROS production is associated with necrosis signaling (Agostinis et al., 2011).

Autophagy is another pathway which can be activated by ROS-based cancer therapy, including PDT (Dewaele et al., 2010; Agostinis et al., 2011). It is a regulated process that disassembles and recycles dysfunctional components within a cell, generally activated by nutrient deprivation but also by cellular damage. The process is divided into different mechanisms which all have in common to transfer damaged components into lysosomes. Photosensitizers damaging the lysosomes may therefore compromise the completion of autophagy, subsequently potentiating photocytotoxicity in apoptosis-dependent cells (Agostinis et al., 2011). Autophagy may, depending on the circumstances, act both as a pro-survival and pro-death mechanism (Dolmans et al., 2003; Kessel et al., 2007; Agostinis et al., 2011; Mroz et al., 2011; Jeon, 2012), but has in general been associated with enhanced survival upon PDT yielding low levels of photodamage.

Growth and Proliferation Signaling While efficient cell death is observed when the PDT dose is high, low PDT doses may also mediate growth inhibition, *e.g.* by arresting cells in the G2/M phase of the cell cycle, which Piette *et al.* linked to damage to microtubules mediated by hypericin-PDT (Piette et al., 2003). Microtubuli-damage has also been reported for endo/-lysosomal photosensitizers (Berg et al., 1997), and suggested as targets for photochemical therapy of cancer.

Growth factors (or *mitogens*) also play a role for cell proliferation. One example is epidermal growth factor (EGF) which, upon binding to epidermal growth factor receptor (EGFR), leads to Ras and Raf activation which subsequently activate the MAPK/ERK signaling pathway. The MAPK/ERK pathway (also known as the Ras-Raf-MEK-ERK pathway) regulates proliferation, differentiation, motility and survival by the signal from a surface receptor to the DNA of the cell. The mitogen-activated protein kinase (MAPK) family constitute the p38MAPK, the c-Jun N-terminal protein kinase (JNK) and extracellular signal-regulated kinase (ERK), all of which have been shown to be readily activated by ROS (Dolado et al., 2007). In (Klotz et al., 1998) it was shown that PDT using 5-aminolevulinic acid (ALA) activated JNK and p38MAPK. These pathways, in addition to ERK, were found to protect cells from cell death after hypericin- and Photofrin-PDT by (Assefa et al., 1999; Tong et al., 2002). The ERK-pathway was, however, not activated in (Klotz et al., 1998), while both ERK and p38MAPK were activated (and JNK-activation found cell line dependent) after $TPPS_{2a}$ in (Weyergang et al., 2008b). In the work of Weyergang *et al.* p38MAPK was identified as a death signal, while JNK was identified as a signal for survival (Weyergang et al., 2008b).

PDT has also been shown to be involved in the expression and regulation of EGFR. *E.g.* Pc4-PDT has been reported both to inhibit the protein expression, but also to activate EGFR (Ahmad et al., 2001), while $TPPS_{2a}$-PDT has been reported to attenuate its activation (Weyergang et al., 2008a).

2.1.3 Drugs and Toxins for PCI

In 1999 Berg *et al.* demonstrated that molecules that do not readily penetrate the plasma membrane, but rather are entrapped in endocytic vesicles (endosomes and lysosomes), are ideal drugs for the use in PCI-combination (Berg et al., 1999). Ideally, the molecules should only exert toxicity when translocated to the cell cytosol and not possess any mechanism for cytosolic translocation without PCI. One family of such molecules include the type I-ribosome inactivating protein (RIP)s produced by plants.

Ribosome Inactivating Proteins

RIPs originating from plants exert N-glycosidase activity against the 60S ribosomal subunit in eukaryotic cells, by removing a specific adenin, A4324, of the 28S rRNA (Endo et al., 1988; Barbieri et al., 1993), thereby halting irreversibly the protein synthesis of the cell. Toxicity induced by RIPs is, however, reported to not only involve inhibition of protein synthesis, but also the capability to induce DNA fragmentation and apoptosis (Polito et al., 2013).

The RIPs are divided into two types depending on the presence of a translocation domain. The type I-RIPs include gelonin, saporin, PAP, momordin and trichosanthin (Walsh et al., 2013). They contain a catalytic A chain, but are by far less toxic than the type II-RIPs that additionally contain both a binding chain (B chain) and a translocation domain (II domain), which provide them with substantial higher toxicity and make

them unsuitable for PCI. PCI of type I-RIP toxins have shown promising *in vitro* and *in vivo* results because of their entrapment in endo-/lysosomes (Selbo et al., 2000; Selbo et al., 2001; Selbo et al., 2006; Norum et al., 2009).

Many receptors are involved in receptor mediated endocytosis triggered by binding of a ligand. The receptors can then be transported within the cell and fuse with Golgi for recycling, or to a lysosome for degradation (Pastan et al., 1983). Overexpression of some receptors involved in control of growth and proliferation (*e.g.* EGFR, VEGFR and cancer stem cell (CSC) receptors) is correlated with cancer aggressiveness and invasiveness (Hirsch et al., 2003; Sok et al., 2006; Rimawi et al., 2010; Li et al., 2014). Surface receptors have, hence, brought attention as targets for several treatment strategies involving mAbs, ADCs and ITs which can trigger or inhibit receptor mediated signaling or deliver a drug/toxin payload to the cancer cells. Since PCI can deliver drugs and toxins lacking a translocation domain, the technology has been potentiated by introducing targeting moieties to the type I-RIPs. This has efficiently and specifically increased the delivery of EGF- (Weyergang et al., 2006; Berstad et al., 2015), VEGF- (Weyergang et al., 2014), HER2- (Berstad et al., 2012), CD133- (Stratford et al., 2013; Bostad et al., 2013; Bostad et al., 2015), CD44- (Bostad et al., 2014) and EpCAM-targeting (Lund et al., 2014; Selbo et al., 2015) gelonin- and saporin-based ITs in several *in vitro* and *in vivo* models.

The ADCs and ITs have, traditionally, been based on chemically conjugated structures of antibodies or ligands to drugs and toxins, resulting in large and immunogenic products. These have been associated with a risk of payload dissociation before reaching the targets (Alewine et al., 2015). Today, recombinant technology allows the production of smaller ITs based on *e.g.* scFv antibody fragments and the enzymatically active domains of the toxins, eliminating many of the challenges associated with the chemically conjugated products. For example, they provide higher specificities, better stabilities and smaller sizes, hence rendering them less immunogenic and more tissue permeable (Shan et al., 2013). Denileukin diftitox is currently the only recombinant IT approved in the clinic. This drug is not suited for PCI due to its capability of cell translocation. It targets IL-2R for treatment of cutaneous T-cell lymphoma, but has been associated with development of off-targets effects (Pai et al., 2003; Rappa et al., 2015).

Chemotherapy

Drugs that are weak bases may also entrap in late endosomes and lysosomes because of protonation in the acidic milieu. One example is the anthracyclin doxorubicin which works by stopping the process of replication by stabilizing the topoisomerase II complex preventing the DNA double helix from being resealed. Doxorubicin could therefore with great success be delivered to the doxorubicin-resistant MCF7/ADR cells by use of the PCI technique (Lou et al., 2006). Bleomycin is another chemotherapeutic. It is a water soluble glycopeptidic antibiotic which cause single-and double-strand DNA breaks, resembling the damage by ionizing radiation. The sensitivity to bleomycin is, however, highly variable due to the limited penetration through the plasma membrane, but was demonstrated to induce synergistic inhibition of tumor growth by the PCI technology (Berg et al., 2005).

To this date, one clinical trial has been completed (NCT00993512) showing tolerable and promising effects of PCI of bleomycin in a Phase I clinical study (Sultan et al., 2016). Recently, PCI was also investigated for the delivery of gemcitabine in locally advanced cholangiocarcinomas (NCT01900158) where tolerability also was concluded. The photosensitizer was recently granted an orphan-drug-designation. Because of its potential

to also activate the immune system through delivery of antigens, PCI is currently also investigated for use as a vaccine-therapy for cancer indications (Håkerud et al., 2015; Otterhaug et al., 2016).

Chapter 3

Treatment Challenges in Chemotherapy and PDT

3.1 General Cancer Therapy Resistance

General resistance mechanisms may be complex involving drug efflux and inactivation, drug-target alteration and cell death inhibition (Gottesman, 2002; Gottesman et al., 2006; Housman et al., 2014) (Fig. 3.1). The resistance can be divided into two main categories; intrinsic and acquired resistance, where intrinsic resistance indicates pre-existing factors mediating resistance before receiving any treatment, and acquired resistance develop during the course of treatment through mutations or adaptive responses (Holohan et al., 2013).

3.1.1 Drug Efflux Pumps

One of the most commonly described resistance mechanisms to cancer treatment, is the efflux of drugs by certain transporters (Schinkel et al., 2003). One important family of transporters is the ATP-binding cassette (ABC) transporter family, which has been shown to be associated with multidrug resistance (MDR) (Fletcher et al., 2010). The family comprise seven subfamilies designated A to G on the basis of their sequence, driven by ATP. They are endogenously responsible for the transport of lipids and metabolic products across the membranes, but also the efflux of xenobiotics including drugs (Fletcher et al., 2010).

Plasma membrane glycoprotein (Pgp) (ABCB1) was the first ABC transporter detected in cancers exerting resistance to chemically unrelated chemostatics (Juliano et al., 1976). It is encoded by the *MDR1*α gene, and has been shown to be expressed in many different cancer types, in addition to normal tissue (Cordon-Cardo et al., 1990). Chemostatics effluxed by Pgp are generally weakly amphiphatic and lipid-soluble (Sharom, 2011), suggesting that photosensitizers also may be potential substrates. Kessel *et al.* showed that doxorubicin-induced overexpression of Pgp impaired the cellular accumulation of a cationic photosensitizer (copper benzochlorin iminium salt) (Kessel et al., 1994), but that affinity to Pgp in general was dependent on photosensitizer structure (Kessel et al., 1992). Although some photosensitizers have been shown to exhibit some affinity to Pgp, only negligible effects on accumulation levels have been detected. Also, cell lines induced by repeated PDT have not been shown to increase the expression of Pgp, and the forced induction of similar photosensitizer accumulation levels in the case of chemo-induced Pgp overexpressing cells, has not always translated into similar toxicities (Casas et al., 2011).

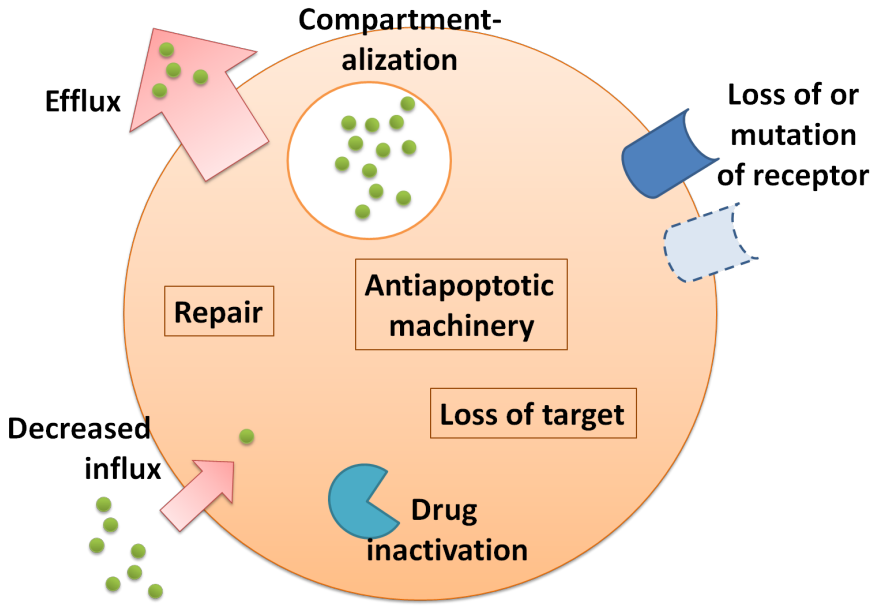

FIGURE 3.1: **General Resistance Mechanisms**

Summary of superior anti-cancer drug resistance mechanisms based on (Gottesman et al., 2006).

Another group of the ABC transporter family is the half-transporters including the MDR associated breast cancer resistance protein (BCRP), also referred to as ABCG2. ABCG2 exhibits high affinity for hydrophilic organic anions, particularly sulfates in addition to glutathione (GSH) (Mao et al., 2015). Pheophorbide A (PhA) and PpIX, among some other photosensitizers, have been identified as substrates of ABCG2 (Jonker et al., 2002; Robey et al., 2005; Morgan et al., 2010; Selbo et al., 2012). PCI-relevant photosensitizers have, however, not been shown to be affected by this transporter (Selbo et al., 2012), (Paper I) and (Paper II).

3.1.2 Inactivation of Drugs

Compartmentalization

Intracellular compartmentalization and degradation of molecules represents an important resistance mechanism with specific implication for drugs that do not cross the cell membrane, and is the main target in PCI. Advanced cancers are highly dependent on the function of lysosomes (Piao et al., 2015) as the lysosomal degradative enzymes (*e.g.* cathepsins and cysteine proteases) may regulate angiogenesis and invasion (Gocheva et al., 2006). Cancer progression and metastasis are therefore associated with changes in lysosomal compartments, including lysosomal size, cellular distribution, and lysosomal enzyme activity (Piao et al., 2015).

Little is known about the implication of alteration in the lysosomal biogenesis for the PCI technology, but studies indicate that it is of some importance. Caruso *et al.* and Nilsson *et al.* reported that lysosomes of different cell lines, but also individual lysosomes within a cell, may differ in their susceptibility to damage and subsequent survival by the photosensitizer NPe6 (Caruso et al., 2004) and oxidative stress (Nilsson

et al., 1997), respectively. Cathepsins were implicated as regulators of this lysosomal fragility (Caruso et al., 2004).

ROS Scavengers

The ROS scavenging system is well known to antagonize ROS induced by PDT and other ROS-generating therapies. It includes the SODs, the glutathione peroxidase (GPx)s, catalase and lipoamide dehydrogenase (Casas et al., 2011).

The SODs compromise the enzymes that catalyze the dismutation of superoxide into oxygen and hydrogen peroxide, utilizing Cu^{2+}, Zn^{2+}, Mn^{2+} and Fe^{2+} as cofactors. They are divided in three subtypes, SOD1, 2 and 3, which primarily locate in the cytoplasm, mitochondria and extracellularly, respectively. Several studies have shown the protective role from SOD on the primary effect from PDT, demonstrated by decreased anti-tumor effect and reduced tissue swelling upon SOD inhibition (Hamblin et al., 2008; Agostinis et al., 2011).

Catalase is the main H_2O_2 detoxifying enzyme, as its scavenging activity is one of the highest known (Casas et al., 2006). Its role in PDT is, however, not well known due to that the majority of studies have investigated the role of exogenous catalase, and not the enzyme produced by cancer cells (Casas et al., 2006).

The GSH system, regarded as a secondary ROS scavenging mechanism, includes GSH, glutathione reductase (GR), glutathione S-transferase (MRP) (GST), and GPx, summerized in Fig. 3.2. GSH is synthesized by GSH synthetase catalyzing the condensation of γ-glutamylcysteine and glycine. Eight isoforms of GPx have in total been identified in humans; GPx1-8. Among them, GPx1 in the cytoplasm is the most abundant and mainly localizes in the cytoplasm, while *e.g.* GPx4 is found in the cellular membrane. All the GPxs have in common that they reduce hydrogen peroxide into water by the redox reaction of GSH (Equation 3.1). GSSG can subsequently be recycled by GR back to GSH (Equation 3.2). Expression of GPx has in general been associated with redox reactions with lipid hydroperoxides, protecting cancer cells from PDT (Hamblin et al., 2008). Likewise, GSH depletion by GSH synthetase-inhibition or genetic modification potentiates the anti-tumor activity of PDT, while the increase of GSH is associated with a decrease in such toxicity (Hamblin et al., 2008; Agostinis et al., 2011).

$$2GSH + H_2O_2 \rightarrow GSSG + 2H_2O \tag{3.1}$$

$$GSSG + NADPH + H^+ \rightarrow 2GSH + NADP^+ \tag{3.2}$$

GSH is not only oxidized in the redox reaction by GPx, but can also be conjugated directly to xenobiotics by GST (Casas et al., 2006). This subsequently forms GS-X products which can be expelled by a GS-X efflux pump, also called multispecific canalicular organic anion transporter (MRP) (MOAT).

3.2 Cancer Stem Cells

3.2.1 Definition of the Cancer Stem Cells and the Cancer Stem Cell Hypothesis

The cancer cells within a tumor have traditionally been described as a homogeneous cell population, and tumor progression has been explained by the stochastic evolution

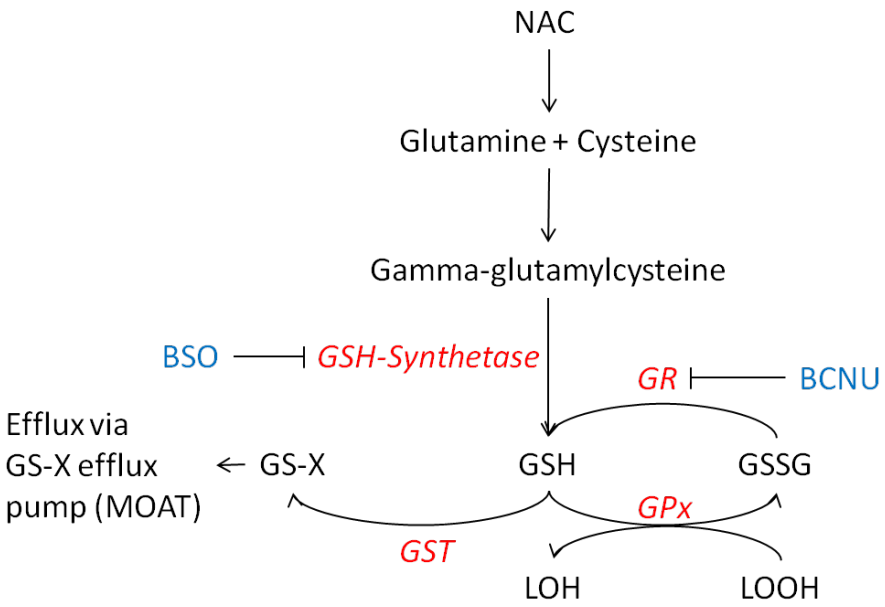

FIGURE 3.2: **The GSH system**

The synthesis of glutathione (GSH) and its involvement in production of GS-X products by glutathione S-transferase (GST) or in the redox reactions of lipids by glutathione peroxidase (GPx) and glutathione reductase (GR). The synthesis or reformation of GSH can be inhibited by the GSH-synthetase inhibitor BSO or by the glutathione reductase (GR) inhibitor BCNU, respectively.

model where all cells within a tumor have tumor-initiating potential. Many advanced tumors are, however, very heterogeneous, exhibiting sub-populations with distinct differentiation, proliferation, vascularity and invasiveness (Hanahan et al., 2011). More recently, such aggressive cancers were attributed to the presence of a subclass of cells, termed cancer stem cells (CSC)s. CSCs are defined by their ability to self-renew, differentiate and to initiate new tumors, and, hence, be partly responsible for the relapses in the clinic. The CSC theory has gained wide acceptance over the last years.

3.2.2 Cancer Stem Cells in Different Cancers

CSCs were first reported in acute myeolid leukemia, as CD34+/CD38- cells (Bonnet et al., 1997). Later they were identified in solid tumors including breast (Al-Hajj et al., 2003), brain (Singh et al., 2003) and colon (Ricci-Vitiani et al., 2007). With time, several tissue-specific markers for CSCs have been identified including *e.g.* EpCAM+, CD133+, CD166+, CD44+, CD24+ (colorectal), EpCAM+, CD44+, CD24- (breast), CD133+ (brain), and EpCAM+, CD44+, CD24+ (pancreatic), in addition to drug efflux pumps like ABCG2 (Dragu et al., 2015). These markers are also present on normal cells. Therefore, also sphere forming capacity in serum-free medium or soft agar is used for *in vitro* identification of CSCs (Dragu et al., 2015). However, only *in vivo* assays can reveal the tumorigenic potential.

3.2.3 Targeting of Cancer Stem Cells

CSCs may show a slow rate of division, and may even be present in a quiescent state (Schulenburg et al., 2006). They exhibit overexpression of drug-efflux pumps and are in general therapy resistant (Colak et al., 2014). Traditional cancer therapy, like chemo- and radiotherapy, hence, result in treatment failure and tumor relapse (Fig. 3.3). Therefore, there has been a focus on strategies targeting the specific surface markers and to inhibit cell signal pathways which are characteristic for the CSCs. CD133, CD44, CD24, EpCAM, CD34 and CD47 are among the markers that have received most attention, in addition to targeting of the drug-efflux pumps. Important signal cascades include the Notch (Hassan et al., 2013), Hedgehog (Huang et al., 2012), Wnt/β-catenin (Cai et al., 2012), PI3K/Akt (Li et al., 2011) and NF-κB (Zhou et al., 2008) pathways, shown to be important factors in CSCs.

Similarities between normal stem- and progenitor cells and CSCs render, however, CSC targeted therapy potentially damaging to healthy tissue. The localization of CSCs in low oxygenated and low vascularized areas, also contribute to preventing efficient delivery of therapy.

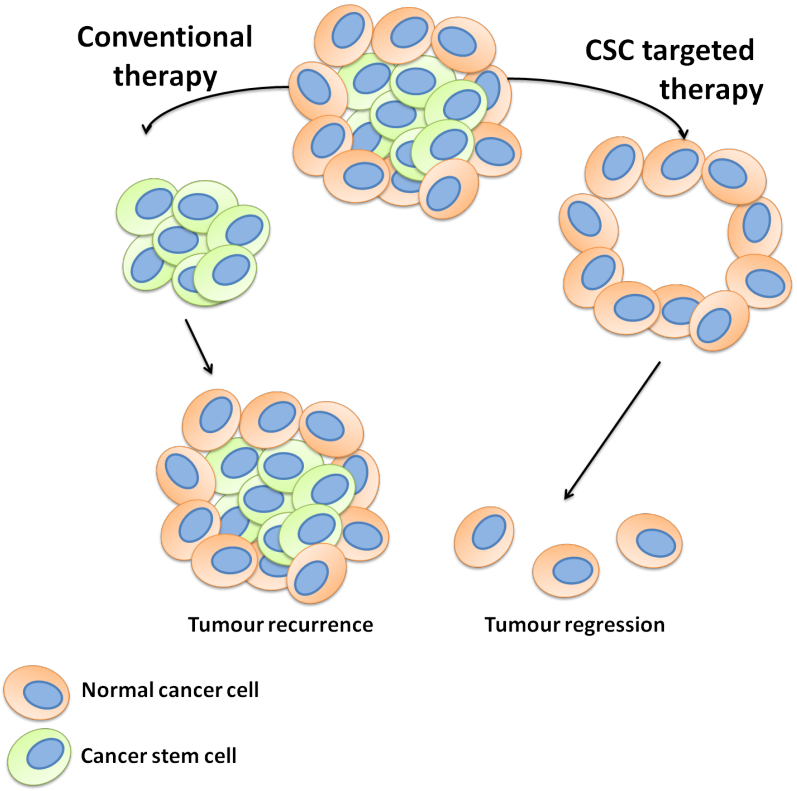

FIGURE 3.3: **Conventional and Cancer Stem Cell Targeted Therapy**

Cancer stem cells are believed to constitute a significant proportion of a tumor. Conventional therapy may leave the CSCs behind leading to tumor regrowth. CSC targeted therapy may eliminate the whole tumor.

Chapter 4

Experimental Conditions

4.1 Cell Lines

The human breast cancer cell lines MA11, MDA-MB-231 and MCF-7 were studied to investigate acquired PhA- and $TPCS_{2a}$-PDT-resistance (Paper I). The MA11 cell line has previously been shown to overexpress ABCG2 and to efflux the photosensitizer PhA but not the PCI-photosensitizer (Selbo et al., 2012). MDA-MB-231, which is triple negative and hence often used as a model for chemotherapy, and MCF-7, which is estrogen- and progesterone receptor positive and often used as a model for hormone therapy, were used as additional cell lines.

To study if doxorubicin-resistance induces cross-resistance to $TPCS_{2a}$-PDT and PCI of recombinant gelonin (rGelonin) (Paper II), the MES-SA and MES-SA/Dx5 uterine soft tissue sarcoma cell lines were used, of which the latter is resistant to doxorubicin. They have previously been studied for cross-resistance to PDT using the *in vitro* relevant PCI-photosensitizer $TPPS_{2a}$ (Selbo et al., 2006). The MES-SA/Dx5 cells were originally developed and described by Harker et al. in 1985 (Harker et al., 1985), and confirmed in Paper II and (Selbo et al., 2006) to retain the doxorubicin resistance.

Pancreatic cancer is a highly aggressive condition with one of the poorest prognosis of all cancers (Ansari et al., 2016). It is mainly treated by surgery with adjuvant 5-fluorouracil (5-FU) - a pyrimidine analog that inhibits thymidylate synthase, and/or gemcitabine (Hartley et al., 2015). The Panc03.27 cell line was used as a model to study the effect of $TPCS_{2a}$-PDT and PCI after induction of 5-FU-resistance (Paper III). Three subclones of Panc03.27 resistant to 5-FU and two untreated control clones were chosen and named B1L, B1Q and B1V, and Nt and Nw, respectively. The 5-FU resistant cells were kept resistant by supplementing the cultivation media with 1 μg/ml 5-FU until 48 hours prior to experiments. All the resistant clones showed an overexpression of CD105, that we exploited for CD105-saporin targeting by PCI.

The uterine and vulvar soft tissue sarcoma cell lines MES-SA and SK-LMS-1 were used to study the effects of $TPCS_{2a}$-PDT and PCI of bleomycin in pheno- and genotypically different cell lines (Paper IV). MES-SA exhibits an epithelial phenotype very similar to carcinomas, and the *P53*-mutated SK-LMS-1 exhibits the typical mesenchymal phenotype.

Aggressive, therapy resistant subpopulations of cells in a tumor has been associated with the presence of CSCs. CD133 is an important CSC marker, and is found glycosylated in the colorectal adenocarcinoma WiDr, breast cancer MDA-MB-231 and the melanoma cell line FEMX-1, hence being a target for the immunotoxin AC133-saporin (Paper V). The CD133 negative MCF-7 cell line was used as a negative control, although other work describes this cell line differently dependent on which CD133 antibody is used for detection (Blancas-Mosqueda, 2012). This may be related to several epitopes

of CD133 recognized both on the extracellular and intracellular part of CD133 (Bidlingmaier et al., 2008).

To study photochemical delivery of the CD133-targeting recombinant IT scFvCD133/-rGelonin (clone 7), the CD133 positive colorectal adenocarcinoma HT29 and WiDr cell lines were used, in addition to the CD133 (clone 7) negative / low-expression murine fibrosarcoma NIH/3T3, human glioblastoma U87, breast cancer MDA-MB-231 and MCF-7 cell lines. Spontaneous conversion of CD133 expression between CD133 positive and negative cells may be a challenge, as reported by Feng et al. (Feng et al., 2012). Our FACS sorted CD133-high and -low HT29 cells were confirmed to preserve the CD133 status when investigated for CD133 specificity by PCI of scFvCD133/rGelonin.

4.2 PDT and PCI

The PCI-photosensitizer $TPCS_{2a}$ (Fimaporfin) (PCI Biotech) absorbs light at several wavelengths, but most efficiently in the blue and red spectrum (430 nm and 652 nm, respectively) (Berg et al., 2011). Even though blue light cannot propagate deeper than 1-2 mm in tissue (Agostinis et al., 2011), it exerts high energy and is excellent for *in vitro* experiments. Illumination of cells was performed using the LumiSource lamp from PCI Biotech with an Emax at 435 nm. The irradiance varied less than 10% among the illumination area, and had an effect range [9.6-13.5] mW/cm^2 (See each respective manuscript). To ensure stable irradiance, the lamp was turned on 15 min prior to treatment.

All experiments with photosensitizers were, other than when illuminated, performed in subdued light. Drugs and toxins were administered either together with the photosensitizer, or added to the experiment during the *chase* period. The wash and *chase* period was introduced to remove the photosensitizer away from the plama membrane so that $TPCS_{2a}$ was preferentially located in the membrane of the endo-/lysosomes.

4.3 Selection of PDT-Resistant Cells

PDT resistant cells were selected by four different strategies in this thesis. In Paper I human breast cancer cells were treated repeatedly with $TPCS_{2a}$-PDT. A similar $TPCS_{2a}$ concentration and incubation time was used for three different cell lines (0.4-0.5 μg/ml at 3 min light exposure). At each treatment, all surviving cells were kept and retreated in total 3 times during 3 weeks. The doses used, resulted in a >90% cell kill in two of three cell lines (MA11 and MDA-MB-231), while one cell line was less affected (MCF-7). In Paper II a doxorubicin resistant sub-cell line selected from the MES-SA cell line was used. The MES-SA/Dx5 cells were originally developed by Harker *et al.* after increasing doxorubicin doses in the MES-SA cell line to a final concentration of $5x10^{-7}$ M, using similar growth criteria as for the MES-SA cells. The advantage of selecting resistant populations as a strategy is that the selected cells may resemble the "real" conditions within a tumor.

The 5-FU resistant cells of Paper III were, in contrast, selected by clonal selection. A disadvantage of this strategy is that such clones in general are not representative for the entire resistant population. Therefore, three individual clones were selected through limited dilution after creation of stable, proliferating 5-FU resistant cells (Lund et al., 2015).

The cell lines of Paper IV were chosen based on their diverse morphology despite both being soft tissue sarcomas. They exhibited an intrinsic slightly different sensitivity to PDT and PCI. In Paper V and Paper VI cancer cell lines were categorized based on their expression of AC133 or CD133. The CD133 marker was used for CD133+ and CD133- cell isolation in Paper VI. This marker has previously been associated with PDT resistance (Bostad et al., 2013).

4.4 Viability Assays

Cellular viability was assessed using the 3-(4,5-dimethylthiazol-2-yl)-2,5-diphenyltetra zolium bromide (MTT) assay. The assay does not differentiate viable cells from dying cells at early time points after treatment as it only measures the mitochondrial activity of the cells, but has been shown to correlate well with the clonogenic assay when used at least 48 hours after PDT in our group (Selbo et al., 2006). The MTT assay is, however, challenging when addressing chemotherapy- or PCI-induced cell death when cytostatic drugs are involved. These drugs require relatively long action durations before an effect can be measured. Clonal experiments were therefore used when appropriate.

Neither the MTT assay or clonogenic assay discriminate between the mode of death or if cells have reached growth arrest. Apoptosis and necrosis was therefore studied by TUNEL- and cell permeabilization (based on propidium iodide) assays on flow cytometry, respectively.

To study the proliferation rate of cells, the IncuCyte proliferation assay was used. The assay is based on percentage from cell confluence and is reliable for the determination of the exponential growth phase. Proliferation assays were used for the determination of seeding densities and to study the photochemically induced effects on cell proliferation.

4.5 ROS Formation

Relative ROS formation was addressed by studying the cell permeable agent 2′,7′-Dichl orofluorescin diacetate (DCFH-DA) (Sigma), which upon deacetylation inside the cells, converts to DCFH. DCFH is rapidly oxidized to highly fluorescent DCF by the reaction with ROS. The fluorescence intensity is proportional to the ROS levels in the cell cytosol and was measured either by plate reading or flow cytometry (section 4.6). The accumulated ROS upon 1 hour was chosen to study immediate effects of the treatments. When flow cytometry was used, only live cells were analyzed, as dying cells are associated with unreliable results. The assay does therefore not include potential ROS formation in these cells, although it is expected that dying cells, indeed, are dying because of the ROS formation. Although DCFH-DA is most widely used for the detection of H_2O_2, several one-electron-oxidizing species may oxidize DCFH to DCF, including $OH^{\cdot}$ and NO_2. An intermediate radical of DCF ($DCF^{\cdot}$) may further react with O_2 to form $O_2^{\cdot-}$ subsequently generating H_2O_2 leading to amplification of the fluorescence signal intensity (Kalyanaraman et al., 2012).

4.6 Flow Cytometry and Fluorescence Microscopy

Flow cytometry is a laser-based method employed in cell counting, bio-marker detection and cell sorting. The method allows simultaneous multiparametic analysis, and can be performed on both live and fixed cells upon immunostaining or use of fluorescent markers. The method can be used for analyses of a high number of cells and many different dyes.

Immunostaining of live cells will typically reveal the presence of surface proteins and was in this thesis used for the identification of the CD133 and CD105 surface receptors. Cells subjected to drug incubation, *e.g.* with $TPCS_{2a}$ or agents for detection of ROS (DCFH-DA) were also analysed by flow cytometry. Internal controls, either gated based on barcoding stains or $TPCS_{2a}$, were used for increased reliability, in addition to live/dead markers, either based on forward and side scattering parameters or on live/dead dyes.

Fixation and permeabilization allows for detection of intracellular targets, and was used for the identification of γH2AX associated with DNA strand breaks and dUTP nicks associated with DNA fragmentation in apoptotic cells. The method was also used for the relative quantification of immunotoxin based on immunodetection post fixation.

Even if flow cytometry is a highly precise method, it does not reveal the intracellular localization of drugs and stains. For this reason phase contrast, fluorescence and electron microscopy was used, as it can visualise both the inside and outside of cells with great magnification. The method can be used to *e.g.* study co-localization of different dyes, which is not possible with flow cytometry.

4.7 Signal Normalization

When comparing signals, either from viability assays or protein expression assays, there is a need of an internal control for the ability to compare different cell lines and individual experiments. For the viability assays, non-treated (NT) cells were used as internal control and hence normalized to 100%. All other treatments were normalized relative to this.

For protein expression assays, such as Western blotting and immunodetection, signals were normalized to untreated controls. If proteins exhibited *decreasing* phosphorylation, the signals were normalized to the total expression of the respective protein (both phosphorylated and non-phosphorylated). If proteins were *gaining* phosphorylation, signals were normalized against phosphorylated proteins within the experiments.

Flow cytometry data were either presented as signal intensities per cell or as intensities relative to cell protein when cell lines exhibited differences in their protein content.

Summary of Publications and Manuscripts

Paper I

Development of resistance to photodynamic therapy (PDT) in human breast cancer cells is photosensitizer-dependent: Possible mechanisms and approaches for overcoming PDT-resistance

Authors

Cathrine Elisabeth Olsen, Anette Weyergang, Victoria Tudor Edwards, Kristian Berg, Andreas Brech, Sabine Weisheit, Anders Høgset and Pål Kristian Selbo

Main findings

This paper provides new knowledge demonstrating that repeating treatment with $TPCS_{2a}$-PDT induces acquired and persistent resistance to PDT, using the breast cancer cell line model MA11. Resistance was also obtained in the breast cancer cell line MDA-MB-231 while not the MCF-7 cell line. It was also found that three cycles or more of PDT using another photosensitizer, PhA, induced persistent resistance that was attributed to a selection of cells with intrinsically high expression of the ABCG2 drug-transporter responsible for efflux of PhA. The resistance to $TPCS_{2a}$-PDT was not conferred by altered $TPCS_{2a}$ accumulation. No difference in ROS scavenging or cross-resistance to doxorubicin or radiotherapy could be found between the $TPCS_{2a}$-PDT resistant and non-resistant cells. Instead, $TPCS_{2a}$-PDT resistant cells (MA11/TR) were growing more rapidly and overexpressed EGFR and ERK1/2, and exhibited a stronger STAT-3 activation after $TPCS_{2a}$-PDT compared to the maternal MA11 cells. The most interesting finding was, however, the highly dysregulated p38MAPK activity with the subsequent lack of MAPKAPK-2 (MK2) phosphorylation upon $TPCS_{2a}$-PDT treatment. Similar p38MAPK-results were obtained in MDA-MB-231 breast cancer cells of which we also managed to evoke PDT resistance, but the p38MAPK signal pathway was only found to mediate cell death in the MA11 cells. As also discussed in Paper II, the mechanism of resistance to PDT did not affect sensitivity to $TPCS_{2a}$-PCI. Targeting EGFR overexpression by PCI of EGF-saporin in the resistant MA11/TR cells showed that PCI circumvents the resistance mechanisms to PDT, and resulted in a synergistic decrease in cell viability of both $TPCS_{2a}$-PDT resistant and sensitive cells.

Submitted manuscript

Paper II

Circumvention of resistance to photodynamic therapy in doxorubicin-resistant sarcoma by photochemical internalization of gelonin.

Authors

Cathrine Elisabeth Olsen, Pål Kristian Selbo, Kristian Berg, Anette Weyergang

Main findings

The aim of this paper was to explore the mechanisms of cross-resistance to $TPCS_{2a}$-PDT induced by resistance to the chemotherapeutical agent doxorubicin in the uterine sarcoma cell line MES-SA/Dx5 originally developed from the MES-SA cells (Harker et al., 1985). The resistance to doxorubicin has previously been shown to involve upregulation of the drug-efflux pump Pgp, which we confirmed by Pgp inhibition that lowered the viability after doxorubicin treatment. Cross-resistance to clinically relevant $TPCS_{2a}$-PDT was demonstrated in line with a previous finding of cross-resistance to $TPPS_{2a}$-PDT. No difference in accumulation of $TPCS_{2a}$ was found between the cell lines, excluding an altered endocytosis/exocytosis rate or alterations in drug transporters. Compared to the MES-SA cells, the MES-SA/Dx5 cells were, however, found to express higher levels of the gluathione peroxidase (GPx)1 and GPx4 enzymes, which are ROS scavengers involved in detoxification of lipid hydroperoxides. In line with this, a lower level of PDT- and doxorubicin-induced ROS was detected in the MES-SA/Dx5 cells and accompanied with lower sensitivity to ionizing radiation. On protein level, an abrogated p38MAPK - MK2 (MAPKAPK-2) signaling was revealed, inhibiting initiation of $TPCS_{2a}$-PDT-induced cell death in the MES-SA/Dx5 cell line. Instead, inhibition of p38MAPK by SB203580 revealed that p38 activation is a death signal after $TPCS_{2a}$-PDT in the MES-SA cells. Endo-/lysosomal release of rGelonin by PCI induced more apoptosis-independent death in MES-SA/Dx5 cells despite the resistance to ROS, and was hypothesized to circumvent ROS resistance because $TPCS_{2a}$ is not in direct proximity to GPx1 and 4 when damaging endosomes and lysosomes in PCI. It was suggested that PCI may be a strategy for treatment of multidrug-resistant cancers.

Published

Free Radical, Biology and Medicine 65 (2013) 1300-1309 (Olsen et al., 2013)

Paper III

5-FU resistant EMT-like pancreatic cancer cells are hypersensitive to photochemical internalization of the novel endoglin-targeting immunotoxin CD105-saporin

Authors

Kaja Lund, **Cathrine Elisabeth Olsen**, Judith Jing Wen Wong, Petter Angell Olsen, Anders Høgset, Stefan Krauss and Pål Kristian Selbo

Main findings

Here we show that three 5-FU resistant sub-clones of the wild type pancreatic cancer cell line Panc03.27, overexpress Endoglin (CD105). CD105 is a membrane receptor overexpressed by the proliferating tumor neovasculature and is under clinical evaluation as a therapeutic target in different solid tumours. In the present work we have used PCI to enhance cytosolic release of a novel immunotoxin, anti-CD105-saporin, to target and kill 5-FU-resistant and epithelial-to-mysenchymal-like pancreatic cancer cells that overexpress CD105. Treatment with CD105-saporin alone significantly reduced the viability of the CD105-expressing 5-FU resistant pancreatic cancer cells, whereas little effect was seen in the CD105-negative non-resistant parental cancer cell lines. Strikingly, PCI of nanomolar levels of CD105-saporin nearly eradicated the 5-FU resistant cell population. In addition, the 5-FU resistant cell lines displayed hypersensitivity to PDT, despite a higher level of ROS-quenching machinery (increased expression of superoxide dismutase (SOD)1 and SOD2, and increased dependency of glutathione (GSH)). The increased sensitivity to PDT was linked to increased uptake of $TPCS_{2a}$, altered lysosomal distribution and increased expression of the lysosomal marker LAMP-1 in the 5-FU resistant cells. We show that inhibition of autophagy, either using chloroquine or PDT, increased the sensitivity to 5-FU in the resistant cells, indicating that acquisition of 5-FU resistance can be linked to alterations in the autophagosomal/lysosomal process in these cells and supporting the notion that alterations in autophagosomal/lysosomal pathways can be linked to acquisition of chemoresistance.

Manuscript

Paper IV

Impact of Genotypic and Phentypic Differences in Sarcoma models on the Outcome of Photochemical Internalization (PCI) of Bleomycin

Authors

Cathrine Elisabeth Olsen, Simen Sellevold, Theodossis Theodossiou, Sebastian Patzke and Kristian Berg

Main findings

In this paper we studied $TPCS_{2a}$-PDT and PCI of bleomycin in two soft tissue sarcomas; the vulvar leiomyosarcoma SK-LMS-1 cell line that exhibits a *P53* mutation rendering them unable to activate p53-mediated apoptosis, and the *P53* competent uterine sarcoma MES-SA cell line. Both cell lines were found intrinsically resistant to low-dose bleomycin, while SK-LMS-1 additionally possessed a slightly lower sensitivity to PDT. The SK-LMS-1 cells expressed higher levels of SOD and GPx enzymes compared to the MES-SA cells. PCI increased the toxicity and amount of DNA damage induced by bleomycin in both cell lines, but was found most effective in the MES-SA cells. Glutathione was found to potentiate the DNA damage in the MES-SA cells, which is in line with the suggested reactivation of bleomycin-Fe(III) to bleomycin-Fe(II) potentiating its action. No such effect was observed in the SK-LMS-1 cells. Depletion of glutathione increased the toxicity from PDT in both cell lines. The MES-SA cells entered apoptosis and cell cycle arrest upon PDT and PCI, in line with their functional *P53* gene upon PCI of bleomycin. The SK-LMS-1 cells did not enter apoptosis to the same degree as the MES-SA cells. Taken together, PCI of bleomycin induces DNA damage that, dependent on cell line, may be potentiated by glutathione.

Submitted manuscript

Paper V

Light-controlled endosomal escape of the novel CD133-targeting immunotoxin AC133-saporin by photochemical internalization - A minimally invasive cancer stem cell-targeting strategy

Authors

Monica Bostad, **Cathrine Elisabeth Olsen**, Qian Peng, Kristian Berg, Anders Høgset and Pål Kristian Selbo.

Main findings

The aim of this study was to use PCI for the delivery of the CD133 targeting IT AC133-saporin. It was demonstrated that AC133-saporin co-localizes with the PCI-photosensitizer $TPCS_{2a}$, which upon light exposure induced cytosolic release of AC133-saporin. PCI of picomolar levels of AC133-saporin blocked cell proliferation and induced inhibition of cell viability and colony forming ability, whereas no cytotoxicity was obtained in the absence of light. Efficient targeting was in addition demonstrated in stem-cell-like and aggressive cancer cells, whereas no enhanced targeting was obtained in CD133-negative cells. PCI of AC133-saporin induced necrosis as the main death response, and resulted in S phase arrest and reduced LC3-II conversion in the presence of the autophagy inhibitor bafilomycin A1, indicating a termination of the autophagic flux. PCI of the CD133 targeted IT was also demonstrated *in vivo*. After only one systemic injection of AC133-saporin and $TPCS_{2a}$, a strong anti-tumor response was observed. However, no cure was obtained, which layed the foundation of developing a smaller recombinant CD133-targeting toxin with presumably better tumor-penetrating capacity (Paper VI).

Published

Journal of Controlled Release 206 (2015) 37-48 (Bostad et al., 2015)

Paper VI

Design, characterization and evaluation of a novel CD133-targeting recombinant immunotoxin scFvCD133/rGelonin for use in combination with the endosomal escape method photochemical internalization

Authors

Cathrine Elisabeth Olsen, Lawrence Cheung, Anette Weyergang, Kristian Berg, Daniel Vallera, Michael Rosenblum and Pål Kristian Selbo

Main findings

The aim of the study was to design, develop and explore a novel recombinant IT for the specific targeting of CD133. In this work, the scFv unit of anti-CD133 (clone 7), was, recombinantly fused to the RIP gelonin by the stable and flexible 218 amino acid linker in *E. Coli* bacteria, and purified by immobilized metal affinity chromatography (IMAC) based on histidine retention. Total yield of the resulting scFvCD133/rGelonin IT was calculated to be 1200 microgram immunotoxin per 10 L bacteria, with a final concentration of 1.8 microM of purified material. The ribosome inactivating property was tested in a cell free system and showed >100-fold loss of activity compared to rGelonin. Nanomolar levels of the IT exhibited, however, a 90% ribosome inhibitory effect. Despite the loss of activity, PCI of the scFvCD133/rGelonin induced log-fold effects on viability after only 2-4 hours incubation in the PCI protocol. By increasing light doses, PCI of 10 nM reduced the viability down to less than 1%, and exceeded the specificity of rGelonin. The recombinant IT did also show a superior binding to the cell membrane of CD133 positive cells over CD133 negative. Surprisingly, PCI of the IT exceeded the toxicity of PCI of rGelonin also in CD133 receptor negative/low cell lines. To study if the effect could be cell line dependent, 5% of the lowest and 5% of the highest CD133 expressing cells in a receptor positive cell line were sorted. The sensitivity to PCI of scFvCD133/rGelonin was, however, not found significantly different between the sorted cells. This implies that minor levels of CD133 is sufficient to achieve cytotoxic effects after PCI of scFvCD133/rGelonin.

Manuscript

Discussion

Chapter 5

$TPCS_{2a}$-PDT and Resistance

PCI is a method developed to increase sensitivity to drugs that are sequestered and may be degraded in the lysosomal compartments of cancer cells. The method is mediated by the localized action of $TPCS_{2a}$-PDT on the endo-/lysosomal membranes subsequently releasing the drugs before they are degraded. In this respect, PCI can be regarded as a method for circumvention of resistance. There is, however, a lack of knowledge about if and how resistance may develop against $TPCS_{2a}$-PDT and, hence, what impact it may have on the effect of PCI. PCI has been investigated as a delivery method in several drug-resistant cancer cell lines (Lou et al., 2006; Selbo et al., 2010; Bostad et al., 2013; Weyergang et al., 2015), but only a few attempts have been made to investigate its own susceptibility to resistance (Selbo et al., 2006; Selbo et al., 2012). This chapter gives an overview of acquisition of altered sensitivity to $TPCS_{2a}$-PDT, and associated mechanisms regarding photosensitizer accumulation, detoxification, cell death and growth/proliferation inhibition.

5.1 Acquired PDT Resistance and PDT Hypersensitivity

Clinical PDT is usually conducted once or twice to achieve a successful result. Although development of clinical PDT-resistance is not well documented (Fiechter et al., 2012; Gilaberte et al., 2014; Bardazzi et al., 2015) it is of high importance that Paper I showed that only three treatment repetitions induce resistance to $TPCS_{2a}$- or PhA-PDT in two different breast cancer cell lines (MA11 (Fig. 5.1) and MDA-MB-231) selected by population selection. Acquired PDT-resistance is not limited to breast cancer. Singh *et al.* showed that also colon adenocarcinoma (HT29) and bladder carcinoma (HT1376) acquire resistance after repeated *in vitro* PDT (Singh et al., 2001), and Casas *et al.* and Mayhew *et al.* isolated PDT-resistant murine adenocarcinoma clones and radiotherapy-induced fibroblast (RIF)-1 cell populations, respectively (Casas et al., 2006; Mayhew et al., 2001).

The $TPCS_{2a}$-PDT resistance in MA11 and MDA-MB-231 was acquired by treating the cells with relative high PDT-doses resulting in >90% kill after first exposure. While this is similar to the doses used by Singh *et al.* and Casas *et al.* for the induction of PDT-resistance, Paper I, however, showed that the less PDT-sensitive MCF-7 cell line did not acquire resistance to $TPCS_{2a}$-PDT upon repeated treatment. This demonstrates that not all cell lines are susceptible to development of $TPCS_{2a}$-PDT resistance or that the level of cell kill may be important for the selection of resistant sub-populations. HT1376 and SK-N-MC cells isolated by Sing *et al.* did in line with this not develop resistance to AlPc4- and Photofrin-, and Photofrin-, Nile Blue- and AlPcS4-PDT, respectively (Singh et al., 2001). These cell lines demonstrated different levels of intrinsic resistance.

More than 8 cycles of PDT had to be used by Singh *et al.* before 1.5-2.81-fold increased survival was confirmed in the resistant cells compared to the maternal cells, while Casas

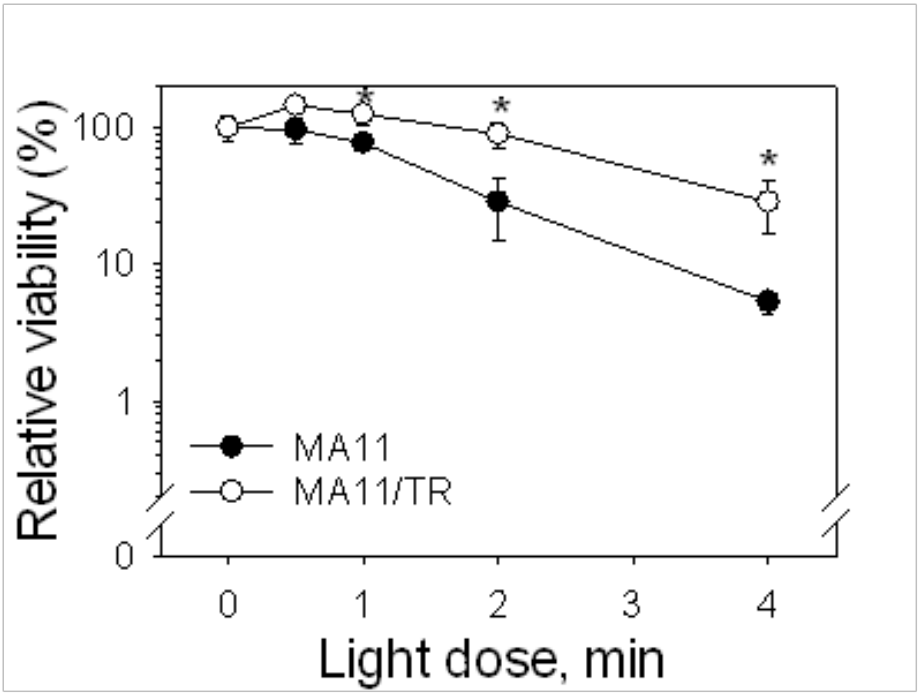

FIGURE 5.1: **PDT resistance in MA11 cells**

More than 3-fold increased survival after $TPCS_{2a}$-PDT MA11/TR cells upon induction of resistance. The data are the average of triplicates from a representative experiment (Error bars: S.D.), * = p<0.001 (Paper I).

et al. treated cells at 13 cycles. Fifteen cycles were used by Mayhew *et al.* for the isolation of cells exhibiting 5.7-7.1-fold increase in resistance. The resistant MA11/TR and MDA-MB-231/TR cells were in comparison >3-fold less sensitive to $TPCS_{2a}$-PDT than their maternal cells after 3 cycles when compared at the same light dose, and the LD_{50} and LD_{90} were >3-fold and close to 2-fold increased, respectively. Such fold-resistance index can, however, be difficult to define, as several parameters such as photosensitizer concentration, incubation time, localization and light dose may be different in different PDT protocols. This was illustrated by Mayhew *et al.* who demonstrated the 5.7-7.1-fold increased PDT-resistance with a fixed light dose and increasing photosensitizer concentration, but showed that the resistance was reduced to 1.7-1.8-fold with increasing light dose and fixed photosensitizer concentration (Mayhew et al., 2001). LD_{50} or LD_{90} (photosensitizer concentration and light dose) are, however, mainly used for comparison between cell lines (Zamarrón et al., 2015).

The first observation of PDT resistance was reported in 1991 by Luna and Gomer which showed that RIFs had generated *in vitro* resistance to Photofrin II-PDT (Luna et al., 1991). This demonstrates that PDT resistance can develop before any PDT treatment has been applied, subsequently also demonstrated *in vivo* (Singh et al., 1991), hence suggesting clinical implications. Selbo *et al.* also demonstrated that the doxorubicin-induced human uterine sarcoma cell line MES-SA/Dx5 had developed resistance to $TPPS_{2a}$-PDT (Selbo et al., 2006), and in Paper II we showed that this cross-resistance also applies for $TPCS_{2a}$-PDT.

Repeated chemotherapy or radiotherapy is often the first line treatment for malignant tumors, hence, rendering development of resistance and cross-resistance a potential prevalent phenomenon. The MES-SA/Dx5 cell line, originally developed by Harker

et al. (Harker et al., 1985), has for example been reported cross-resistant to several different chemotherapies (daunorubicin, dactinomycin, mitoxantrone, colchicine, vincristine, vinblastine, etoposide, mitomycin C and melphalan) (Wesolowska et al., 2005; Ambudkar et al., 2003; Sharom, 2008; Zilfou et al., 1995; Consoli et al., 1997), in addition to radiotherapy (as demonstrated in Paper II). Fortunately, in most cases no cross-resistance between chemotherapy and PDT has been reported (Casas et al., 2011). Demonstrations of cross-resistance include, however, the chemo-resistant P388/ADR (Kessel et al., 1994), CHO-MDR (DiProspero et al., 1997) and MCF-7/ADR (Wang et al., 2016) cell lines, exhibiting resistance to copper benzochlorin iminium salt, Photofrin- and Ce6-PDT, respectively. Interestingly, Paper I showed that the $TPCS_{2a}$-PDT-resistance in MA11/TR did not confer resistance to doxorubicin or radiotherapy, suggesting that $TPCS_{2a}$-PDT resistance not always is mediated by the same mechanism. However, while certain cancer cell sub-populations have been reported to undergo epigenetic changes and acquire transient resistance (Sharma et al., 2010), the resistance to $TPCS_{2a}$-PDT both in the MA11/TR and MES-SA/Dx5 cells in Paper I and Paper II were found persistent (more than 20 passages).

Chemotherapy-resistance (*e.g.* resistance to doxorubicin) has not only been reported to induce cross-resistance, but also to *increase* sensitivity to PDT (*hypersensitivity*), *e.g.* to meta-tetrahydroxy-phenyl-chlorin (m-THPC)-PDT in doxorubicin resistant breast cancer (MCF-7/DXR) cells (Teiten et al., 2001). Similar to this, Paper III revealed that 5-FU-resistance may confer hypersensitivity to $TPCS_{2a}$-PDT, demonstrated in the pancreas adenocarcinoma Panc03.27 sub-cell lines (B1L, B1Q and B1V). Similar results were recently obtained in a clinical study where pretreatment with 5-FU increased the efficacy of PDT in actinic keratosis (Nissen et al., 2017). Interestingly, $TPCS_{2a}$-PDT pretreatment of the B1L, B1Q and B1V sub-cell lines did also confer increased sensitivity to 5-FU in Paper III, suggesting that $TPCS_{2a}$-PDT influences on the resistance mechanism to 5-FU.

5.2 Mechanisms affecting Sensitivity to $TPCS_{2a}$-PDT

Some general resistance mechanisms to PDT have been suggested and discussed as similar to mechanisms conferring resistance to conventional cancer drugs, *e.g.* efflux, inactivation, target alterations and repair of damage (Casas et al., 2011). It can therefore be hypothesized that specific resistance mechanisms may be shared among cross-resistant drugs. This has, indeed, been confirmed for all the chemotherapeutics subjected to cross-resistance in the MES-SA/Dx5 cell line described in section 5.1. The main targets are, however, very different between doxorubicin and $TPCS_{2a}$-PDT; doxorubicin acts directly on the DNA while $TPCS_{2a}$ exerts its action on endo-/lysosomes. Both treatments share, however, the capability of generating ROS as part of their mechanism of action, indicating that the cross-resistance may be associated with adaption to excess ROS. However, as acquired resistance to $TPCS_{2a}$-PDT did not induce cross-resistance to doxorubicin in the MA11/TR cell line of Paper I, there are likely several mechanisms conferring alterations in sensitivity to $TPCS_{2a}$-PDT.

5.2.1 Photosensitizer Accumulation

Accumulation studies in Paper I and Paper II showed that there were no difference in $TPCS_{2a}$ uptake/efflux between the MES-SA and MA11 cell lines and their resistant counterparts MES-SA/Dx5 and MA11/TR. It was, accordingly, recently reported that

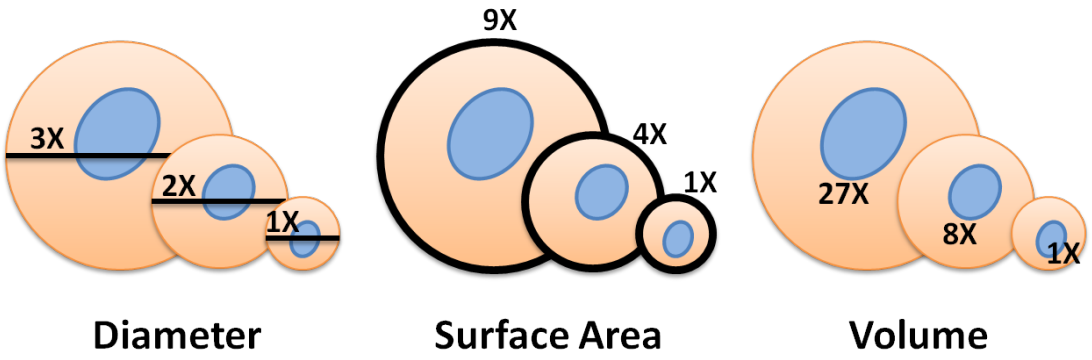

FIGURE 5.2: **The Relationship between Radius, Surface Area and Volume of a Cell**

While the diameter doubles, the surface area and volume of a cell increases to 4x and 8x, respectively. An increase from 1x to 3x, increases the surface area and volume 9x and 27x, respectively. Figure based on http://www.nature.com/scitable/topicpage/eukaryotic-cells-14023963 (Date entered: 4th of April 2017).

amphiphilic photosensitizers, such as $TPPS_{2a}$ and $TPCS_{2a}$ are not substrates of the ABC transporter ABCG2 (Selbo et al., 2012), which has been discussed to be conferred by the amphiphilic character of these photosensitizers possessing low ABCG2 affinities. In Paper II, doxorubicin resistance in MES-SA/Dx5 induced cross-resistance to $TPCS_{2a}$-PDT. Although upregulation of Pgp was identified as the resistance mechanism towards chemotherapy in this cell line, in line with previous reports (Ambudkar et al., 2003; Sharom, 2008; Zilfou et al., 1995; Consoli et al., 1997), Pgp inhibition did not increase the toxicity induced by $TPCS_{2a}$-PDT, demonstrating that $TPCS_{2a}$ is not a Pgp substrate.

Due to the localization and anchoring of $TPCS_{2a}$ in the cell membrane, the intracellular accumulation is mainly mediated by an endocytic process. In Paper III, accumulation studies demonstrated a time- and concentration-dependent uptake of $TPCS_{2a}$ in the maternal and $TPCS_{2a}$-PDT hypersensitive Panc03.27 cells. Interestingly, it was shown that the hypersensitive cells exhibited a 1.6-fold increased $TPCS_{2a}$ accumulation compared to the maternal cells, and that they were larger by volume. Similar results have also been observed after induction of resistance to 5-FU (Trigueros-Motos et al., 2012), Photofrin II-PDT- (Luna et al., 1991) and ALA-PDT (Casas et al., 2006) in breast cancer, RIFs and adenocarcinoma cells, respectively. As cells increase in size, their surface area, and thus the ability to take up the photosensitizer, does not increase to the same degree as their volume (Fig. 5.2). Therefore, as was calculated based on volume- and area-equations, the increase in cell volume (which was observed in the 5-FU resistant cells of Paper III) translated into an increase in surface area by 51%. This demonstrated that the 1.6-fold increased accumulation of $TPCS_{2a}$ was, at least partly, due to their increased surface area.

Paper IV also addressed $TPCS_{2a}$ accumulation. At the PDT timepoint (18 hours incubation + 4 hours chase), 3.3 times more $TPCS_{2a}$ was measured per cell in the SK-LMS-1 cell line compared to the MES-SA cells. Similar to Paper III it was found that the SK-LMS-1 cells were larger by volume (3.7 times, addressed by protein measurements), hence, accumulating slightly less $TPCS_{2a}$ than the MES-SA cells when corrected for protein content. When further estimating the surface area of SK-LMS-1 (>11 times larger

than in MES-SA based on area calculations), the accumulation of $TPCS_{2a}$ in the SK-LMS-1 cells is >3 times lower than expected.

The accumulation data from Paper IV do not explain how the change in accumulation is mediated. Factors that may be of importance include different endocytosis rates and cell membrane composition, *e.g.* presence of LDL receptors, previously demonstrated to affect the binding affinity of photosensitizers (Kessel, 1986; Kascakova et al., 2008). Membrane composition was not investigated in this work, but should be included when investigating the potential of $TPCS_{2a}$ in PDT and PCI.

5.2.2 ROS Detoxification

$TPCS_{2a}$ in combination with light is an efficient ROS inducer, as shown by the high ROS generation shortly after PDT. As described in section 3.1.2, ROS generation depends on oxygen availability, but to the greatest extent on the presence of the photosensitizer. It is, accordingly, expected that cells accumulating high levels of $TPCS_{2a}$ may generate more ROS than other cells.

Cells exhibit properties that may protect them from excess ROS, *e.g.* the ROS scavengers SOD and GPx. The cells of Paper III and Paper IV which accumulated the highest levels of $TPCS_{2a}$ (per cell), also expressed the highest levels of ROS scavenging enzymes. The ROS scavengers in the 5-FU resistant cells of Paper III did, however, not seem to detoxify the excess ROS to an adequate extent, and were hypersensitive to $TPCS_{2a}$-PDT. The cells were, nevertheless, highly dependent on the presence of GSH which decreased the sensitivity to $TPCS_{2a}$-PDT.

The specific role of GSH for intrinsic PDT resistance was recently investigated by us (Theodossiou et al., 2017), where we demonstrated that GSH may exhibit different roles depending on cell line; either being utilized in a redox reaction by GPx for the reduction of oxygenated products, or being involved in GST-mediated conjugation of GSH to the photosensitizer or photo-oxidized products. In the study, the intrinsically hypericin-PDT resistant MCF-7 cell line was found to overexpress GPx when compared to MDA-MB-231, which instead overexpressed GSTP1 relevant for efflux of photo-oxidized products. The impact of total GSH depletion, hence, affected both cell lines, but in different manners. It can, hence, be concluded that the importance of GSH is dependent on cell line, which also seems to be the case in Paper III and Paper IV.

In Paper II it was suggested that $TPCS_{2a}$-PDT-resistant MES-SA/Dx5 cells detoxified PDT-induced ROS by their increased expression of GPx1 and GPx4 upon acquiring resistance to doxorubicin. mRNA level and activity of ROS detoxifying enzymes has, in line with this, also been reported in other doxorubicin resistant cell lines such as K562/DOX and SKVLB (Kalinina et al., 2006). Accordingly, resistance to other ROS-inducing agents has also mediated increased antioxidant capacity (Deavall et al., 2012; Trachootham et al., 2009). As further shown in Paper II, doxorubicin treatment yielded less ROS generation in the MES-SA/Dx5 cells, indicating that the ROS scavenging enzymes confer the doxorubicin resistance. ROS detoxification can, however, not be identified as a prevalent resistance mechanism against $TPCS_{2a}$-PDT-induced toxicity, as the PDT-resistant MA11/TR cells of Paper I did not exhibit less ROS or more ROS-detoxifying enzymes than the sensitive maternal cells.

Taken together, ROS scavengers contribute to the mechanisms conferring resistance mechanism to $TPCS_{2a}$-PDT. The role seems, however, different in different cell lines.

5.2.3 $TPCS_{2a}$ Localization, Cell Death and Signaling

As described above, PCI induces cytosolic delivery of a drug/toxin, which on its own lacks a mode of efficient translocation. The localized effect of PDT on endo-/lysosomal membranes is therefore decisive for the PCI method. Lysosomal photosensitizers may, nevertheless, also relocate to other membranes upon the primary activation (*e.g.* to endoplasmic reticulum (ER) (Berg et al., 1991; Rodal et al., 1998)). Cell death may therefore, to a great extent, also be mediated by secondary effects (Wood et al., 1997) and, hence, be initiated by different intracellular signaling pathways.

Apoptosis

Activated photosensitizers damaging lysosomes have been suggested to have the ability to activate the apoptotic pathway through release of cathepsins and subsequent activation of the caspase cascade (Berg et al., 1997; Berg et al., 2010). In Paper II and Paper V it was, however, shown that $TPCS_{2a}$-PDT did not activate the caspases to a significant extent, but rather cleaved the caspase-substrate PARP independently of the caspases. This is in line with previous reports showing that cathepsins themselves can cleave PARP in a caspase independent manner (Gobeil et al., 2001) and that PDT with hexaminolevulinate (HAL) may initiate caspase independent apoptosis (Furre et al., 2006). Cells can survive a moderate release of cathepsins because of cathepsin inhibitors intrinsically present in the cytosol (Berg et al., 1994). Inhibition of cathepsins was of interest found as the mechanism of resistance in ATX-s10-PDT-resistant MCF-7c3 cells (Ichinose et al., 2006).

Neither Paper IV nor Paper V demonstrated $TPCS_{2a}$-PDT-induced apoptosis to the same degree as expected based on MTT viability measurements. Paper I additionally showed that $TPCS_{2a}$-PDT mediated an equal distribution of apoptotic and necrotic cells in the dead fraction of the $TPCS_{2a}$-PDT-resistant and sensitive MA11 breast cancer cell lines. It can therefore be suggested that the main death mechanism induced by $TPCS_{2a}$-PDT is not mediated by apoptosis, and, hence, that reduced susceptibility to apoptosis-mediated cell death is not a prevalent resistance mechanism to $TPCS_{2a}$-PDT.

Autophagy

Paper I, Paper III and Paper V showed that $TPCS_{2a}$-PDT increases the accumulation of the autophagy marker LC3 II, which in general is associated with LC3 conversion (LC3 I to LC3 II) indicating the initiation of autophagy. During the autophagic flux, lysosomes fuse with autophagosomes and subsequently degrade LC3 II localized on the inside of the autophagosomes. Agents which inhibit this fusion are therefore used as autophagy inhibitors and to reveal the total amount of LC3 II before it gets degraded. Examples of such agents include chloroquine and bafilomycin A1.

Interestingly, as $TPCS_{2a}$ localizes to and damages the endo-/lysosomes upon activation, it is possible that $TPCS_{2a}$-PDT may compromise the fusion of lysosomes and autophagsomes (Fig. 5.3), as previously described for PDT using other lysosomal photosensitizers (Agostinis et al., 2011). It is, hence, expected that $TPCS_{2a}$-PDT, in a similar manner as the autophagy inhibitors, would increase the LC3 II accumulation. Our results therefore suggested that $TPCS_{2a}$-PDT could act as an inhibitor of autophagy and, hence, implicate on the treatment outcome of drugs subjected to resistance by autophagy. Not surprisingly, Paper III showed that both chloroquine and $TPCS_{2a}$-PDT

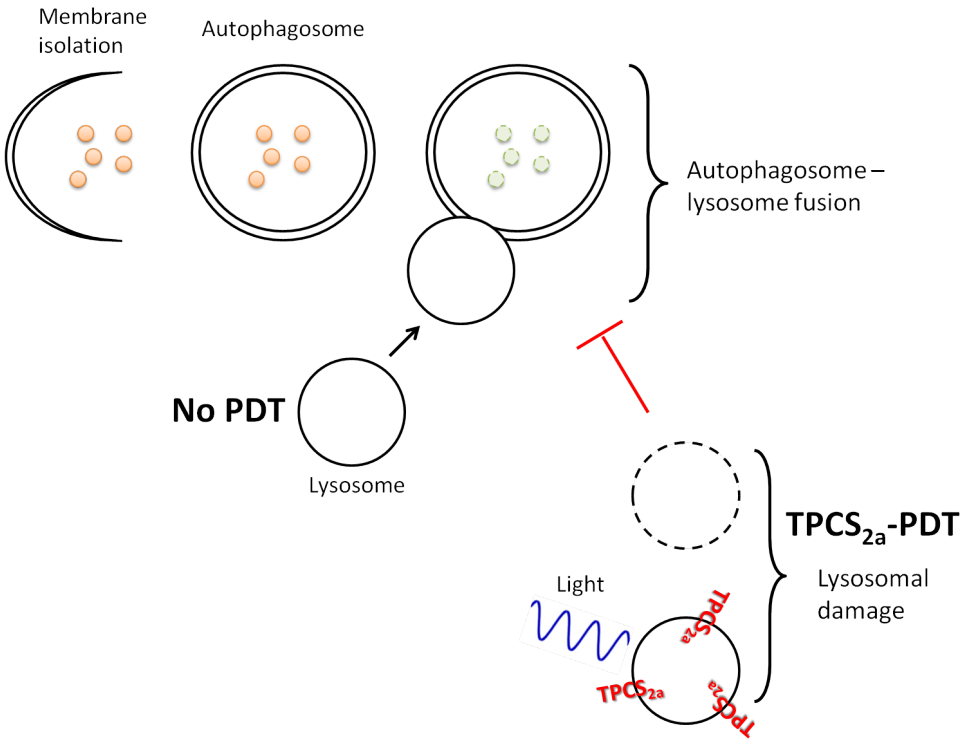

FIGURE 5.3: **Possible Inhibition of autophagy by TPCS$_{2a}$-PDT**

TPCS$_{2a}$-PDT may damage the lysosomes, resulting in the inhibition of autophagosome - lysosome fusion.

independently resensitized the Panc03.27R cell lines to 5-FU, likely through the inhibition of autophagic flux.

The 5-FU-resistant pancreatic cells in Paper III also exhibited altered endo-/lysosomal sizes and numbers, and were as described above hypersensitive to TPCS$_{2a}$-PDT. The results of Paper III are comparable to the results reported by Teiten *et al.* who demonstrated that doxorubicin resistant MCF-7/DXR cells exhibited a different intracellular m-THPC distribution pattern than their maternal cells and were hypersensitive to m-THPC-PDT (Teiten et al., 2001). It is difficult to address whether hypersensitivity to PDT is directly mediated by alterations in the lysosomal biogenesis, but as photosensitizer localization in general is considered as an important parameter in PDT-mediated toxicity, lysosomal distribution should warrant more investigation.

Cell Cycle Arrest

Hanahan *et al.* describe the evading of cell death as a cancer hallmark (Hanahan et al., 2000). Such ability has been related to cell cycle arrest where the cells may repair their damage before continuing their DNA replication. Paper IV showed, indeed, the arrest of MES-SA cells in G2/M phase upon TPCS$_{2a}$-PDT. According to indications that microtubuli are targets of PCI-relevant photosensitizers (Berg et al., 1997), it is likely that the G2/M arrest in MES-SA cells (Paper IV) can be linked to TPCS$_{2a}$-PDT-induced microtubuli-damage. Piette *et al.*, indeed, demonstrated that hypericin co-localizes with microtubuli and suggested that damage to microtubuli is an inducer of G2/M arrest (Piette et al., 2003). No G2/M arrest was, however, observed in the SK-LMS-1 cell line,

perhaps related to their mutated *P53* gene which may impair with mechanisms of cell cycle arrest, although multiple pathways may regulate the G2/M transition. Although a G2/M arrest was demonstrated after $TPCS_{2a}$-PDT in Paper I, no difference between $TPCS_{2a}$-PDT-sensitive and resistant MA11 cells was observed, indicating that G2/M arrest is not associated with the PDT-resistance in this model. $TPCS_{2a}$-PDT seems therefore to induce G2/M arrest dependent on cell line, and cannot be completely ruled out as a mechanism of $TPCS_{2a}$-PDT resistance.

ERK and p38MAPK

A few studies have reported on increased cell proliferation (Wolf et al., 1997; Varma et al., 2000; Maydan et al., 2006) and alterations in the MAPK/ERK pathway (Klotz et al., 1998; Tong et al., 2002) upon repeated PDT treatment, including $TPPS_{2a}$-PDT (Weyergang et al., 2008a; Weyergang et al., 2008b). In line with this, we showed that the breast cancer cell line MA11/TR in Paper I increased its proliferation capacity and expression of the growth related EGFR and ERK1/2 proteins upon the induction of acquired resistance to $TPCS_{2a}$-PDT. EGFR has, interestingly, previously been reported to be a target of $TPPS_{2a}$-PDT (Weyergang et al., 2007) and shown to be downregulated or deactivated by Pc4- or ALA-PDT (Ahmad et al., 2001; Tsai et al., 2009). EGFR was, however, not found to be significantly downregulated upon $TPCS_{2a}$-PDT in the MA11 or MA11/TR cells, although the upregulation of EGFR in untreated MA11/TR may seem as some sort of compensatory mechanism.

While ERK1/2 was found equally deactivated in the MA11 and MA11/TR cells relative to total ERK1/2 upon $TPCS_{2a}$-PDT, the transcription activator STAT-3 was found downregulated after PDT in both cell lines, but, interestingly, regained a higher level of phosphorylation in the MA11/TR cells after the initial dephosphorylation. This is in line with the increased EGFR expression and a possible increased stimuli by EGF.

In two of the papers in this thesis, p38MAPK was investigated after $TPCS_{2a}$-PDT (Paper I and Paper II). In both papers it was found that p38MAPK was phosphorylated rapidly after $TPCS_{2a}$-PDT, in line with Weyergang *et al.*'s previous observations involving $TPPS_{2a}$ (Weyergang et al., 2008b). Interestingly, $TPCS_{2a}$-PDT resistant cells either exhibited a high and prolonged p38MAPK phosphorylation (as the MA11/TR and MDA-MB-231/TR cells in Paper I) or a low phosphorylation (MES-SA/Dx5 in Paper II). In both cases the downstream activation of MK2 was abrogated in the resistant cell lines.

The work of Weyergang *et al.* showed that $TPPS_{2a}$-PDT was an inducer of p38MAPK-mediated cell death (Weyergang et al., 2008b), while in Paper II p38MAPK was recognized as a death signal only in the PDT-sensitive MES-SA cells. Further, Paper I identified p38MAPK as a death inducer only in the $TPCS_{2a}$-PDT sensitive MA11 cell line, while not in the MDA-MB-231 cell line. However, in the PDT-resistant MA11/TR and MDA-MB-231/TR cell lines' activation of MK2 was blocked, consistent with the abrogated p38MAPK phosphorylation. No effect was, accordingly, gained by the inhibition of p38MAPK, and p38MAPK could, hence, not be recognized as a death signal in these cells. The results show, nevertheless, that p38MAPK is involved in the development of $TPCS_{2a}$-PDT resistance, but that it is of different importance for $TPCS_{2a}$-PDT-mediated cell death.

Chapter 6

PCI and Cirumvention of Resistance

All the papers of the thesis showed that $TPCS_{2a}$-PDT-resistance did not affect the sensitivity to PCI. Chemotherapeutics and targeted and non-targeted toxins were, hence, with great success delivered by the PCI method to all the different PDT-resistant cell lines. In the following sections mechanisms of how PCI may circumvent the $TPCS_{2a}$-PDT resistance are discussed.

6.1 $TPCS_{2a}$ Localization

The amphiphilic stucture is the most important feature of $TPCS_{2a}$ for being used in PCI. This way it mediates the specific endo-/lysosome-directed generation of ROS, as described above. $TPCS_{2a}$ showed, indeed, localization to endo-/lysosomes independently of PDT sensitivity, when addressed in Paper I, Paper II, Paper III and Paper V. Even when the $TPCS_{2a}$ distribution pattern changed upon induction of 5-FU-resistance in Paper III, $TPCS_{2a}$ was still found co-localized with lysosomal markers, hence able to initiate the endo-/lysosomal rupture required for the PCI effect. The rupture was demonstrated by the observations of absent or weaker LysoTracker staining after $TPCS_{2a}$ activation.

In addition to alterations in size and number of lysosomes, other changes to the lysosomal biogenesis have also been reported in chemotherapy-resistant cells. Important for the PCI method, they include alkalization of the lysosomal pH in some MDR cancers (Larsen et al., 2000). However, as alkalized pH increases the deprotonation of the SO_3 groups of $TPCS_{2a}$, its anchoring to the endo-/lysosomal membranes should be further increased, thereby, if possible increasing the specificity of $TPCS_{2a}$ for endocytic vesicles. This may explain the increased effect of PCI observed in MDR cancers (Selbo et al., 2006) and (Paper II).

6.2 Reactive Oxygen Species

6.2.1 ROS Scavengers

Paper II showed that prolonged doxorubicin exposure was the reason for the elevated levels of ROS scavengers in the MES-SA/Dx5 cell line, and suggested that the ROS scavengers protected the cells against PDT-induced ROS *e.g.* in the cytosol and ER. Regarding PCI, the localization of the ROS scavengers is of high importance, as the primary ROS produced from the photosensitizer is short-lived (Moan et al., 1991) and located to the endo-/lysosomes. The ROS scavengers identified in Paper II (GPx1 and GPx4) are, importantly, not localized to the endo-/lysosomes, but reported to be expressed in the cytosol, mitochondria, nucleus and ER (Brigelius-Flohé et al., 2013; Liang et al.,

2009). The increased GPx1 and GPx4 expression in the MES-SA/Dx5 cells was therefore suggested to be able to inhibit the $TPCS_{2a}$-PDT-mediated toxicity without decreasing the efficacy of PCI. In this way, PCI was believed to circumvent the resistance towards $TPCS_{2a}$-induced ROS.

In Paper III, increased expression of SOD1 and SOD2 was detected in the 5-FU resistant cell lines. SOD1 and SOD2 are localized to the cytoplasm and mitochondria, respectively, and it is therefore expected that PCI is unaffected by this protection mechanism. As the cells, however, were hypersensitive to both PDT and PCI, it is likely that the ROS protection instead was surpassed by the increased $TPCS_{2a}$ accumulation. The hypersensitive cells were, nevertheless, more dependent on the presence of GSH for survival upon PDT than the maternal cells, suggesting that the ROS scavenging machinery in general contributes to some protection against PDT.

The SK-LMS-1 cells of Paper IV also expressed more ROS scavengers (SOD2 and GPx1) than the MES-SA cells, and the sensitivity to PCI of bleomycin and the DNA damage were lower in the SK-LMS-1 cells when compared to MES-SA. As GPx1 has been shown to be located in the cytosol, mitochondria and nucleus (Miranda et al., 2009), the expression of GPx1 and inverse correlation with double strand DNA breaks upon PCI of bleomycin may indicate that GPx1 attenuates the level of double strand breaks in the SK-LMS-1 cells, as discussed in Paper IV and (Jerome-Morais et al., 2013). The role of GPx1 is, however, not fully understood.

Taken together, the results demonstrate that ROS scavengers may confer resistance to $TPCS_{2a}$-induced ROS. However, because PCI-induced ROS-generation is in close vicinity to the endo-/lysosomal membranes, which are not the main localization of the ROS scavengers, PCI may be able to release sequestered drugs and toxins circumventing PDT resistance. Importantly, the PCI toxicity further depends on what drug is being released.

6.2.2 The Dual Role of Glutathione for DNA Damage

As described in section 5.2.2 GSH may exhibit different roles with implication for sensitivity to PDT, but as the GPxs are not localized to the endo-/lysosomes, the role of GSH for the effect of PCI is not expected to be mediated by the redox reaction of GSH by GPx. Instead, when using PCI for the delivery of bleomycin in Paper IV, it was shown that GSH may affect the PCI efficacy in a different manner:

Bleomycin is a glycopeptide antibiotic that mainly acts by inducing DNA strand breaks (Dorr, 1992). This action is to a high extent dependent on bleomycin's cytosolic translocation, but is limited due to bleomycin's hydrophilic structure and big size (Berg et al., 2005). Bleomycin-resistance in Paper IV was shown to be conferred by endo-/lysosomal entrapment, and was circumvented by PCI-induced bleomycin-release. The subsequent DNA damage by bleomycin increased with increasing PCI-light dose, and affected the MES-SA cells by the most.

If getting in close vicinity to the DNA, the action of bleomycin has been reported to depend on presence of metal ions, electron reductants and oxygen for the efficient production of ROS causing DNA strand breaks (Chen et al., 2005). Hypoxic regions may therefore be less sensitive to bleomycin treatment. The dependency of GSH as an electron reductant was demonstrated by a decrease in DNA damage upon GSH depletion (Fig. 6.1), but the depletion only had an influence in MES-SA cells regarding PCI. Interestingly, this was the cell line gaining highest DNA damage from PCI of bleomycin.

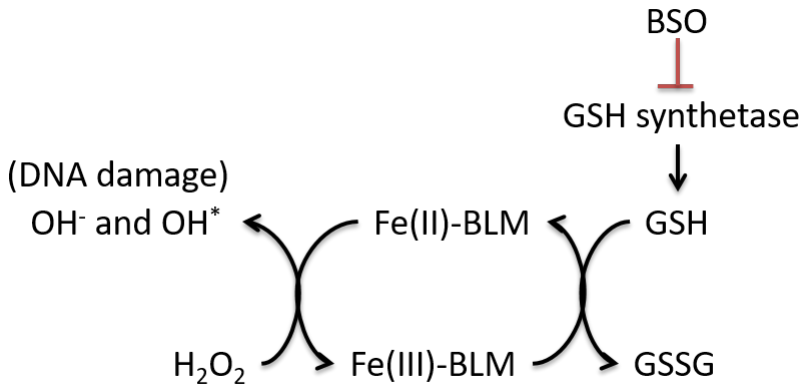

FIGURE 6.1: **Redox Reactions by Ferric and Ferrous Bleomycin**

The redox reaction of H_2O_2 to OH^- and $OH^{\cdot}$ by ferrous bleomycin (Fe(II)-BLM), and the subsequent reduction of ferric bleomycin by GSH oxidation. The redox reaction can be inhibited by inhibition of GSH synthetase.

Taken together the results show that, despite that GSH may contribute to a lower sensitivity to $TPCS_{2a}$-PDT (and probably not affecting the endo-/lysosomal escape of drugs in PCI), it may be important for the activity of the drug that is released by PCI *e.g.* bleomycin. Therefore, instead of being irrelevant for PCI, GSH may instead increase the PCI-mediated toxicity, here shown by the increase of DNA damage.

6.3 Utilization of Resistance-induced Markers in PCI

In Paper I an increased expression of EGFR was demonstrated in the $TPCS_{2a}$-PDT resistant MA11/TR cells, associated with an increased proliferation capacity. EGFR may, indeed, be an interesting target in cancer therapy as it may be a marker for aggressive tumors. Additionally, binding of a ligand to EGFR may induce alterations in its trafficking pattern towards an accelerated and enhanced lysosomal targeting (Wiley, 2003). This makes EGFR an especially interesting target in PCI. EGF-based ITs such as EGF-saporin and EGF-gelonin have, accordingly, been delivered by the PCI method by great success (Weyergang et al., 2006; Selbo et al., 2012; Berstad et al., 2015).

Compared to the toxicity mediated by PDT, the PDT-resistant MA11/TR cells in Paper I were found 3-fold more sensitive to PCI of EGF-saporin as compared to the maternal MA11 cell line when measured at the same PDT/PCI dose. As previously demonstrated by Selbo *et al.*, PCI of EGF-saporin efficiently surpasses the toxicity mediated by PCI of non-targeted saporin (Selbo et al., 2012), indicating receptor dependence. This was demonstrated in the MA11 cells, which express EGFR, but yet less than the MA11/TR cell line as shown in Paper I. Although a substantial toxicity was mediated by PCI of EGF-saporin when compared to PDT, Paper I did not show a stronger toxicity from PCI of EGF-saporin in the MA11/TR cells when directly compared to PCI of EGF-saporin in the MA11 cells. This may indicate that it may not be the *level*, but rather the *presence*, of EGFR expression being the important factor for targeted toxicity in the MA11 and MA11/TR cells, and that the sensitivity may be further complicated by different sensitivities to PDT or to the toxin part of the IT. Similar results were discussed

in Paper VI, where it was shown that PCI of scFvCD133/rGelonin surpassed the toxicity from PCI of rGelonin in cell lines suggested to express very low levels of CD133. Although not detected by our methods, all the cell lines in Paper VI have been reported to express CD133 to some extent in the literature (U87 (Wang et al., 2015), MDA-MB-231 (Paper V) and (Liu et al., 2012), MCF-7 (Blancas-Mosqueda, 2012), and NIH/3T3 (Product Datasheet CD133 Antibody NBP2-44249, Novusbio)). Similar results were obtained by Bostad *et al.* in the BxPc cell line (Bostad et al., 2013), reported to express CD133 in <1% of the cell population (Hermann et al., 2017).

CD133 expression is controlled by the levels of cholesterol in the cell membrane (Corbeil et al., 2001; Corbeil et al., 2010). Therefore, as amino acids, fatty acids and cholesterol are the main targets of singlet oxygen generated by the photochemical reactions from PCI, PCI of CD133-targeting ITs can be considered as highly advantageous. It is, hence, likely that PCI mediates a synergistic effect to the release of CD133-targeting ITs compared to other receptor-targeting toxins. This, in particular, was suggested to compensate for loss of IT RIP-activity compared to rGelonin, as discussed in Paper VI.

Sensitivity to ITs may also be dependent on other parameters, as *e.g.* shown in the work of Bull-Hansen *et al*. Correction for toxin sensitivity was decisive for the correlation between HER2 expression and sensitivity to PCI of a HER2-targeting IT (Bull-Hansen et al., 2015).

In Paper III, PCI of the CD105-targeting IT CD105-saporin mediated profound toxicity to the 5-FU resistant cells which overexpressed CD105. Although the PCI-mediated toxicity was highly associated with this overexpression, it is not unlikely that the increased accumulation of $TPCS_{2a}$ and the altered lysosomal distribution in the 5-FU resistant cells to some extent may contribute to their increased sensitivity to PDT and PCI.

Certain surface receptors (*e.g.* EGFR and HER2) have been associated with receptor mutations linked to therapy resistance towards *e.g.* gefitinib (Kobayashi et al., 2005), Herceptin (Anido et al., 2006) and trastuzumab (Mitra et al., 2009). Sometimes, mutations have affected signal transduction (Lynch et al., 2004), while in other cases affected epitope recognition (Okamoto et al., 1996). Normal signal transduction is, however, not a prerequisite for the utilization in PCI, as long as receptor binding and subsequent endocytosis is retained. Compared to other targeted therapies, *e.g.* mAbs which depend both on binding and the signal transduction, PCI may be a promising strategy even when receptors have altered their signaling and subsequently conferred resistance to other therapies. Receptor-targeting ITs together with a light-guided $TPCS_{2a}$-activation therefore suggest PCI as a promising strategy in resistant cancers.

6.4 PCI for Targeted Treatment of Cancer Stem Cells

Eradication of CSCs may be a prerequisite for complete tumor eradication as CSCs are suggested to be the drivers of tumorigenesis within a tumor. Several challenges are, however, associated with CSCs, *e.g.* that they can be quiescent and that they thrive under hypoxic conditions making them potentially less sensitive to therapies depending on oxygen (radiotherapy, PDT and some chemotherapeutics). CSCs have in addition been reported to exhibit strong ROS scavenging systems, of which Diehn *et al.* discussed could contribute to their clonogenicity and radioresistance (Diehn et al., 2009). The treatment challenges are further complicated by the expression of ABC efflux transporters, *e.g.* ABCG2, further contributing to resistance to several different drugs (Mao et al., 2015) and photosensitizers (Selbo et al., 2012).

The $TPCS_{2a}$-accumulation-studies by Selbo *et al.* (Selbo et al., 2012) and Paper I and Paper II showed that $TPCS_{2a}$ is not a substrate of ABCG2. Further, because photosensitizers can transfer energy directly to bio-substrates under low-oxygen conditions (Type I reaction) and PCI exhibits a capability to circumvent ROS-resistance, PCI using $TPCS_{2a}$ is a promising delivery strategy in the therapy-resistant CSCs. Importantly, quiescent cells also perform endocytosis (Bar-Sagi et al., 1986).

Many of the CSC associated markers described in the introduction of this thesis have been suggested as potential treatment targets, but are often challenged by the expression on normal stem- and progenitor cells, making CSC-targeted therapy a potential risk for healthy tissues. This thesis includes two papers with focus on PCI-based targeting of the CSC marker CD133. CD133 is shown to be an independent prognostic marker (Horst et al., 2008), and has been shown to have tumor-initiating capacity with only 10 $CD133^{high}$ cells inoculated in mice (Bostad et al., 2013). In the latter study it was also shown that the $CD133^{high}$ cells expressing the AC133 epitope were resistant to PDT. Beneficial for ITs targeting CD133 is that they only yield modest cytotoxic effects on normal progenitor cells, related to their low CD133 expression compared to the expression on CSCs (Schmohl et al., 2016). The confined light-induced targeting by PCI may, however, contribute to even less toxic effects on healthy tissue. In Paper V colocalization of AC133-saporin and $TPCS_{2a}$ in endo-/lysosomes was demonstrated, and PCI of picomolar levels of the IT blocked cell proliferation and induced cytosolic release of AC133-saporin. The work suggested, however, that the chemically conjugated IT was too large to be clinically relevant.

6.5 Recombinant Immunotoxins for Clinical PCI

Conventional ITs, based on chemical linkers, are perhaps mostly optimal for use in *in vitro*-PCI as they possess large sizes and risk of payload dissociation before reaching their targets. One hundred and ninety kDa have been set as the threshold for adequate tumor penetration (Shan et al., 2013), but it is also important that the sizes exceed the cut-off size for renal clearance (50-60 kDa) (Rennen et al., 2001). Non-specificity of ITs have in general been associated with the development of vascular leak syndrome (VLS).

Saporin-based ITs have been used as model-drugs in several of the *in vitro* and *in vivo* PCI studies. Compared to the toxicity of other type I-RIPs, *e.g.* gelonin, saporin is rather toxic upon cellular internalization. The use of gelonin, being 5-10 times less toxic than saporin, has, hence, been suggested as a better toxin payload for clinically relevant ITs (French et al., 1995). As gelonin further is rigidly packed and relative inaccessible to proteolytic cleavage (Rosenblum et al., 1995), it may be a better RIP for making ITs suitable for PCI. HuM195-Gelonin was the first IT used in a (non-PCI) clinical trial based on rGelonin, chemically, linked to the humanized monoclonal CD33-targeting antibody HuM195 (Pagliaro et al., 1998). HuM195-Gelonin has shown a favorable toxicity profile (Borthakur et al., 2013), but the large size (190 kDa) renders it, however, on the borderline for optimal tumor penetration (Scheinberg et al., 2004). The efficacy in the clinical phase I study was, indeed, limited (Borthakur et al., 2013; Alewine et al., 2015). Other smaller fusion constructs containing recombinant gelonin studied *in vivo* include e23-L-rGel and C6.5-L-rGel (55 kDa), rGel/BLyS (136.5 kDa), VEGF121/rGel (84 kDa), as described in (Lyu et al., 2012), in addition to rGel/EGF (Berstad et al., 2015) and MH3-B1/rGel (Bull-Hansen et al., 2015) investigated for PCI delivery. All these fusion toxins

qualify as candidates for clinical trials based on their size and expected toxicity and are relevant for clinical PCI.

In Paper VI a 58.97 kDa IT was constructed based on the scFv fragment of CD133 and deglycosylated gelonin, produced by recombinant technology. The IT did, however, not qualify as targeting regarding toxicity as its RIP activity was lost by more than 100-fold compared to that of rGelonin. PCI mediated, nevertheless, profound toxicity compared to PCI of rGelonin, and was shown to bind to and accumulate specifically in CD133+ cell lines. PCI of the IT did, however, also mediate cell death to CD133- cells as discussed above. CD133 receptor targeted recombinant gelonin-based ITs therefore warrant more research on alternative constructs for further optimization and *in vivo* evaluations.

Chapter 7

Conclusions

7.1 Summary

$TPCS_{2a}$-PCI exploits endocytic sequestration and the principle of PDT for the delivery of drugs into cancer cells. This thesis provides insight into the susceptibility and mechanisms behind development of resistance to PDT using $TPCS_{2a}$. It was shown that $TPCS_{2a}$ was susceptible to PDT-resistance induced both by cross-resistance from chemotherapy and by repeated treatment with $TPCS_{2a}$-PDT. Some cell lines were also found intrinsically less sensitive to PDT. Resistance to $TPCS_{2a}$-PDT was, however, not found to induce cross-resistance to chemotherapy nor radiotherapy, and did not decrease the sensitivity to PCI.

Several mechanisms were found to confer PDT-resistance. These included an increased EGFR related proliferation capacity and a dysregulated p38MAPK pathway attenuating photochemical cell death, in addition to an increased ROS scavenging capacity after $TPCS_{2a}$-PDT. Increased ROS scavenging capacity did, however, not protect all cell lines from toxicity from $TPCS_{2a}$-PDT, suggesting that $TPCS_{2a}$-PDT-resistance may be controlled by a combination of several factors.

The resistance mechanisms to $TPCS_{2a}$-PDT were, to the extent this thesis has investigated, not found to implicate cross-resistance to $TPCS_{2a}$-PCI. This was suggested to be because the resistance towards $TPCS_{2a}$-PDT was developed against secondary effects mediated by $TPCS_{2a}$-PDT and not against the primary action on the endo-/lysosomes, *e.g.* ROS scavengers located other places than in the endo-/lysosomal membranes. The primary ROS generation and endo-/lysosomal release of sequestered drugs and toxins could, hence, be delivered by the use of PCI to all PDT-sensitive and -resistant cell lines. It was also suggested that $TPCS_{2a}$-PDT may act as an inhibitor of autophagic flux and hence be used to improve the efficacy of drugs degraded by the autophagosomal pathway.

Even though the ROS scavenger GSH was found to protect cells against $TPCS_{2a}$-PDT, it was shown that it could mediate increased DNA damage from PCI of the chemotherapeutic bleomycin, likely due to GSH-mediated bleomycin reactivation. This showed that resistance mechanisms to PDT sometimes may be utilized in PCI.

Resistance-induced markers were also investigated for utilization in PCI by the use of targeting ITs. Both EGF- and CD105-targeting saporin-based ITs were found to mediate several-fold increased toxicities compared to PCI of the non-targeted toxins, and circumvented resistance to $TPCS_{2a}$-PDT. Recombinant technology was further used to improve the clinical relevance of a CSC targeting IT based on anti-CD133 and gelonin. Production of a recombinant scFvCD133- and gelonin-based IT yielded a clinically relevant size and mediated cytotoxic responses better than that of rGelonin when delivered

by the PCI method. Despite a profound loss in RIP activity, PCI of the IT also mediated toxicity to CD133- cell lines.

7.2 Future Perspectives

The work of this thesis demonstrates the involvement of several mechanisms towards development of resistance to $TPCS_{2a}$-PDT. Although many resistance mechanisms were identified, they were not found to affect the PCI method, demonstrating that PCI is a reasonable approach to overcome PDT resistance.

The results show, however, that not all cell lines are prone to development of PDT resistance, hence, more research should be put into investigating cell line differences, which are also important for the search of prognostic markers for sensitivity to PDT. The use of DNA microarrays to measure the expression level of genes would be a rational first approach to understand the cell line-specific diversity.

The results propose that PCI has the potential to overcome clinical PDT resistance. The next approach would, therefore, be to document that PCI can circumvent PDT resistance in clinically relevant models. The first step would, hence, be to document the development of $TPCS_{2a}$-PDT resistance *in vivo*. This can be performed by either inoculating mice with PDT resistant cancer cells or treating tumors in cycles. The latter method would resemble a clinical situation.

The PCI technology is optimized for drugs that are sequestered in endo-/lysosomes, but as $TPCS_{2a}$-PDT also may act as an inhibitor of autophagy, hence, its use should also be investigated further in combination with drugs where autophagy is shown to be a resistance/survival mechanism.

Further, overexpression of EGFR, CD105 and CD133, present intrinsically or as a result of acquired resistance to PDT or chemotherapy, suggests that studies should also be performed for further investigating the targeting potential of PCI in PDT- and chemotherapy-resistant cancers. Although recombinant ITs were assumed to be advantageous over conventional ITs in this regard, they may benefit from construct- and production-optimization. Focus should be laid on preserving RIP activity and improving selectivity.

Bibliography

Agostinis, P., Berg, K., Cengel, K. A., Foster, T. H., Girotti, A. W., Gollnick, S. O., Hahn, S. M., Hamblin, M. R., Juzeniene, A., Kessel, D., Korbelik, M., Moan, J., Mroz, P., Nowis, D., Piette, J., Wilson, B. C., and Golab, J. (2011). "Photodynamic therapy of cancer: An update". In: *CA: A Cancer Journal for Clinicians* 61.4, pp. 250–281. DOI: 10.3322/caac.20114.

Ahmad, N., Kalka, K., and Mukhtar, H. (2001). "In vitro and in vivo inhibition of epidermal growth factor receptor-tyrosine kinase pathway by photodynamic therapy." In: *Oncogene* 20.18, pp. 2314–2317. DOI: 10.1038/sj.onc.1204313.

Al-Hajj, M., Wicha, M. S., Benito-Hernandez, A., Morrison, S. J., and Clarke, M. F. (2003). "Prospective identification of tumorigenic breast cancer cells". In: *Proceedings of the National Academy of Sciences* 100.7, pp. 3983–3988. DOI: 10.1073/pnas.0530291100.

Alberts, B., Bray, D., Hopkin, K., Johnson, A., Lewis, J., Raff, M., Roberts, K., and Walter, P. (2004). *Essential Cell Biology*. Ed. by E. Hunt. 2nd ed. ISBN: 0-8153-3481-8.

Alewine, C., Hassan, R., and Pastan, I. (2015). "Advances in anticancer immunotoxin therapy." In: *The oncologist* 20 (2), pp. 176–185. DOI: 10.1634/theoncologist.2014-0358.

Ambudkar, S. V., Kimchi-Sarfaty, C., Sauna, Z. E., and Gottesman, M. M. (2003). "P-glycoprotein: from genomics to mechanism." In: *Oncogene* 22 (47), pp. 7468–7485. DOI: 10.1038/sj.onc.1206948.

Anagnostou, V. K. and Brahmer, J. R. (2015). "Cancer immunotherapy: a future paradigm shift in the treatment of non-small cell lung cancer." In: *Clinical cancer research : an official journal of the American Association for Cancer Research* 21 (5), pp. 976–984. DOI: 10.1158/1078-0432.CCR-14-1187.

Anido, J., Scaltriti, M., Serra, J. J. B., Josefat, B. S., Todo, F. R., Baselga, J., and Arribas, J. (2006). "Biosynthesis of tumorigenic HER2 C-terminal fragments by alternative initiation of translation". In: *The EMBO Journal* 25.13, pp. 3234–3244. DOI: 10.1038/sj.emboj.7601191.

Ansari, D., Tingstedt, B., Andersson, B., Holmquist, F., Sturesson, C., Williamsson, C., Sasor, A., Borg, D., Bauden, M., and Andersson, R. (2016). "Pancreatic cancer: yesterday, today and tomorrow." In: *Future oncology (London, England)* 12 (16), pp. 1929–1946. DOI: 10.2217/fon-2016-0010.

Assefa, Z., Vantieghem, A., Declercq, W., Vandenabeele, P., Vandenheede, J. R., Merlevede, W., de Witte, P., and Agostinis, P. (1999). "The activation of the c-Jun N-terminal kinase and p38 mitogen-activated protein kinase signaling pathways protects HeLa cells from apoptosis following photodynamic therapy with hypericin." In: *Journal of Biological Chemistry* 274.13, pp. 8788–8796. DOI: 10.1074/jbc.274.13.8788.

Bacellar, I. O. L., Tsubone, T. M., Pavani, C., and Baptista, M. S. (2015). "Photodynamic Efficiency: From Molecular Photochemistry to Cell Death." In: *International Journal of Molecular Sciences* 16 (9), pp. 20523–20559. DOI: 10.3390/ijms160920523.

Baier, J., Maier, M., Engl, R., Landthaler, M., and Bäumler, W. (2005). "Time-Resolved Investigations of Singlet Oxygen Luminescence in Water, in Phosphatidylcholine,

and in Aqueous Suspensions of Phosphatidylcholine or HT29 Cells". In: *The Journal of Physical Chemistry B* 109.7 (7), pp. 3041–3046. DOI: 10.1021/jp0455531.

Bar-Sagi, D and Feramisco, J. R. (1986). "Induction of membrane ruffling and fluid-phase pinocytosis in quiescent fibroblasts by ras proteins." In: *Science (New York, N.Y.)* 233 (4768), pp. 1061–1068. DOI: 10.1126/science.3090687.

Barbieri, L, Battelli, M. G., and Stirpe, F (1993). "Ribosome-inactivating proteins from plants." In: *Biochimica et Biophysica Acta* 1154 (3-4), pp. 237–282. DOI: 10.1016/0304-4157(93)90002-6.

Bardazzi, F, Loi, C, Magnano, M, Burtica, E. C., Giordano, F, and Patrizi, A (2015). "Methyl-aminolevulinic acid photodynamic therapy for actinic keratoses: a useful treatment or a risk factor? A retrospective study." In: *The Journal of dermatological treatment* 26 (2), pp. 168–170. DOI: 10.3109/09546634.2014.915004.

Berg, K, Bommer, J. C., and Moan, J (1989). "Evaluation of sulfonated aluminum phthalocyanines for use in photochemotherapy. Cellular uptake studies." In: *Cancer Letters* 44 (1), pp. 7–15. DOI: 10.1016/0304-3835(89)90101-8.

Berg, K, Madslien, K, Bommer, J. C., Oftebro, R, Winkelman, J. W., and Moan, J (1991). "Light induced relocalization of sulfonated meso-tetraphenylporphines in NHIK 3025 cells and effects of dose fractionation." In: *Photochemistry and Photobiology* 53 (2), pp. 203–210. DOI: 10.1111/j.1751-1097.1991.tb03924.x.

Berg, K and Moan, J (1994). "Lysosomes as photochemical targets." In: *International Journal of Cancer* 59 (6), pp. 814–822. DOI: 10.1002/ijc.2910590618.

— (1997). "Lysosomes and microtubules as targets for photochemotherapy of cancer." In: *Photochemistry and Photobiology* 65 (3), pp. 403–409. DOI: 10.1111/j.1751-1097.1997.tb08578.x.

Berg, K, Selbo, P. K., Prasmickaite, L, Tjelle, T. E., Sandvig, K, Moan, J, Gaudernack, G, Fodstad, O, Kjølsrud, S, Anholt, H, Rodal, G. H., Rodal, S. K., and Høgset, A (1999). "Photochemical internalization: a novel technology for delivery of macromolecules into cytosol." In: *Cancer Research* 59 (6), pp. 1180–1183.

Berg, K., Dietze, A., Kaalhus, O., and Høgset, A. (2005). "Site-specific drug delivery by photochemical internalization enhances the antitumor effect of bleomycin." In: *Clinical cancer research : an official journal of the American Association for Cancer Research* 11 (23), pp. 8476–8485. DOI: 10.1158/1078-0432.CCR-05-1245.

Berg, K., Berstad, M., Prasmickaite, L., Weyergang, A., Selbo, P. K., Hedfors, I., and Høgset, A. (2010). "Photochemical internalization: a new tool for gene and oligonucleotide delivery." In: *Topics in Current Chemistry* 296, pp. 251–281. DOI: 10.1007/128_2010_63.

Berg, K., Nordstrand, S., Selbo, P. K., Tran, D. T. T., Angell-Petersen, E., and Høgset, A. (2011). "Disulfonated tetraphenyl chlorin (TPCS2a), a novel photosensitizer developed for clinical utilization of photochemical internalization." In: *Photochemistry & Photobiological Sciences* 10.10, pp. 1637–1651. DOI: 10.1039/c1pp05128h.

Berstad, M. B., Cheung, L. H., Berg, K., Peng, Q., Fremstedal, A. S. V., Patzke, S., Rosenblum, M. G., and Weyergang, A. (2015). "Design of an EGFR-targeting toxin for photochemical delivery: in vitro and in vivo selectivity and efficacy." In: *Oncogene*. DOI: 10.1038/onc.2015.15.

Berstad, M. B., Weyergang, A., and Berg, K. (2012). "Photochemical internalization (PCI) of HER2-targeted toxins: synergy is dependent on the treatment sequence." In: *Biochimica et Biophysica Acta* 1820 (12), pp. 1849–1858. DOI: 10.1016/j.bbagen.2012.08.027.

Bidlingmaier, S., Zhu, X., and Liu, B. (2008). "The utility and limitations of glycosylated human CD133 epitopes in defining cancer stem cells." In: *Journal of Molecular Medicine* 86.9 (9), pp. 1025–1032. DOI: 10.1007/s00109-008-0357-8.

Blancas-Mosqueda, M. (2012). "CD133 antisense suppresses cancer cell growth and increases sensitivity to cisplatin in vitro". In: *Experimental and Therapeutic Medicine*. DOI: 10.3892/etm.2012.692.

Bonnet, D. and Dick, J. E. (1997). "Human acute myeloid leukemia is organized as a hierarchy that originates from a primitive hematopoietic cell". In: *Nature Medicine* 3.7, pp. 730–737. DOI: 10.1038/nm0797-730.

Borthakur, G., Rosenblum, M. G., Talpaz, M., Daver, N., Ravandi, F., Faderl, S., Freireich, E. J., Kadia, T., Garcia-Manero, G., Kantarjian, H., and Cortes, J. E. (2013). "Phase 1 study of an anti-CD33 immunotoxin, humanized monoclonal antibody M195 conjugated to recombinant gelonin (HUM-195/rGEL), in patients with advanced myeloid malignancies." In: *Haematologica* 98 (2), pp. 217–221. DOI: 10.3324/haematol.2012.071092.

Bossu, E, A'Amar, O, Parache, R. M., Notter, D, Labrude, P, Vigneron, C, and Guillemin, F (1997). "Determination of the maximal tumor/normal skin ratio after HpD or m-THPC administration in hairless mouse (SKh-1) by fluorescence spectroscopy–a non-invasive method." In: *Anti-Cancer Drugs* 8 (1), pp. 67–72. DOI: 10.1097/00001813-199701000-00009.

Bostad, M., Berg, K., Høgset, A., Skarpen, E., Stenmark, H., and Selbo, P. K. (2013). "Photochemical internalization (PCI) of immunotoxins targeting CD133 is specific and highly potent at femtomolar levels in cells with cancer stem cell properties." In: *Journal of controlled release : official journal of the Controlled Release Society* 168 (3), pp. 317–326. DOI: 10.1016/j.jconrel.2013.03.023.

Bostad, M., Kausberg, M., Weyergang, A., Olsen, C. E., Berg, K., Høgset, A., and Selbo, P. K. (2014). "Light-triggered, efficient cytosolic release of IM7-saporin targeting the putative cancer stem cell marker CD44 by photochemical internalization." In: *Molecular Pharmaceutics* 11.8, pp. 2764–2776. DOI: 10.1021/mp500129t.

Bostad, M., Olsen, C. E., Peng, Q., Berg, K., Høgset, A., and Selbo, P. K. (2015). "Light-controlled endosomal escape of the novel CD133-targeting immunotoxin AC133-saporin by photochemical internalization - A minimally invasive cancer stem cell-targeting strategy." In: *Journal of controlled release : official journal of the Controlled Release Society* 206, pp. 37–48. DOI: 10.1016/j.jconrel.2015.03.008.

Brigelius-Flohé, R. and Maiorino, M. (2013). "Glutathione peroxidases." In: *Biochimica et Biophysica Acta* 1830 (5), pp. 3289–3303. DOI: 10.1016/j.bbagen.2012.11.020.

Broekgaarden, M., Weijer, R., Gulik, T. M. van, Hamblin, M. R., and Heger, M. (2015). "Tumor cell survival pathways activated by photodynamic therapy: a molecular basis for pharmacological inhibition strategies". In: *Cancer and Metastasis Reviews* 34.4, pp. 643–690. DOI: 10.1007/s10555-015-9588-7.

Bugelski, P. J., Porter, C. W., and Dougherty, T. J. (1981). "Autoradiographic distribution of hematoporphyrin derivative in normal and tumor tissue of the mouse." In: *Cancer Research* 41 (11 Pt 1), pp. 4606–4612.

Bull-Hansen, B., Berstad, M. B., Berg, K., Cao, Y., Skarpen, E., Fremstedal, A. S., Rosenblum, M. G., Peng, Q., and Weyergang, A. (2015). "Photochemical activation of MH3-B1/rGel: a HER2-targeted treatment approach for ovarian cancer." In: *Oncotarget* 6 (14), pp. 12436–12451. DOI: 10.18632/oncotarget.3814.

Cai, C. and Zhu, X. (2012). "The Wnt/β-catenin pathway regulates self-renewal of cancer stem-like cells in human gastric cancer." In: *Molecular Medicine Reports* 5 (5), pp. 1191–1196. DOI: 10.3892/mmr.2012.802.

Caruso, J. A., Mathieu, P. A., Joiakim, A., Leeson, B., Kessel, D., Sloane, B. F., and Reiners, J. J. (2004). "Differential susceptibilities of murine hepatoma 1c1c7 and Tao cells to the lysosomal photosensitizer NPe6: influence of aryl hydrocarbon receptor on lysosomal fragility and protease contents." In: *Molecular Pharmacology* 65 (4), pp. 1016–1028. DOI: 10.1124/mol.65.4.1016.

Casas, A., Di Venosa, G., Hasan, T., and Batlle, A. (2011). "Mechanisms of resistance to photodynamic therapy." In: *Current Medicinal Chemistry* 18.16, pp. 2486–2515. DOI: 10.2174/092986711795843272.

Casas, A., Perotti, C., Ortel, B., Venosa, G. D., Saccoliti, M., Batlle, A., and Hasan, T. (2006). "Tumor cell lines resistant to ALA-mediated photodynamic therapy and possible tools to target surviving cells". In: *International Journal of Oncology*. DOI: 10.3892/ijo.29.2.397.

Castano, A. P., Demidova, T. N., and Hamblin, M. R. (2004). "Mechanisms in photodynamic therapy: part one—photosensitizers, photochemistry and cellular localization". In: *Photodiagnosis and Photodynamic Therapy* 1.4, pp. 279–293. DOI: 10.1016/s1572-1000(05)00007-4.

Chen, B., Pogue, B. W., Hoopes, P. J., and Hasan, T. (2006). "Vascular and cellular targeting for photodynamic therapy." In: *Critical Reviews in Eukaryotic Gene Expression* 16 (4), pp. 279–305.

Chen, J. and Stubbe, J. (2005). "Bleomycins: towards better therapeutics." In: *Nature Reviews. Cancer* 5 (2), pp. 102–112. DOI: 10.1038/nrc1547.

Colak, S. and Medema, J. P. (2014). "Cancer stem cells–important players in tumor therapy resistance." In: *The FEBS journal* 281 (21), pp. 4779–4791. DOI: 10.1111/febs.13023.

Consoli, U, Van, N. T., Neamati, N, Mahadevia, R, Beran, M, Zhao, S, and Andreeff, M (1997). "Cellular pharmacology of mitoxantrone in p-glycoprotein-positive and -negative human myeloid leukemic cell lines." In: *Leukemia* 11 (12), pp. 2066–2074. DOI: 10.1038/sj.leu.2400511.

Corbeil, D, Röper, K, Fargeas, C. A., Joester, A, and Huttner, W. B. (2001). "Prominin: a story of cholesterol, plasma membrane protrusions and human pathology." In: *Traffic (Copenhagen, Denmark)* 2 (2), pp. 82–91. DOI: 10.1034/j.1600-0854.2001.020202.x.

Corbeil, D., Marzesco, A.-M., Fargeas, C. A., and Huttner, W. B. (2010). "Prominin-1: a distinct cholesterol-binding membrane protein and the organisation of the apical plasma membrane of epithelial cells." In: *Sub-Cellular Biochemistry* 51, pp. 399–423. DOI: 10.1007/978-90-481-8622-8_14.

Cordon-Cardo, C, O'Brien, J. P., Boccia, J, Casals, D, Bertino, J. R., and Melamed, M. R. (1990). "Expression of the multidrug resistance gene product (P-glycoprotein) in human normal and tumor tissues." In: *The journal of histochemistry and cytochemistry : official journal of the Histochemistry Society* 38 (9), pp. 1277–1287. DOI: 10.1177/38.9.1974900.

Deavall, D. G., Martin, E. A., Horner, J. M., and Roberts, R. (2012). "Drug-Induced Oxidative Stress and Toxicity". In: *Journal of Toxicology* 2012, pp. 1–13. DOI: 10.1155/2012/645460.

Dewaele, M., Maes, H., and Agostinis, P. (2010). "ROS-mediated mechanisms of autophagy stimulation and their relevance in cancer therapy". In: *Autophagy* 6.7, pp. 838–854. DOI: 10.4161/auto.6.7.12113.

Diehn, M., Cho, R. W., Lobo, N. A., Kalisky, T., Dorie, M. J., Kulp, A. N., Qian, D., Lam, J. S., Ailles, L. E., Wong, M., Joshua, B., Kaplan, M. J., Wapnir, I., Dirbas, F. M., Somlo, G., Garberoglio, C., Paz, B., Shen, J., Lau, S. K., Quake, S. R., Brown, J. M., Weissman, I. L., and Clarke, M. F. (2009). "Association of reactive oxygen species levels and radioresistance in cancer stem cells." In: *Nature* 458 (7239), pp. 780–783. DOI: 10.1038/nature07733.

DiProspero, L, Singh, G, Wilson, B. C., and Rainbow, A. J. (1997). "Cross-resistance to photofrin-mediated photodynamic therapy and UV light and recovery from photodynamic therapy damage in Rif-8A mouse fibrosarcoma cells measured using viral capacity." In: *Journal of Photochemistry and Photobiology. B, Biology* 38 (2-3), pp. 143–151. DOI: 10.1016/s1011-1344(96)07462-3.

Dolado, I., Swat, A., Ajenjo, N., De Vita, G., Cuadrado, A., and Nebreda, A. R. (2007). "p38alpha MAP kinase as a sensor of reactive oxygen species in tumorigenesis." In: *Cancer Cell* 11.2, pp. 191–205.

Dolmans, D. E., Fukumura, D., and Jain, R. K. (2003). "TIMELINE: Photodynamic therapy for cancer". In: *Nature Reviews. Cancer* 3.5, pp. 380–387. DOI: 10.1038/nrc1071.

Dorr, R. T. (1992). "Bleomycin pharmacology: mechanism of action and resistance, and clinical pharmacokinetics." In: *Seminars in Oncology* 19 (2 Suppl 5), pp. 3–8.

Dougherty, T. J., Kaufman, J. E., Goldfarb, A, Weishaupt, K. R., Boyle, D, and Mittleman, A (1978). "Photoradiation therapy for the treatment of malignant tumors." In: *Cancer Research* 38 (8), pp. 2628–2635.

Dougherty, T. J., Gomer, C. J., Henderson, B. W., Jori, G, Kessel, D, Korbelik, M, Moan, J, and Peng, Q (1998). "Photodynamic therapy." In: *Journal of the National Cancer Institute* 90 (12), pp. 889–905. DOI: 10.1093/jnci/90.12.889.

Dragu, D. L., Necula, L. G., Bleotu, C., Diaconu, C. C., and Chivu-Economescu, M. (2015). "Therapies targeting cancer stem cells: Current trends and future challenges." In: *World journal of stem cells* 7 (9), pp. 1185–1201. DOI: 10.4252/wjsc.v7.i9.1185.

Endo, Y, Tsurugi, K, and Lambert, J. M. (1988). "The site of action of six different ribosome-inactivating proteins from plants on eukaryotic ribosomes: the RNA N-glycosidase activity of the proteins." In: *Biochemical and Biophysical Research Communications* 150 (3), pp. 1032–1036. DOI: 10.1016/0006-291x(88)90733-4.

Feng, J.-M., Miao, Z.-H., Jiang, Y., Chen, Y., Li, J.-X., Tong, L.-J., Zhang, J., Huang, Y.-R., and Ding, J. (2012). "Characterization of the conversion between CD133+ and CD133- cells in colon cancer SW620 cell line." In: *Cancer biology & therapy* 13 (14), pp. 1396–1406. DOI: 10.4161/cbt.22000.

Fiechter, S., Skaria, A., Nievergelt, H., Anex, R., Borradori, L., and Parmentier, L. (2012). "Facial basal cell carcinomas recurring after photodynamic therapy: a retrospective analysis of histological subtypes." In: *Dermatology (Basel, Switzerland)* 224 (4), pp. 346–351. DOI: 10.1159/000339335.

Fletcher, J. I., Haber, M., Henderson, M. J., and Norris, M. D. (2010). "ABC transporters in cancer: more than just drug efflux pumps." In: *Nature Reviews. Cancer* 10 (2), pp. 147–156. DOI: 10.1038/nrc2789.

Freeman, S. A. and Grinstein, S. (2014). "Phagocytosis: receptors, signal integration, and the cytoskeleton". In: *Immunological Reviews* 262.1, pp. 193–215. DOI: 10.1111/imr.12212.

French, R. R., Penney, C. A., Browning, A. C., Stirpe, F, George, A. J., and Glennie, M. J. (1995). "Delivery of the ribosome-inactivating protein, gelonin, to lymphoma cells via CD22 and CD38 using bispecific antibodies." In: *British Journal of Cancer* 71 (5), pp. 986–994. DOI: 10.1038/bjc.1995.190.

Furre, I. E., Møller, M. T. N., Shahzidi, S., Nesland, J. M., and Peng, Q. (2006). "Involvement of both caspase-dependent and -independent pathways in apoptotic induction by hexaminolevulinate-mediated photodynamic therapy in human lymphoma cells." In: *Apoptosis : an international journal on programmed cell death* 11 (11), pp. 2031–2042. DOI: 10.1007/s10495-006-0190-x.

Gilaberte, Y., Milla, L., Salazar, N., Vera-Alvarez, J., Kourani, O., Damian, A., Rivarola, V., Roca, M. J., Espada, J., González, S., and Juarranz, A. (2014). "Cellular intrinsic factors involved in the resistance of squamous cell carcinoma to photodynamic therapy." In: *Journal of Investigative Dermatology* 134.9, pp. 2428–2437. DOI: 10.1038/jid.2014.178.

Girotti, A. W. (1998). "Lipid hydroperoxide generation, turnover, and effector action in biological systems." In: *Journal of Lipid Research* 39 (8), pp. 1529–1542.

Gobeil, S, Boucher, C. C., Nadeau, D, and Poirier, G. G. (2001). "Characterization of the necrotic cleavage of poly(ADP-ribose) polymerase (PARP-1): implication of lysosomal proteases." In: *Cell Death and Differentiation* 8 (6), pp. 588–594. DOI: 10.1038/sj.cdd.4400851.

Gocheva, V., Zeng, W., Ke, D., Klimstra, D., Reinheckel, T., Peters, C., Hanahan, D., and Joyce, J. A. (2006). "Distinct roles for cysteine cathepsin genes in multistage tumorigenesis." In: *Genes & development* 20 (5), pp. 543–556. DOI: 10.1101/gad.1407406.

Gottesman, M. M. (2002). "Mechanisms of cancer drug resistance." In: *Annual Review of Medicine* 53, pp. 615–627. DOI: 10.1146/annurev.med.53.082901.103929.

Gottesman, M. M., Ludwig, J., Xia, D., and Szakács, G. (2006). "Defeating drug resistance in cancer." In: *Discovery Medicine* 6 (31), pp. 18–23.

Grant, B. D. and Donaldson, J. G. (2009). "Pathways and mechanisms of endocytic recycling". In: *Nature Reviews. Molecular Cell Biology* 10.9, pp. 597–608. DOI: 10.1038/nrm2755.

Hamblin, M. and Mróz, P., eds. (2008). *Advances in Photodynamic Therapy: Basic, Translational, and Clinical*.

Hamblin, M. R. and Huang, Y. (2013). *Handbook of Photomedicine*. Ed. by M. R. Hamblin and Y. Huang. Taylor & Francis Inc. 886 pp. ISBN: 1439884692.

Hanahan, D. and Weinberg, R. A. (2000). "The Hallmarks of Cancer". In: *Cell* 100.1, pp. 57–70. DOI: 10.1016/s0092-8674(00)81683-9.

Hanahan, D. and Weinberg, R. A. (2011). "Hallmarks of Cancer: The Next Generation". In: *Cell* 144.5, pp. 646–674. DOI: 10.1016/j.cell.2011.02.013.

Harker, W. G. and Sikic, B. I. (1985). "Multidrug (pleiotropic) resistance in doxorubicin-selected variants of the human sarcoma cell line MES-SA." In: *Cancer Research* 45 (9), pp. 4091–4096.

Hartley, M. L., Bade, N. A., Prins, P. A., Ampie, L., and Marshall, J. L. (2015). "Pancreatic cancer, treatment options, and GI-4000." In: *Human vaccines & immunotherapeutics* 11 (4), pp. 931–937. DOI: 10.1080/21645515.2015.1011017.

Hassan, K. A., Wang, L., Korkaya, H., Chen, G., Maillard, I., Beer, D. G., Kalemkerian, G. P., and Wicha, M. S. (2013). "Notch pathway activity identifies cells with cancer stem cell-like properties and correlates with worse survival in lung adenocarcinoma." In: *Clinical cancer research : an official journal of the American Association for Cancer Research* 19 (8), pp. 1972–1980. DOI: 10.1158/1078-0432.CCR-12-0370.

Hermann, P. C., Huber, S. L., Herrler, T., Aicher, A., Ellwart, J. W., Guba, M., Bruns, C. J., and Heeschen, C. (2017). "Distinct populations of cancer stem cells determine tumor growth and metastatic activity in human pancreatic cancer." In: *Cell stem cell* 1 (3), pp. 313–323. DOI: 10.1016/j.stem.2007.06.002.

Hirsch, F. R., Varella-Garcia, M., Bunn, P. A., Di Maria, M. V., Veve, R., Bremmes, R. M., Barón, A. E., Zeng, C., and Franklin, W. A. (2003). "Epidermal growth factor receptor in non-small-cell lung carcinomas: correlation between gene copy number and protein expression and impact on prognosis." In: *Journal of clinical oncology : official journal of the American Society of Clinical Oncology* 21 (20), pp. 3798–3807. DOI: 10.1200/JCO.2003.11.069.

Håkerud, M., Selbo, P. K., Waeckerle-Men, Y., Contassot, E., Dziunycz, P., Kündig, T. M., Høgset, A., and Johansen, P. (2015). "Photosensitisation facilitates cross-priming of adjuvant-free protein vaccines and stimulation of tumour-suppressing CD8 T cells." In: *Journal of controlled release : official journal of the Controlled Release Society* 198, pp. 10–17. DOI: 10.1016/j.jconrel.2014.11.032.

Holohan, C., Van Schaeybroeck, S., Longley, D. B., and Johnston, P. G. (2013). "Cancer drug resistance: an evolving paradigm." In: *Nature Reviews. Cancer* 13.10, pp. 714–726. DOI: 10.1038/nrc3599.

Horst, D, Kriegl, L, Engel, J, Kirchner, T, and Jung, A (2008). "CD133 expression is an independent prognostic marker for low survival in colorectal cancer." In: *British Journal of Cancer* 99 (8), pp. 1285–1289. DOI: 10.1038/sj.bjc.6604664.

Housman, G., Byler, S., Heerboth, S., Lapinska, K., Longacre, M., Snyder, N., and Sarkar, S. (2014). "Drug resistance in cancer: an overview." In: *Cancers* 6 (3), pp. 1769–1792. DOI: 10.3390/cancers6031769.

Huang, F.-T., Zhuan-Sun, Y.-X., Zhuang, Y.-Y., Wei, S.-L., Tang, J., Chen, W.-B., and Zhang, S.-N. (2012). "Inhibition of hedgehog signaling depresses self-renewal of pancreatic cancer stem cells and reverses chemoresistance." In: *International Journal of Oncology* 41 (5), pp. 1707–1714. DOI: 10.3892/ijo.2012.1597.

Ichinose, S., Usuda, J., Hirata, T., Inoue, T., Ohtani, K., Maehara, S., Kubota, M., Imai, K., Tsunoda, Y., Kuroiwa, Y., Yamada, K., Tsutsui, H., Furukawa, K., Okunaka, T., Oleinick, N. L., and Kato, H. (2006). "Lysosomal cathepsin initiates apoptosis, which is regulated by photodamage to Bcl-2 at mitochondria in photodynamic therapy using a novel photosensitizer, ATX-s10 (Na)." In: *International Journal of Oncology* 29 (2), pp. 349–355. DOI: 10.3892/ijo.29.2.349.

Jeon, K. W., ed. (2012). *International Review of Cell and Molecular Biology*. Vol. 295. ACADEMIC PR INC. 348 pp. ISBN: 0123943086.

Jerome-Morais, A, Bera, S, Rachidi, W, Gann, P. H., and Diamond, A. M. (2013). "The effects of selenium and the GPx-1 selenoprotein on the phosphorylation of H2AX." In: *Biochimica et Biophysica Acta* 1830 (6), pp. 3399–3406. DOI: 10.1016/j.bbagen.2013.03.010.

Jonker, J. W., Buitelaar, M., Wagenaar, E., Van Der Valk, M. A., Scheffer, G. L., Scheper, R. J., Plosch, T., Kuipers, F., Elferink, R. P.J. O., Rosing, H., Beijnen, J. H., and Schinkel, A. H. (2002). "The breast cancer resistance protein protects against a major chlorophyll-derived dietary phototoxin and protoporphyria." In: *Proceedings of the National academy of Sciences of the United States of America* 99.24, pp. 15649–15654.

Juliano, R. L. and Ling, V (1976). "A surface glycoprotein modulating drug permeability in Chinese hamster ovary cell mutants." In: *Biochimica et Biophysica Acta* 455 (1), pp. 152–162. DOI: 10.1016/0005-2736(76)90160-7.

Kalinina, E. V., Chernov, N. N., Saprin, A. N., Kotova, Y. N., Andreev, Y. A., Solomka, V. S., and Scherbak, N. P. (2006). "Changes in expression of genes encoding antioxidant enzymes, heme oxygenase-1, Bcl-2, and Bcl-xl and in level of reactive oxygen species in tumor cells resistant to doxorubicin." In: *Biochemistry. Biokhimiia* 71 (11), pp. 1200–1206. DOI: 10.1134/s0006297906110058.

Kalyanaraman, B., Darley-Usmar, V., Davies, K. J., Dennery, P. A., Forman, H. J., Grisham, M. B., Mann, G. E., Moore, K., Roberts, L. J., and Ischiropoulos, H. (2012). "Measuring reactive oxygen and nitrogen species with fluorescent probes: challenges and limitations". In: *Free Radical Biology and Medicine* 52.1, pp. 1–6. DOI: 10.1016/j.freeradbiomed.2011.09.030.

Kascakova, S., Nadova, Z., Mateasik, A., Mikes, J., Huntosova, V., Refregiers, M., Sureau, F., Maurizot, J.-C., Miskovsky, P., and Jancura, D. (2008). "High level of low-density lipoprotein receptors enhance hypericin uptake by U-87 MG cells in the presence of LDL." In: *Photochemistry and Photobiology* 84 (1), pp. 120–127. DOI: 10.1111/j.1751-1097.2007.00207.x.

Kessel, D (1986). "Porphyrin-lipoprotein association as a factor in porphyrin localization." In: *Cancer Letters* 33 (2), pp. 183–188. DOI: 10.1016/0304-3835(86)90023-6.

Kessel, D and Erickson, C (1992). "Porphyrin photosensitization of multi-drug resistant cell types." In: *Photochemistry and Photobiology* 55 (3), pp. 397–399. DOI: 10.1111/j.1751-1097.1992.tb04253.x.

Kessel, D, Woodburn, K, and Skalkos, D (1994). "Impaired accumulation of a cationic photosensitizing agent by a cell line exhibiting multidrug resistance." In: *Photochemistry and Photobiology* 60 (1), pp. 61–63. DOI: 10.1111/j.1751-1097.1994.tb03943.x.

Kessel, D. and Reiners, J. J. (2007). "Apoptosis and autophagy after mitochondrial or endoplasmic reticulum photodamage." In: *Photochemistry and Photobiology* 83 (5), pp. 1024–1028. DOI: 10.1111/j.1751-1097.2007.00088.x.

Kessel, D. and Oleinick, N. L. (2010). "Photodynamic therapy and cell death pathways." In: *Methods in molecular biology (Clifton, N.J.)* 635, pp. 35–46. DOI: 10.1007/978-1-60761-697-9_3.

Klotz, L. O., Fritsch, C., Briviba, K., Tsacmacidis, N., Schliess, F., and Sies, H. (1998). "Activation of JNK and p38 but not ERK MAP kinases in human skin cells by 5-aminolevulinate-photodynamic therapy." In: *Cancer Research* 58.19, pp. 4297–4300.

Kobayashi, S., Boggon, T. J., Dayaram, T., Jänne, P. A., Kocher, O., Meyerson, M., Johnson, B. E., Eck, M. J., Tenen, D. G., and Halmos, B. (2005). "EGFR mutation and resistance of non-small-cell lung cancer to gefitinib." In: *The New England journal of medicine* 352 (8), pp. 786–792. DOI: 10.1056/NEJMoa044238.

Larsen, A. K., Escargueil, A. E., and Skladanowski, A (2000). "Resistance mechanisms associated with altered intracellular distribution of anticancer agents." In: *Pharmacology & therapeutics* 85 (3), pp. 217–229. DOI: 10.1016/s0163-7258(99)00073-x.

Li, H., Gao, Q., Guo, L., and Lu, S. H. (2011). "The PTEN/PI3K/Akt pathway regulates stem-like cells in primary esophageal carcinoma cells." In: *Cancer biology & therapy* 11 (11), pp. 950–958. DOI: 10.4161/cbt.11.11.15531.

Li, S. and Li, Q. (2014). "Cancer stem cells and tumor metastasis (Review)." In: *International Journal of Oncology* 44 (6), pp. 1806–1812. DOI: 10.3892/ijo.2014.2362.

Liang, H., Ran, Q., Jang, Y. C., Holstein, D., Lechleiter, J., McDonald-Marsh, T., Musatov, A., Song, W., Van Remmen, H., and Richardson, A. (2009). "Glutathione peroxidase 4 differentially regulates the release of apoptogenic proteins from mitochondria." In: *Free radical biology & medicine* 47 (3), pp. 312–320. DOI: 10.1016/j.freeradbiomed.2009.05.012.

Lilletvedt, M, Tønnesen, H. H., Høgset, A, Sande, S. A., and Kristensen, S (2011). "Evaluation of physicochemical properties and aggregation of the photosensitizers TPCS2a and TPPS2a in aqueous media." In: *Die Pharmazie* 66 (5), pp. 325–333.

Lim, J. P. and Gleeson, P. A. (2011). "Macropinocytosis: an endocytic pathway for internalising large gulps". In: *Immunology and Cell Biology* 89.8, pp. 836–843. DOI: 10.1038/icb.2011.20.

Liu, T. J., Sun, B. C., Zhao, X. L., Zhao, X. M., Sun, T, Gu, Q, Yao, Z, Dong, X. Y., Zhao, N, and Liu, N (2012). "CD133+ cells with cancer stem cell characteristics associates with vasculogenic mimicry in triple-negative breast cancer". In: *Oncogene* 32.5, pp. 544–553. DOI: 10.1038/onc.2012.85.

Lou, P.-J., Lai, P.-S., Shieh, M.-J., Macrobert, A. J., Berg, K., and Bown, S. G. (2006). "Reversal of doxorubicin resistance in breast cancer cells by photochemical internalization." In: *International Journal of Cancer* 119 (11), pp. 2692–2698. DOI: 10.1002/ijc.22098.

Luna, M. C. and Gomer, C. J. (1991). "Isolation and initial characterization of mouse tumor cells resistant to porphyrin-mediated photodynamic therapy." In: *Cancer Research* 51.16, pp. 4243–4249.

Lund, K., Bostad, M., Skarpen, E., Braunagel, M., Kiprijanov, S., Krauss, S., Duncan, A., Høgset, A., and Selbo, P. K. (2014). "The novel EpCAM-targeting monoclonal antibody 3-17I linked to saporin is highly cytotoxic after photochemical internalization in breast, pancreas and colon cancer cell lines". In: *mAbs* 6.4, pp. 1038–1050. DOI: 10.4161/mabs.28207.

Lund, K., Dembinski, J. L., Solberg, N., Urbanucci, A., Mills, I. G., and Krauss, S. (2015). "Slug-dependent upregulation of L1CAM is responsible for the increased invasion potential of pancreatic cancer cells following long-term 5-FU treatment." In: *PLOS ONE* 10 (4), e0123684. DOI: 10.1371/journal.pone.0123684.

Lynch, T. J., Bell, D. W., Sordella, R., Gurubhagavatula, S., Okimoto, R. A., Brannigan, B. W., Harris, P. L., Haserlat, S. M., Supko, J. G., Haluska, F. G., Louis, D. N., Christiani, D. C., Settleman, J., and Haber, D. A. (2004). "Activating mutations in the epidermal growth factor receptor underlying responsiveness of non-small-cell lung cancer to gefitinib." In: *The New England journal of medicine* 350 (21), pp. 2129–2139. DOI: 10.1056/NEJMoa040938.

Lyu, M.-A., Cao, Y. J., Mohamedali, K. A., and Rosenblum, M. G. (2012). "Cell-targeting fusion constructs containing recombinant gelonin." In: *Methods in Enzymology* 502, pp. 167–214. DOI: 10.1016/B978-0-12-416039-2.00008-2.

Mao, Q. and Unadkat, J. D. (2015). "Role of the breast cancer resistance protein (BCRP/ABCG2) in drug transport–an update." In: *The AAPS journal* 17 (1), pp. 65–82. DOI: 10.1208/s12248-014-9668-6.

Maxfield, F. R. and McGraw, T. E. (2004). "Endocytic recycling". In: *Nature Reviews. Molecular Cell Biology* 5.2, pp. 121–132. DOI: 10.1038/nrm1315.

Maydan, E., Nootheti, P. K., and Goldman, M. P. (2006). "Development of a keratoacanthoma after topical photodynamic therapy with 5-aminolevulinic acid." In: *Journal of Drugs in Dermatology* 5.8, pp. 804–806.

Mayhew, S, Vernon, D. I., Schofield, J, Griffiths, J, and Brown, S. B. (2001). "Investigation of cross-resistance to a range of photosensitizers, hyperthermia and UV light in two radiation-induced fibrosarcoma cell strains resistant to photodynamic therapy in vitro." In: *Photochemistry and Photobiology* 73 (1), pp. 39–46. DOI: 10.1562/0031-8655(2001)073<0039:iocrta>2.0.co;2.

McMahon, H. T. and Boucrot, E. (2011). "Molecular mechanism and physiological functions of clathrin-mediated endocytosis". In: *Nature Reviews. Molecular Cell Biology* 12.8, pp. 517–533. DOI: 10.1038/nrm3151.

Mellman, I, Fuchs, R, and Helenius, A (1986). "Acidification of the endocytic and exocytic pathways." In: *Annual Review of Biochemistry* 55, pp. 663–700. DOI: 10.1146/annurev.bi.55.070186.003311.

Miranda, S. G., Wang, Y. J., Purdie, N. G., Osborne, V. R., Coomber, B. L., and Cant, J. P. (2009). "Selenomethionine stimulates expression of glutathione peroxidase 1 and 3 and growth of bovine mammary epithelial cells in primary culture." In: *Journal of Dairy Science* 92 (6), pp. 2670–2683. DOI: 10.3168/jds.2008-1901.

Mitra, D., Brumlik, M. J., Okamgba, S. U., Zhu, Y., Duplessis, T. T., Parvani, J. G., Lesko, S. M., Brogi, E., and Jones, F. E. (2009). "An oncogenic isoform of HER2 associated with locally disseminated breast cancer and trastuzumab resistance". In: *Molecular Cancer Therapeutics* 8.8, pp. 2152–2162. DOI: 10.1158/1535-7163.mct-09-0295.

Moan, J and Berg, K (1991). "The photodegradation of porphyrins in cells can be used to estimate the lifetime of singlet oxygen." In: *Photochemistry and Photobiology* 53 (4), pp. 549–553. DOI: 10.1111/j.1751-1097.1991.tb03669.x.

Moan, J. and Peng, Q. (2003). "An outline of the hundred-year history of PDT." In: *Anticancer Research* 23 (5A), pp. 3591–3600.

Moor, A. C. (2000). "Signaling pathways in cell death and survival after photodynamic therapy." In: *Journal of Photochemistry and Photobiology. B, Biology* 57.1, pp. 1–13. DOI: 10.1016/s1011-1344(00)00065-8.

Morgan, J., Jackson, J. D., Zheng, X., Pandey, S. K., and Pandey, R. K. (2010). "Substrate affinity of photosensitizers derived from chlorophyll-a: the ABCG2 transporter affects the phototoxic response of side population stem cell-like cancer cells to photodynamic therapy." In: *Mol Pharm* 7.5, pp. 1789–1804. DOI: 10.1021/mp100154j.

Mroz, P., Hashmi, J. T., Huang, Y.-Y., Lange, N., and Hamblin, M. R. (2011). "Stimulation of anti-tumor immunity by photodynamic therapy." In: *Expert review of clinical immunology* 7 (1), pp. 75–91. DOI: 10.1586/eci.10.81.

Nilsson, E, Ghassemifar, R, and Brunk, U. T. (1997). "Lysosomal heterogeneity between and within cells with respect to resistance against oxidative stress." In: *The Histochemical journal* 29 (11-12), pp. 857–865.

Nissen, C. V., Heerfordt, I. M., Wiegell, S. R., Mikkelsen, C. S., and Wulf, H. C. (2017). "Pretreatment with 5-Fluorouracil Cream Enhances the Efficacy of Daylight-mediated Photodynamic Therapy for Actinic Keratosis." In: *Acta Dermato-Venereologica*. DOI: 10.2340/00015555-2612.

Norum, O.-J., Selbo, P. K., Weyergang, A., Giercksky, K.-E., and Berg, K. (2009). "Photochemical internalization (PCI) in cancer therapy: From bench towards bedside medicine". In: *Journal of Photochemistry and Photobiology, B: Biology* 96.2, pp. 83–92. DOI: 10.1016/j.jphotobiol.2009.04.012.

Okamoto, S, Yoshikawa, K, Obata, Y, Shibuya, M, Aoki, S, Yoshida, J, and Takahashi, T (1996). "Monoclonal antibody against the fusion junction of a deletion-mutant epidermal growth factor receptor." In: *British Journal of Cancer* 73 (11), pp. 1366–1372. DOI: 10.1038/bjc.1996.260.

Olsen, C. E., Berg, K., Selbo, P. K., and Weyergang, A. (2013). "Circumvention of resistance to photodynamic therapy in doxorubicin-resistant sarcoma by photochemical internalization of gelonin." In: *Free Radical Biology and Medicine* 65, pp. 1300–1309. DOI: 10.1016/j.freeradbiomed.2013.09.010.

Otterhaug, T., Haug, M., Brede, G., Håkerud, M., Nedberg, A. G., Edwards, V., Selbo, P. K., Johansen, P., Halaas, Ø., and Høgset, A. (2016). "Abstract A008: Photochemical internalization: Light-induced enhancement of MHC Class I antigen presentation, giving strong enhancement of cytotoxic T-cell responses to vaccination". In: *Cancer Immunology Research* 4.11 Supplement, A008–A008. DOI: 10.1158/2326-6066.imm2016-a008.

Pagliaro, L. C., Liu, B, Munker, R, Andreeff, M, Freireich, E. J., Scheinberg, D. A., and Rosenblum, M. G. (1998). "Humanized M195 monoclonal antibody conjugated to recombinant gelonin: an anti-CD33 immunotoxin with antileukemic activity." In: *Clinical cancer research : an official journal of the American Association for Cancer Research* 4 (8), pp. 1971–1976.

Pai, V., Pandey, P., DiGiovine, B., and Iannuzzi, M. (2003). "Severe vascular leak syndrome from denileukin diftitox presenting as acute respiratory distress syndrome (ards)". In: *Chest* 124.4_MeetingAbstracts, 253S–253S. DOI: 10.1378/chest.124.4_MeetingAbstracts.253S.

Parton, R. G. and Pozo, M. A. del (2013). "Caveolae as plasma membrane sensors, protectors and organizers". In: *Nature Reviews. Molecular Cell Biology* 14.2, pp. 98–112. DOI: 10.1038/nrm3512.

Pastan, I. and Willingham, M. C. (1983). "Receptor-mediated endocytosis: coated pits, receptosomes and the Golgi". In: *Trends in Biochemical Sciences* 8.7, pp. 250–254. DOI: 10.1016/0968-0004(83)90351-1.

Piao, S. and Amaravadi, R. K. (2015). "Targeting the lysosome in cancer". In: *Annals of the New York Academy of Sciences* 1371.1, pp. 45–54. DOI: 10.1111/nyas.12953.

Piette, J., Volanti, C., Vantieghem, A., Matroule, J.-Y., Habraken, Y., and Agostinis, P. (2003). "Cell death and growth arrest in response to photodynamic therapy with membrane-bound photosensitizers." In: *Biochemical Pharmacology* 66.8, pp. 1651–1659. DOI: 10.1016/s0006-2952(03)00539-2.

Pinedo, H. M. (2007). *Drug Resistance in the Treatment of Cancer*. CAMBRIDGE UNIVERSITY PRESS. ISBN: 0521030749.

Polito, L., Bortolotti, M., Mercatelli, D., Battelli, M., and Bolognesi, A. (2013). "Saporin-S6: A Useful Tool in Cancer Therapy". In: *Toxins* 5.10, pp. 1698–1722. DOI: 10.3390/toxins5101698.

Rapozzi, V. and Jori, G., eds. (2015). *Resistance to Photodynamic Therapy in Cancer*. Springer-Verlag GmbH. ISBN: 3319127292.

Rappa, G., Fargeas, C. A., Le, T. T., Corbeil, D., and Lorico, A. (2015). "Letter to the Editor: An Intriguing Relationship Between Lipid Droplets, Cholesterol-Binding Protein CD133 and Wnt/β-Catenin Signaling Pathway in Carcinogenesis". In: *STEM CELLS* 33.4, pp. 1366–1370. DOI: 10.1002/stem.1953.

Reiners, J. J., Caruso, J. A., Mathieu, P, Chelladurai, B, Yin, X.-M., and Kessel, D (2002). "Release of cytochrome c and activation of pro-caspase-9 following lysosomal photodamage involves Bid cleavage." In: *Cell Death and Differentiation* 9 (9), pp. 934–944. DOI: 10.1038/sj.cdd.4401048.

Rennen, H. J., Makarewicz, J., Oyen, W. J., Laverman, P., Corstens, F. H., and Boerman, O. C. (2001). "The effect of molecular weight on nonspecific accumulation of 99mT-labeled proteins in inflammatory foci". In: *Nuclear Medicine and Biology* 28.4, pp. 401–408. DOI: 10.1016/s0969-8051(01)00208-6.

Ricci-Vitiani, L., Lombardi, D. G., Pilozzi, E., Biffoni, M., Todaro, M., Peschle, C., and De Maria, R. (2007). "Identification and expansion of human colon-cancer-initiating cells." In: *Nature* 445 (7123), pp. 111–115. DOI: 10.1038/nature05384.

Rimawi, M. F., Shetty, P. B., Weiss, H. L., Schiff, R., Osborne, C. K., Chamness, G. C., and Elledge, R. M. (2010). "Epidermal growth factor receptor expression in breast cancer association with biologic phenotype and clinical outcomes." In: *Cancer* 116 (5), pp. 1234–1242. DOI: 10.1002/cncr.24816.

Robey, R. W., Steadman, K., Polgar, O., and Bates, S. E. (2005). "ABCG2-mediated transport of photosensitizers: potential impact on photodynamic therapy." In: *Cancer Biology and Therapy* 4.2, pp. 187–194. DOI: 10.4161/cbt.4.2.1440.

Rodal, G. H., Rodal, S. K., Moan, J, and Berg, K (1998). "Liposome-bound Zn (II)-phthalocyanine. Mechanisms for cellular uptake and photosensitization." In: *Journal of Photochemistry and Photobiology. B, Biology* 45 (2-3), pp. 150–159. DOI: 10.1016/s1011-1344(98)00175-4.

Rosenblum, M. G., Kohr, W. A., Beattie, K. L., Beattie, W. G., Marks, W, Toman, P. D., and Cheung, L (1995). "Amino acid sequence analysis, gene construction, cloning, and expression of gelonin, a toxin derived from Gelonium multiflorum." In: *Journal of interferon & cytokine research : the official journal of the International Society for Interferon and Cytokine Research* 15 (6), pp. 547–555. DOI: 10.1089/jir.1995.15.547.

Sanlorenzo, M., Vujic, I., Posch, C., Dajee, A., Yen, A., Kim, S., Ashworth, M., Rosenblum, M. D., Algazi, A., Osella-Abate, S., Quaglino, P., Daud, A., and Ortiz-Urda, S. (2014). "Melanoma immunotherapy." In: *Cancer biology & therapy* 15 (6), pp. 665–674. DOI: 10.4161/cbt.28555.

Scheinberg, D. A. and Jurcic, J. G., eds. (2004). *Treatment of Leukemia and Lymphoma*. Vol. 51. ISBN: 0-12-032952-2.

Schinkel, A. H. and Jonker, J. W. (2003). "Mammalian drug efflux transporters of the ATP binding cassette (ABC) family: an overview." In: *Advanced Drug Delivery Reviews* 55 (1), pp. 3–29. DOI: 10.1016/s0169-409x(02)00169-2.

Schmohl, J. U., Felices, M., Todhunter, D., Taras, E., Miller, J. S., and Vallera, D. A. (2016). "Tetraspecific scFv construct provides NK cell mediated ADCC and self-sustaining stimuli via insertion of IL-15 as a cross-linker." In: *Oncotarget* 7 (45), pp. 73830–73844. DOI: 10.18632/oncotarget.12073.

Schulenburg, A., Ulrich-Pur, H., Thurnher, D., Erovic, B., Florian, S., Sperr, W. R., Kalhs, P., Marian, B., Wrba, F., Zielinski, C. C., and Valent, P. (2006). "Neoplastic stem cells: a novel therapeutic target in clinical oncology." In: *Cancer* 107 (10), pp. 2512–2520. DOI: 10.1002/cncr.22277.

Selbo, P. K., Sandvig, K, Kirveliene, V, and Berg, K (2000). "Release of gelonin from endosomes and lysosomes to cytosol by photochemical internalization." In: *Biochimica et Biophysica Acta* 1475 (3), pp. 307–313. DOI: 10.1016/s0304-4165(00)00082-9.

Selbo, P. K., Sivam, G, Fodstad, O, Sandvig, K, and Berg, K (2001). "In vivo documentation of photochemical internalization, a novel approach to site specific cancer therapy." In: *International Journal of Cancer* 92 (5), pp. 761–766. DOI: 10.1002/1097-0215(20010601)92:5<761::aid-ijc1238>3.0.co;2-4.

Selbo, P. K., Weyergang, A., Bonsted, A., Bown, S. G., and Berg, K. (2006). "Photochemical internalization of therapeutic macromolecular agents: a novel strategy to kill

multidrug-resistant cancer cells." In: *Journal of Pharmacology and Experimental Therapeutics* 319.2, pp. 604–612.

Selbo, P. K., Weyergang, A., Høgset, A., Norum, O.-J., Berstad, M. B., Vikdal, M., and Berg, K. (2010). "Photochemical internalization provides time- and space-controlled endolysosomal escape of therapeutic molecules." In: *Journal of Controlled Release* 148.1, pp. 2–12. DOI: 10.1016/j.jconrel.2010.06.008.

Selbo, P. K., Weyergang, A., Eng, M. S., Bostad, M., Mælandsmo, G. M., Høgset, A., and Berg, K. (2012). "Strongly amphiphilic photosensitizers are not substrates of the cancer stem cell marker ABCG2 and provides specific and efficient light-triggered drug delivery of an EGFR-targeted cytotoxic drug." In: *Journal of Controlled Release* 159.2, pp. 197–203. DOI: 10.1016/j.jconrel.2012.02.003.

Selbo, P. K., Bostad, M., Olsen, C. E., Edwards, V. T., Høgset, A., Weyergang, A., and Berg, K. (2015). "Photochemical internalisation, a minimally invasive strategy for light-controlled endosomal escape of cancer stem cell-targeting therapeutics". In: *Photochem. Photobiol. Sci*. DOI: 10.1039/c5pp00027k.

Settembre, C., Fraldi, A., Medina, D. L., and Ballabio, A. (2013). "Signals from the lysosome: a control centre for cellular clearance and energy metabolism". In: *Nature Reviews. Molecular Cell Biology* 14.5, pp. 283–296. DOI: 10.1038/nrm3565.

Shan, L., Liu, Y., and Wang, P. (2013). "Recombinant Immunotoxin Therapy of Solid Tumors: Challenges and Strategies." In: *Journal of basic and clinical medicine* 2 (2), pp. 1–6.

Sharma, S. V., Lee, D. Y., Li, B., Quinlan, M. P., Takahashi, F., Maheswaran, S., McDermott, U., Azizian, N., Zou, L., Fischbach, M. A., Wong, K.-K., Brandstetter, K., Wittner, B., Ramaswamy, S., Classon, M., and Settleman, J. (2010). "A Chromatin-Mediated Reversible Drug-Tolerant State in Cancer Cell Subpopulations". In: *Cell* 141.1, pp. 69–80. DOI: 10.1016/j.cell.2010.02.027.

Sharom, F. J. (2008). "ABC multidrug transporters: structure, function and role in chemoresistance." In: *Pharmacogenomics* 9 (1), pp. 105–127. DOI: 10.2217/14622416.9.1.105.

— (2011). "The P-glycoprotein multidrug transporter." In: *Essays in Biochemistry* 50 (1), pp. 161–178. DOI: 10.1042/bse0500161.

Singh, G, Wilson, B. C., Sharkey, S. M., Browman, G. P., and Deschamps, P (1991). "Resistance to photodynamic therapy in radiation induced fibrosarcoma-1 and Chinese hamster ovary-multi-drug resistant. Cells in vitro." In: *Photochemistry and Photobiology* 54 (2), pp. 307–312. DOI: 10.1111/j.1751-1097.1991.tb02021.x.

Singh, G., Espiritu, M., Shen, X. Y., Hanlon, J. G., and Rainbow, A. J. (2001). "In vitro induction of PDT resistance in HT29, HT1376 and SK-N-MC cells by various photosensitizers." In: *Photochemistry and Photobiology* 73.6, pp. 651–656. DOI: 10.1562/0031-8655(2001)0730651iviopr2.0.co2.

Singh, S. K., Clarke, I. D., Terasaki, M., Bonn, V. E., Hawkins, C., Squire, J., and Dirks, P. B. (2003). "Identification of a cancer stem cell in human brain tumors." In: *Cancer Research* 63 (18), pp. 5821–5828.

Skovsen, E., Snyder, J. W., Lambert, J. D. C., and Ogilby, P. R. (2005). "Lifetime and Diffusion of Singlet Oxygen in a Cell". In: *The Journal of Physical Chemistry B* 109.18, pp. 8570–8573. DOI: 10.1021/jp051163i.

Snook, A. E. and Waldman, S. A. (2013). "Advances in cancer immunotherapy." In: *Discovery Medicine* 15 (81), pp. 120–125.

Sok, J. C., Coppelli, F. M., Thomas, S. M., Lango, M. N., Xi, S., Hunt, J. L., Freilino, M. L., Graner, M. W., Wikstrand, C. J., Bigner, D. D., Gooding, W. E., Furnari, F. B.,

and Grandis, J. R. (2006). "Mutant epidermal growth factor receptor (EGFRvIII) contributes to head and neck cancer growth and resistance to EGFR targeting." In: *Clinical cancer research : an official journal of the American Association for Cancer Research* 12 (17), pp. 5064–5073. DOI: 10.1158/1078-0432.CCR-06-0913.

Stratford, E. W., Bostad, M., Castro, R., Skarpen, E., Berg, K., Høgset, A., Myklebost, O., and Selbo, P. K. (2013). "Photochemical internalization of CD133-targeting immunotoxins efficiently depletes sarcoma cells with stem-like properties and reduces tumorigenicity". In: *Biochimica et Biophysica Acta (BBA) - General Subjects* 1830.8, pp. 4235–4243. DOI: 10.1016/j.bbagen.2013.04.033.

Sultan, A. A., Jerjes, W., Berg, K., Høgset, A., Mosse, C. A., Hamoudi, R., Hamdoon, Z., Simeon, C., Carnell, D., Forster, M., and Hopper, C. (2016). "Disulfonated tetraphenyl chlorin (TPCS2a)-induced photochemical internalisation of bleomycin in patients with solid malignancies: a phase 1, dose-escalation, first-in-man trial." In: *The Lancet. Oncology* 17 (9), pp. 1217–1229. DOI: 10.1016/S1470-2045(16)30224-8.

Teiten, M. H., Bezdetnaya, L, Merlin, J. L., Bour-Dill, C, Pauly, M. E., Dicato, M, and Guillemin, F (2001). "Effect of meta-tetra(hydroxyphenyl)chlorin (mTHPC)-mediated photodynamic therapy on sensitive and multidrug-resistant human breast cancer cells." In: *Journal of Photochemistry and Photobiology. B, Biology* 62 (3), pp. 146–152. DOI: 10.1016/s1011-1344(01)00178-6.

Theodossiou, T. A., Olsen, C. E., Jonsson, M., Kubin, A., Hothersall, J. S., and Berg, K. (2017). "The diverse roles of glutathione-associated cell resistance against hypericin photodynamic therapy". In: *Redox Biology* 12, pp. 191–197. DOI: 10.1016/j.redox.2017.02.018.

Tong, Z., Singh, G., and Rainbow, A. J. (2002). "Sustained activation of the extracellular signal-regulated kinase pathway protects cells from photofrin-mediated photodynamic therapy." In: *Cancer Research* 62.19, pp. 5528–5535.

Trachootham, D., Alexandre, J., and Huang, P. (2009). "Targeting cancer cells by ROS-mediated mechanisms: a radical therapeutic approach?" In: *Nature Reviews. Drug Discovery* 8 (7), pp. 579–591. DOI: 10.1038/nrd2803.

Trigueros-Motos, L., Pérez-Torras, S., Casado, F. J., Molina-Arcas, M., and Pastor-Anglada, M. (2012). "Aquaporin 3 (AQP3) participates in the cytotoxic response to nucleoside-derived drugs". In: *BMC Cancer* 12.1. DOI: 10.1186/1471-2407-12-434.

Tsai, T., Ji, H. T., Chiang, P.-C., Chou, R.-H., Chang, W.-S. W., and Chen, C.-T. (2009). "ALA-PDT results in phenotypic changes and decreased cellular invasion in surviving cancer cells." In: *Lasers in Surgery and Medicine* 41 (4), pp. 305–315. DOI: 10.1002/lsm.20761.

Varma, S., Holt, P. J., and Anstey, A. V. (2000). "Erythroplasia of queyrat treated by topical aminolaevulinic acid photodynamic therapy: a cautionary tale." In: *British Journal of Dermatology* 142.4, pp. 825–826. DOI: 10.1046/j.1365-2133.2000.03441.x.

Vikdal, M., Weyergang, A., Selbo, P. K., and Berg, K. (2013). "Vascular endothelial cells as targets for photochemical internalization (PCI)." In: *Photochemistry and Photobiology* 89 (5), pp. 1185–1192. DOI: 10.1111/php.12126.

von Tappeiner, H.A. J. (1904). "Über die Wirkung der photodynamischen (fluorescierenden) Stoffe auf Protozoen und Enzyme". In: *Deutsches Archiv für klinische Medizin* 80, 427–487.

Walsh, M. J., Dodd, J. E., and Hautbergue, G. M. (2013). "Ribosome-inactivating proteins: potent poisons and molecular tools." In: *Virulence* 4 (8), pp. 774–784. DOI: 10.4161/viru.26399.

Wang, D., Guo, Y., Li, Y., Li, W., Zheng, X., Xia, H., and Mao, Q. (2015). "Detection of CD133 expression in U87 glioblastoma cells using a novel anti-CD133 monoclonal antibody". In: *Oncology Letters*. DOI: 10.3892/ol.2015.3079.

Wang, H., Li, L., Wang, P., Wang, X., Zhang, K., and Liu, Q. (2016). "Comparison of photodynamic treatment produced cell damage between human breast cancer cell MCF-7 and its multidrug resistance cell." In: *Photodiagnosis and Photodynamic Therapy* 16, pp. 1–8. DOI: 10.1016/j.pdpdt.2016.07.004.

Wesolowska, O., Paprocka, M., Kozlak, J., Motohashi, N., Dus, D., and Michalak, K. (2005). "Human sarcoma cell lines MES-SA and MES-SA/Dx5 as a model for multidrug resistance modulators screening." In: *Anticancer Research* 25.1A, pp. 383–389.

Weyergang, A., Selbo, P. K., and Berg, K. (2006). "Photochemically stimulated drug delivery increases the cytotoxicity and specificity of EGF-saporin." In: *Journal of Controlled Release* 111.1-2, pp. 165–173. DOI: 10.1016/j.jconrel.2005.12.002.

Weyergang, A., Selbo, P. K., and Berg, K. (2007). "Y1068 phosphorylation is the most sensitive target of disulfonated tetraphenylporphyrin-based photodynamic therapy on epidermal growth factor receptor". In: *Biochemical Pharmacology* 74.2, pp. 226–235. DOI: 10.1016/j.bcp.2007.04.018.

Weyergang, A., Kaalhus, O., and Berg, K. (2008a). "Photodynamic targeting of EGFR does not predict the treatment outcome in combination with the EGFR tyrosine kinase inhibitor Tyrphostin AG1478." In: *Photochemistry & Photobiological Sciences* 7.9, pp. 1032–1040. DOI: 10.1039/b806209a.

— (2008b). "Photodynamic therapy with an endocytically located photosensitizer cause a rapid activation of the mitogen-activated protein kinases extracellular signal-regulated kinase, p38, and c-Jun NH2 terminal kinase with opposing effects on cell survival." In: *Molecular Cancer Therapeutics* 7.6, pp. 1740–1750. DOI: 10.1158/1535-7163.mct-08-0020.

Weyergang, A., Cheung, L. H., Rosenblum, M. G., Mohamedali, K. A., Peng, Q., Waltenberger, J., and Berg, K. (2014). "Photochemical internalization augments tumor vascular cytotoxicity and specificity of VEGF121/rGel fusion toxin". In: *Journal of Controlled Release* 180, pp. 1–9. DOI: 10.1016/j.jconrel.2014.02.003.

Weyergang, A., Berstad, M. E. B., Bull-Hansen, B., Olsen, C. E., Selbo, P. K., and Berg, K. (2015). "Photochemical activation of drugs for the treatment of therapy-resistant cancers." In: *Photochemistry & Photobiological Sciences* 14.8, pp. 1465–1475. DOI: 10.1039/c5pp00029g.

WHO. *WHO, Cancer Fact sheet, February 2017*. URL: http://www.who.int/mediacentre/factsheets/fs297/en/.

Wiley, H. S. (2003). "Trafficking of the ErbB receptors and its influence on signaling." In: *Experimental Cell Research* 284 (1), pp. 78–88. DOI: 10.1016/b978-012160281-9/50007-4.

Wolf, P., Fink-Puches, R., Reimann-Weber, A., and Kerl, H. (1997). "Development of malignant melanoma after repeated topical photodynamic therapy with 5-aminolevulinic acid at the exposed site." In: *Dermatology* 194.1, pp. 53–54. DOI: 10.1159/000246057.

Wood, S. R., Holroyd, J. A., and Brown, S. B. (1997). "The subcellular localization of Zn(II) phthalocyanines and their redistribution on exposure to light." In: *Photochemistry and Photobiology* 65.3, pp. 397–402. DOI: 10.1111/j.1751-1097.1997.tb08577.x.

Zamarrón, A., Lucena, S. R., Salazar, N., Sanz-Rodríguez, F., Jaén, P., Gilaberte, Y., González, S., and Juarranz, n. (2015). "Isolation and characterization of PDT-resistant cancer

cells." In: *Photochemical & photobiological sciences : Official journal of the European Photochemistry Association and the European Society for Photobiology* 14 (8), pp. 1378–1389. DOI: 10.1039/c4pp00448e.

Zhou, J., Zhang, H., Gu, P., Bai, J., Margolick, J. B., and Zhang, Y. (2008). "NF-kappaB pathway inhibitors preferentially inhibit breast cancer stem-like cells." In: *Breast Cancer Research and Treatment* 111 (3), pp. 419–427. DOI: 10.1007/s10549-007-9798-y.

Zilfou, J. T. and Smith, C. D. (1995). "Differential interactions of cytochalasins with P-glycoprotein." In: *Oncology Research* 7 (9), pp. 435–443.

Research Papers

Paper I

Development of resistance to photodynamic therapy (PDT) in human breast cancer cells is photosensitizer-dependent: Possible mechanisms and approaches for overcoming PDT-resistance

Cathrine Elisabeth Olsen [a], Anette Weyergang [a], Victoria Tudor Edwards [a,b], Kristian Berg [a], Andreas Brech [c], Sabine Weisheit [c], Anders Høgset [b], Pål Kristian Selbo [a,*]

[a] Department of Radiation Biology, Institute for Cancer Research, Oslo University Hospital - Radiumhospitalet, Montebello, N-0379 Oslo, Norway.

[b] PCI Biotech, Ullernchauséen 64, N-0379 Oslo, Norway.

[c] Department of Molecular Cell Biology, Institute for Cancer Research, Oslo University Hospital - Radiumhospitalet, Montebello, N-0379 Oslo, Norway.

[*] Corresponding author E-mail: selbo@rr-research.no)

Abstract

Here we report on the induction of resistance to photodynamic therapy (PDT) in the ABCG2-high human breast cancer cell line MA11 after repetitive PDT, using either Pheophorbide A (PhA) or di-sulphonated meso-tetraphenylchlorin ($TPCS_{2a}$) as photosensitizer. Resistance to PhA-PDT was associated with enhanced expression of the efflux pump ABCG2. $TPCS_{2a}$-PDT-resistance was neither found to correspond with lower $TPCS_{2a}$-accumulation nor reduced generation of reactive oxygen species (ROS). Cross-resistance to chemotherapy (doxorubicin) or radiotherapy was not observed. $TPCS_{2a}$-PDT-resistant cells acquired a higher proliferation capacity and an enhanced expression of EGFR and ERK1/2. Activation of p38 MAPK was found to be a death-signal in the MA11 cells post $TPCS_{2a}$-PDT, contrasting the MA11/TR cells in which PDT generated a sustained phosphorylation of p38 that had lost its death-mediated signalling, and an abrogated activation of its downstream effector MAPKAPK2 (MK-2). No difference in apoptosis, necrosis or autophagy responses was found between the treated cell lines. Development of $TPCS_{2a}$-PDT resistance in the MDA-MB-231 cell line was also established, however, p38 MAPK did not play a role in the PDT-resistance. MCF-7 cells did not develop $TPCS_{2a}$-PDT-resistance. Photochemical internalisation (PCI) of 1 pM of EGF-saporin induced equal strong cytotoxicity in both MA11 and MA11/TR cells. In conclusion, loss of p38 MAPK-inducing death signalling is the main mechanism of resistance to $TPCS_{2a}$-PDT in the MA11/TR cell line. This work provides mechanistic knowledge of intrinsic and acquired PDT-resistance which is dependent on choice of photosensitizer, and suggests PCI as a rational therapeutic intervention for the elimination of PDT-resistant cells.

Keywords: Resistance, Reactive oxygen species, Breast cancer, Immunotoxin, Photodynamic

therapy, Photochemical internalization

Compounds: Fimaporfin (CID: 73211805 and 73211806); Pheophorbide A (CID: 5323510); LysoTracker Green (CID: 15410444); 2',7'-Dichlorofluorescin diacetate (CID: 24894058); Doxorubicin hydrochloride (CID: 24893465); SB 203580 (CID: 24899788)

1. Introduction

Intrinsic or acquired resistance to cancer therapies, including photodynamic therapy (PDT), is a major cause of treatment failure and relapse [1]; [2]; [3]. Thus, identification of cellular resistance mechanisms and development of novel strategies that overcome resistance is imperative for the development of successful anti-cancer therapies.

PDT is approved worldwide as a treatment of several cancer types [4]. PDT is based on the preferential accumulation of a nontoxic, light sensitive compound (photosensitizer) in the tumour tissue, and a subsequent light excitation of the photosensitizer by an appropriate wavelength. This leads to energy transfer from the photosensitizer to molecular oxygen (O_2) or to other cellular components, resulting in generation of cytotoxic concentration of reactive oxygen species (ROS), of which singlet oxygen is the most abundant, resulting in peroxidation of vital cellular components and initiation of cell death mechanisms such as apoptosis, necrosis or autophagy [4]. PDT depends on the presence of oxygen, and lack of cytotoxic responses in hypoxic regions of the tumour is a major obstacle [4]. Moreover, intracellular antioxidants such as the glutathione system, superoxide dismutase, catalase and lipoamide de-hydrogenase may detoxify PDT-

induced ROS, resulting in treatment resistance [4]; [5]. Prosurvival signalling have also been shown to be important cytoprotective factors causing PDT resistance [2]; [6]; [7]; [8]; [9]; [10]. Of relevance for this study, several independent reports have also shown that repeated *in vitro* PDT-treatments with different photosensitizers result in acquired resistance [3]; [11]; [12].

Photochemical internalization (PCI) is a minimally invasive intracellular drug delivery method under clinical evaluation [13]. PCI is based on endosomal or lysosomal membrane- localization of the photosensitizers $TPCS_{2a}$ (di-sulfonated meso-tetraphenyl chlorin or Fimaporfin), $TPPS_{2a}$ (di-sulfonated meso-tetraphenylporphine) or $AlPcS_{2a}$ (di-sulfonated aluminium phtalocyanine) and co-treatment with drugs that are sequestered and degraded in the same vesicles. By light-controlled activation of the PCI-photosensitizer the membranes of these vesicles are ruptured, and the entrapped drugs are released into the cell cytosol (endosomal escape) where they can exert their effect [14]. PCI-induced circumvention of resistance to several clinically approved drugs (*e.g.* bleomycin and doxorubicin) and model drugs (*e.g.* ribosome-inactivating protein (RIP) toxins and immunotoxins) has been demonstrated [15]; [16]; [17]. We have in addition shown the feasibility of using PCI as an efficient strategy to kill cancer cells by immunotoxins targeting putative cancer stem cell (CSC) markers including CD133, CD44, CSPG4 and EpCAM [18].

A variety of clinical photosensitizers are substrates of the efflux pump ABCG2 (BCRP) [19]; [20], which may have therapeutic implications due to the overexpression of ABCG2 in drug-resistant cancer stem cells (CSCs) [21]. PCI photosensitizers, including $TPCS_{2a}$, $TPPS_{2a}$ and $AlPcS_{2a}$ are, however, not substrates of this marker [21]. In addition, we have also shown that $TPPS_{2a}$ and $TPCS_{2a}$ are not substrates of ABCB1/p-glycoprotein (Pgp)/MDR1 [16]; [17]. We

recently reported that the ABCG2-overexpressing human breast cancer cell line MA11 is intrinsically resistant to Pheophorbide A (PhA)-PDT, in contrast to PDT with the non-ABCG2 substrate PCI photosensitizer $TPCS_{2a}$ [21]. Altogether, these findings suggest that PCI-photosensitizers are candidates for PCI-mediated targeting of multi drug resistant (MDR) and CSCs.

We hypothesized that repeated cycles of PhA-PDT in MA11 will increase intrinsic PDT-resistance due to selection of cells overexpressing ABCG2, while repeated cycles of $TPCS_{2a}$-PDT will not cause acquired resistance. Since $TPCS_{2a}$ is under clinical evaluation as a photosensitizer for PCI-enhanced drug delivery [13], we also aimed to elucidate death or survival responses after $TPCS_{2a}$-PDT in breast cancer cells. In this study, we demonstrate that three cycles with PhA-PDT induce enhanced intrinsic PDT-resistance and, surprisingly, repeated cycles of $TPCS_{2a}$-PDT result in acquired PDT-resistance. While increased expression of ABCG2 was indicated as the mechanism for acquired PhA-PDT-resistance, increased proliferation capacity and loss of death signalling in the p38 MAPK pathway was indicated as the mechanisms for acquired $TPCS_{2a}$-PDT-resistance in the MA11 cells. Development of $TPCS_{2a}$-PDT resistance in the MDA-MB-231 cell line also resulted in dysregulation of p38 MAPK signalling; however this was not found to play a role for cytoprotection. On the other side MCF-7 cells did not develop resistance after repeated $TPCS_{2a}$-PDT. EGFR was found to be overexpressed in the $TPCS_{2a}$-PDT resistant MA11/TR cells. PCI of the EGFR-targeting toxin EGF-saporin was equally efficient in MA11 and MA11/TR cells, and this put forward PCI-based drug delivery as a rational intervention to overcome PDT-resistance.

2. MATERIALS AND METHODS

2.1. Cell lines and culturing

The MA11 human breast cancer cell line was originally obtained from Dr. Gunhild Mælandsmo, Department of Tumour Biology at Oslo University Hospital - Radiumhospitalet. Two PDT-resistant sub-cell lines (not clones) of MA11, MA11/PAR and MA11/TR, were generated by 3 repeated cycles of PhA-PDT and $TPCS_{2a}$-PDT, respectively. The oestrogen (+) and progesterone (+) and HER2 (-) human breast cancer cell line MCF-7 (#HTB-22) and the triple negative (oestrogen, progesterone and HER2 negative) human breast cancer cell line MDA-MB-231 (#HTB-26) were both purchased from ATCC (Manassas, VA, USA). One resistant sub-line of MDA-MB-231, MDA-MB-231/TR, was generated after 3 repeated cycles of $TPCS_{2a}$-PDT. The cell lines were cultured in L-glutamine-containing RPMI-1640 medium (R8758, Sigma-Aldrich, St. Louis, MO) supplemented with 10% foetal calf serum (FCS) (PAA Laboratories GmbH, Pasching, Austria), 100 U/ml penicillin (Sigma-Aldrich) and 100 µg/ml streptomycin (Sigma-Aldrich) and grown and incubated at 37ºC in a humidified atmosphere containing 5% CO_2.

2.2. Light source and photosensitizers

Illumination of cells was performed by using LumiSource ® (PCI Biotech AS, Oslo, Norway), a lamp consisting of four 18-W Osram L 18/67 light tubes. The lamp delivers blue light (Emission max =435 nm) with an output of 12.6 mW/cm^2 (1 min light exposure = 0.81 J/cm^2). $TPCS_{2a}$ was provided by PCI Biotech AS. $TPCS_{2a}$ (0.35 mg/ml in polysorbate 80, 2.8% mannitol, 50 mM Tris, pH 8.5) stock solution was kept light protected at 4ºC in aliquots (Stability of TPCS2a is >4 years). Pheophorbide A (PhA) was purchased from Frontier Scientific (Salt Lake City, UT, USA)

and dissolved in 100% dimethyl sulfoxide (10 nM stock concentration). Aliquots were kept at -20ºC (Stability of PhA is >2 years). All work with the photosensitizers was performed under subdued light.

2.3. PDT and development of the PDT-resistant sub-cell lines

Cells were seeded at a density of $5x10^3$ MA11, $1.5x10^3$ MDA-MB-231 or $1x10^3$ MCF-7 cells per well in 96-well plates (Nunc) (0.3 cm^2 per well) and left over night to attach. The cells were then incubated with 0.5 µg/mL $TPCS_{2a}$ (MA11) and 0.4 µg/mL $TPCS_{2a}$ (MDA-MB-231 and MCF-7) in cell culture medium for 18 hrs, and washed twice with PBS and further incubated with drug-free medium for 4 hrs to remove membrane-bound $TPCS_{2a}$ prior to light exposure. Alternatively, cells were incubated with 1 µM (0.59 µg/mL) Pheophorbide A (PhA) for 1 hr followed by 2 washes with PBS prior to light exposure in cell culture media as indicated. MA11/TR, MA11/PAR, MDA-MB-231/TR and MCF7/NTR (NTR = not $TPCS_{2a}$-PDT resistant after 3 cycles of PDT) were developed by treatment of naïve cells with 3 min (2.43 J/cm^2, inducing 90-99% reduction of MA11 or MDA-MB-231 cell viability and 50% reduction of cell viability in MCF-7 cells) of $TPCS_{2a}$-PDT (designated /TR), or 0.5 min of PhA-PDT (designated /PAR) (0.4 J/cm^2, inducing 90-99% reduction of MA11 viability) in cell culture flasks. Cells that survived were re-exposed to PDT twice (totally 3 treatments in the course of 3 weeks). To allow the cells to recover, PDT-induced cytotoxicity was assessed the following week at day 5-7 after the last PDT cycle.

2.4. PCI

In the PCI protocol, cells were co-incubated with 0.5 µg/mL $TPCS_{2a}$ and 1 pM EGF-saporin for

18 hrs. Then cells were washed twice with PBS and incubated in drug-free medium for 4 hrs before 1 min light exposure as described in the Figure legend. EGF-saporin was prepared as described by Weyergang et al. by combining biotinylated EGF and streptavidin-saporin by non-covalent binding in a 4:1 ratio [22].

2.5. Viability and cytotoxicity assays

Cells were seeded at a density of $5x10^3$ (MA11, MA11/TR and MA11/PAR), $1.5x10^3$ (MDA-MB-231 and MDA-MB-231/TR) and $1x10^3$ (MCF-7 and MCF7/NTR) per well in 96 well plates (Nunc). Cell metabolic activity/viability was assayed by the 3-(4,5-Dimethylthiazol-2-yl)-2,5-diphenyltetrazolium bromide (MTT) method
[16] at 24, 48 or 72 hrs after light exposure as indicated. For the clonogenic cell survival assay [16] $1.5x10^3$ (MA11 and MA11/TR) and $0.3x10^3$ (MDA-MB-231/-TR and MCF7/NTR cells were seeded per well in 6-well plates. The assay was performed 10-14 days post light exposure by methylene blue staining. Real-time monitoring of cell confluency (proliferation) was determined by the IncuCyte live cell imaging system IncuCyte ZOOM ® (Essen BioScience, Hertfordshire, UK). Five thousand MA11 and MA11/TR cells were seeded in 96 well plates, treated with PDT and analysed for proliferation by detection of cell confluency from 0 to 300 hrs (12.5 days). Live cell phase contrast images were acquired every 3 hrs and processed by IncuCyte Software Rev2. (Image resolution: 1.49 microns, image format: 1280x1024 pixels, field of view: 1.90x1.52 mm, magnification: 10x).

2.6. Intracellular localization of TPCS$_{2a}$

MA11 and MA11/TR cells 5 x 10^4 were seeded on 0.17 (+/- 0.01)-mm-thick coverslips

(Assistent, Glaswarenfabrik Karl Hecht, Sondheim, Germany) in 4-well plates and allowed to attach overnight. Then the cells were incubated with 0.5 µg/ml $TPCS_{2a}$ for 18 hrs, and washed twice with PBS prior to 4 hrs incubation with drug-free medium. The coverslips were washed with cold PBS with Ca^{2+} and Mg^{2+} and carefully inverted onto a microscope slide (Menzel-Gläser, Gerhard Menzel, Braunschweig, Germany). Fluorescence microscopy was carried out with a Zeiss Axioplan epi-fluorescence and phase-contrast microscope using 63 x magnification with an oil immersion objective (Carl Zeiss AG, Oberkochen, Germany). The $TPCS_{2a}$ fluorescence was recorded with an AxioCamMR3 camera (Carl Zeiss) using a 395-440 nm band pass excitation filter, a 460 nm dichroic mirror and a 620 nm long pass emission filter. Co-localization of $TPCS_{2a}$ with LysoTracker Green (LTG) (Life Technologies, Carlsbad, CA, USA) was investigated by fluorescence microscopy after incubation of 0.33 µM LTG for 30 min prior to (co-localization) or after (lysosomal photodamage) PDT. For recording LTG fluorescence, a 470/40 nm band pass excitation filter, a 495 nm dichroic mirror and a 525/50 nm band pass emission filter were used.

2.7. Flow Cytometry

Flow cytometry was performed by using an LSRII Flow Cytometer (Becton-Dickinson, San Jose, CA), and data were processed by the FlowJo version 7.6.5 software (Treestar, OR), as recommended by the Flow Cytometry Core Facility (Institute for Cancer Research, Oslo University Hospital). Cells were treated as indicated and filtered through a 5 ml round-bottom tube with a cell strainer cap (Becton-Dickinson) prior to flow cytometry. Details concerning cell numbers are described in 2.8 (TPCS2a-accumulation study), 2.9 (ROS-detection study) and 2.16 (apoptosis and necrosis study).

2.8. Cellular accumulation of $TPCS_{2a}$

For quantification of $TPCS_{2a}$ accumulation in the MA11 cell lines, $2x10^5$ cells were seeded per well in 6-well plates (Nunc), and incubated with 0.5 µg/ml $TPCS_{2a}$ for 18 hrs. Then the cells were washed twice with PBS prior to 4 hrs incubation with drug-free medium. Subsequently, the cells were detached with trypsin, washed and analysed by flow cytometry. Live and single cells were gated based on forward (FSC) and side (SSC) scattering parameters. $TPCS_{2a}$ was excited by a 100 mW 407 nm laser, and fluorescence was collected through a 660/20 nm emission filter combined with a 635 nm longpass dichroic filter.

2.9. Intracellular ROS detection

2×10^5 cells were seeded per well in 6 well plates and subjected to PDT as described above. Immediately after light exposure, the cells were incubated with 0.1 mM 2',7'-Dichlorofluorescin diacetate (DCFH-DA) (Sigma-Aldrich). After 1 hr incubation, cells were detached with trypsin, washed once in PBS, and subsequently analysed by flow cytometry to detect the fluorescent DCF product which forms upon DCFH oxidation by ROS. DCF fluorescence was detected in live cells by excitation with a 50 mW 488 nm laser, and collected through a 525/50 nm or a 530/30 nm emission filter combined with a 505 nm longpass dichroic filter.

2.10. Ionizing radiation therapy

Cells were seeded in 6-well plates (Nunc) to obtain 100, 200, 400 and 800 colonies for doses of 0, 2, 4 and 6 Gy, respectively. The plating efficiency of MA11 and MA11/TR cells is 15% (1 of 6.67 cells). Hence, e.g. to obtain 800 colonies in one well (800 x 6.67), 5336 cells were seeded out. Ionizing radiation was delivered by an X-ray generator (Faxitron CP160), Tucson, AZ, USA)

(160 kV, 6.3 mA, dose rate 1 Gy/min). Relative colony-forming ability of the cells was measured 10 days after radiation. The plating efficiency (PE) and surviving fraction (SF) were calculated as shown in Eq 1 PE_{NT} = No of colonies formed from NT cells / No of cells seeded and Eq 2 SF = No of colonies formed after treatment / (No of cells seeded x PE_{NT}), respectively.

2.11. Doxorubicin treatment

8 x 10^3 MA11 or MA11/TR cells were seeded per well in 96 well plates (Nunc) and left over night for proper attachment prior to incubation with 3.3 -1000 nM doxorubicin (Doxorubicin hydrochloride, Sigma-Aldrich) for 72 hrs before MTT analysis.

2.12. Immunodetection of proteins by Western blotting

Cells were lysed with 70 µl 1x Lane Marker Reducing Sample Buffer (Thermo Fischer Scientific, Waltham, MA, USA), or lysis buffer containing 62.5 mM Tris-HCl, pH 6.8, 2% (w/v) SDS, 10% glycerol, 50 mM dithiothreitol, 0.01% bromphenol blue, 1 mM NaF, and 20 mM β-glycerol phosphate, added 10 µl/ml protease inhibitor cocktail (Sigma-Aldrich), 10 µl/ml phosphatase inhibitor cocktail I (Sigma-Aldrich), 10 µl/ml phosphatase inhibitor cocktail II (Sigma-Aldrich), 1 mM phenylmethanesulfonyl fluoride and 1 mM Na_3VO_4. Due to the incompatibility of the protein assay (DC protein assay, BioRad) and dithiothreitol, even cell lysate loading was instead based on the nucleic acid concentration measured by absorption at 260 nm as previously reported [23]. The samples were sonicated for 10-15 sec and heated (95ºC for 5 min). Then samples were subjected to gel electrophoresis on 4-20% precast gradient polyacrylamide gels (Bio-Rad) and Western blotting by the Transblot Turbo system (Bio-Rad, Hercules, CA, USA) as recommended

by the producers. Protein expression and activation was detected by antibody stains of western blots as described in [17], using primary antibodies for phospho-p38 (#9216, 1:2000 dilution), phospho-MAPKAPK-2 (Thr222) (#3316, 1:1000 dilution), LC3B (#2775, 1:1000 dilution), EGFR (#2232, 1:1000 dilution), STAT-3 (#8719, 1:1000 dilution), phospho-STAT-3 (#9131, 1:1000 dilution), ERK1/2 (#9120, 1:1000 dilution), phospho-ERK1/2 (#9106, 1:2000 dilution), GPx1 (sc-3206, 1:1000 dilution) and biotin (#7075) (Cell Signaling Technologies, Danvers, MA, USA) and secondary HRP conjugated antibodies for rabbit (goat anti-rabbit IgG, #7074) and mouse (horse anti-mouse IgG, #7076) (Cell Signaling) in concentrations recommended by the producers. In addition to nucleic acid measurements to ensure even loading of cell lysates as described above, control of loading was performed by Ponceau S. staining (Sigma-Aldrich). Quantification was performed by volume integrating measurements of the protein signals using the Image Lab 4.1 Software (Bio-Rad).

2.13. Immunocytochemistry

Exponentially growing MA11 and MA11/TR cells were transferred by cytospin on glass slides and fixed in acetone prior to immunocytochemical (ICC) detection of either EGFR or ABCG2. Primary antibody against EGFR (clone H11, #M3563, 1:200) was purchased from Dako (Glostrup, Denmark) and primary antibody against ABCG2 (clone BXP-21, #B7059, 1:100) was purchased from Sigma-Aldrich. Primary antibodies were incubated for 1 hr in room temperature prior to target retrieval and ICC staining by EnVision FLEX+, Mouse, High pH (#K8002, Dako) at 1:50 dilution for 30 min at room temperature.

2.14. Inhibition of the p38 MAPK pathway

To study the impact of p38 MAPK activation on the PDT-induced viability response, 0.02 mM of

the p38 MAPK inhibitor SB203580 (Calbiochem, Merck, Darmstadt, Germany) was added to cells 1 hr prior to and removed 1.5 hrs after PDT. We previously demonstrated that this concentration and incubation time of SB203580 is non-toxic and block activation of p-38 or MK-2 in different cancer cell lines [24, 25]. Cell viability was assessed by the MTT method 48 hrs after light exposure.

2.15. ELISA assay

Apoptosis (addressed by p53, caspase-3, PARP and Bcl-2-associated death promotor (BAD) detection), and growth signalling (addressed by Akt1, ERK1/2 (p44/p42) and S6 detection) was analysed by using the PathScan ® Apoptosis (#7105) and Growth (#7239) Multi-Target Sandwich ELISA Kits (Cell Signaling). Protein expression was detected according to the producer's protocol and related to the total protein concentration measured by the DC Protein Assay (Bio-Rad, Hercules, CA, USA). 2.5 x 10^5 cells were seed out per well in 6-well plates and incubated over-night prior to 18 hrs incubation with 0.5 µg/mL $TPCS_{2a}$. Cells were then chased in drug-free medium for 4 hrs and then exposed to 1.5 min of blue light exposure. Subsequently, cells were harvested 10 min (for growth signalling analysis) and 20 hrs after (for apoptotic signalling analysis) PDT.

2.16. Apoptosis, necrosis and cell cycle analysis

The TUNEL, and propidium iodide / thiazole orange (PI/TO) based necrosis assays were used to study apoptotic and necrotic responses 20 hrs after PDT, respectively. The TUNEL assay relies on the identification of nicks present in fragmented DNA of apoptotic cells, identified by deoxynucleotidyl transferase (TdT). TdT catalyses the addition of labelled dUTPs which can be

detected by flow cytometry [26]. 2 x 10^5 cells were seeded per well in 6-well plates (Nunc) and treated with PDT (1 and 5 min light exposure). Twenty hours post treatment, cells in the medium and trypsinated cells were harvested together. Subsequently, cells were washed with PBS and resuspended in either 400 µL ice cold methanol (drop wise while vortexing) for TUNEL assay, or in PBS for necrosis assay. Methanol fixed cells were stored in -20◦C for later analysis. Cells in PBS were immediately incubated with thiazole orange (TO) (diluted 1:250) on ice for 5 min, followed by propidium iodide (PI) (diluted 1:500) (both from the BD Cell Viability kit (Becton-Dickinson, San Jose, CA)) immediately before flow cytometry analysis. Single cells were gated based on SSC parameters, and fragments discriminated based on SSC and TO area. Necrotic cells were further gated based on SSC and PI area. TO and PI were excited by a 50 mW 488 nm and 40 mW 561 nm laser, respectively, and fluorescence collected through a 525/50 and 610/20 nm emission filter, combined with 505 and 600 nm longpass dichroic filter. Methanol fixed cells stored for TUNEL assay, were washed once with PBS, and added 35 µL TdT reaction mix (3.5 µL TdT Reaction Buffer, 2.1 µL 25 mM $CoCl_2$, 0.35 µL Biotin-16-dUTP, 0.35 µL 10 mM DTT, 0.14 µL TdT enzyme, 28.58 µL ddH_2O) (Roche) and left for 30 min incubation at 37◦C. Then the cells were washed twice with PBS and incubated with 50 µL streptavidin-Cy5 1:400 (GE Healthcare) in 5% milk in PBS for 30 min at room temperature. Then the cells were washed once with PBS and resuspended in 500 µL Hoechst 33258 (1.5 µg/mL) in PBS, and left overnight at 4◦C before flow cytometry. The apoptotic fraction was gated based on Cy5 and Hoechst area. Cy5 and Hoechst 33258 were excited by a 40 mW 640 nm and 25 mW 405 nm or 100 mW 407 nm laser, respectively, and fluorescence collected through a 670/14 (Cy5) and 450/50 (Hoechst 33258) nm emission filter. REH cells (acute lymphocytic leukaemia) harvested 24 hrs after treatments with ionizing radiation (4 Gy) were used as positive control in the TUNEL

experiments. Cell cycle analysis was performed on Hoechst 33258-stained cells from the TUNEL experiment, based on Hoechst area, and analysed by using the Dean-Jett-Fox model to define cell cycle distribution.

2.17. High-content microscopy for detection of LC3 puncta

4 x 10^4 MA11 or MA11/TR cells grown on coverslips were fixed in 10% neutral buffered formalin (Sigma-Aldrich) for at least 20 min. After three washes in PBS cells were treated with 50 mM NH_4Cl in PBS for 10 min to quench free aldehyde groups, and washed another three times in PBS. Then cells were blocked and permeabilized for 1 hr in PBS containing 1% BSA (Sigma-Aldrich) and 0.05% saponin, incubated with primary antibody rabbit anti-LC3 (MBL, PM036, detecting both LC3-I and LC3-II) for 1 hr, washed three times in PBS/BSA/saponin, incubated with secondary antibody Alexa488-donkey anti-rabbit (Jackson ImmunoResearch Laboratories, 711-545-152) for 1 hr, washed three times in PBS and one time in water. The cells were then mounted in Mowiol containing 1 µg/ml Hoechst 33342 (Sigma-Aldrich). Images were obtained with an Olympus ScanR automated microscope system with an UPLSAPO 40x/0.95 objective. All images were taken with the same settings and the Olympus ScanR analysis software was used to count the number of cells, calculate the percentage of cells with LC3 puncta (granular fluorescence signal of autophagosomes) and the average number of LC3 puncta per cell.

2.18. Electron microscopy

1.5 x 10^5 cells were seeded per well in 6 well plates and treated with $TPCS_{2a}$-PDT (1 min /0.81 J/cm^2 of light) as described above. At different time points post PDT the cells were fixed with 2%

glutaraldehyde in 0.1 M cacodylate buffer and centrifuged after 10 min at room temperature at 10 000 rpm in a table top centrifuge. Postfixation was done in 1% Osmium (1 hr) followed by 30 min 0.1% tannic acid, 1% Na_2SO_4 for 5 min for neutralization, and en bloc staining for 30 min in 4% uranyl acetate. After dehydration in graded ethanol series, cells were embedded in Epon and polymerized for 48 hours. Ultrathin sections were cut by Leica Ultracut, transferred onto formvar/carbon coated grids and observed at 80 kV in a Jeol JEM 1203 transmission electron microscope. Images were recorded with a Morada digital camera and iTEM software (Olympus, Muenster, Germany).

2.19. Statistical evaluations of data

To assess whether the means of the different treatment results were significantly different we used the two-sided Student's t test by Sigma Plot 12.5 if not otherwise stated. A significance level of $p<0.05$ was considered as significant. When appropriate, significance was assessed by the two-way ANOVA with Bonferroni correction as post-hoc tests.

3. RESULTS

3.1. Acquired resistance to PDT is cell line dependent

MA11 cells challenged with ≥ 3 cycles of PhA-PDT (designated MA11/PAR) were found highly resistant to further treatment with PhA-PDT compared to the control naïve MA11 cells (Fig. 1A). Efflux of PhA by the ABCG2 transporter has previously been reported as a mechanism of resistance to PhA-PDT [19]; [21]; [27]. Although the naïve MA11 cells have an intrinsically high expression of ABCG2, the ICC analysis of ABCG2 revealed an enhanced expression of the drug

efflux pump in MA11/PAR cells as compared to the MA11 cells (Fig. 1B). In addition, we observed a shift towards enhanced plasma membrane expression of ABCG2 in the MA11/PAR side population cells (this is the population of cells with lowest Hoechst 33343 fluorescence due to ABCG2 efflux).

A single treatment of MA11 cells with $TPCS_{2a}$-PDT resulted in a light dose-dose dependent decrease of cell viability 24 hrs post light exposure, while development of resistance to $TPCS_{2a}$-PDT (designated MA11/TR) was acquired after ≥3 treatment cycles of PDT (Fig. 1C). The light dose needed to inactivate 50% of the MA11/TR cells viability (LD_{50}) was >3-fold higher compared to that of the naïve MA11 cells. In addition, the MA11 cells were found to be 3-fold more sensitive (p=0.010) to $TPCS_{2a}$-PDT compared to the MA11/TR cells at a 2 min light dose. In addition, we observed a distinct shoulder of the viability curve of the MA11/TR cells (Fig. 1C) compared to the MA11 cells, which suggests activation of cytoprotective pathway(s) in the PDT-resistant cells. In fact, we observed a minor increase of MTT activity of the MA11/TR cell for the two lowest light doses. These results were validated by three independent clonogenic assays (data not shown).

Since $TPCS_{2a}$ is a clinical relevant photosensitizer used in PCI, we decided to further elucidate the cellular mechanisms of the $TPCS_{2a}$-PDT-induced resistance in the MA11/TR cells. By quantifying the dynamics of changes in the cell confluency after $TPCS_{2a}$-PDT during a time course of 12.5 days (300 h), the IncuCyte live-cell imaging system revealed a much higher proliferation capacity of the MA11/TR cells compared to the MA11 cells (Fig.1D), based on phase contrast micrographs acquired up to 300 hrs after PDT (Fig. 1E). Interestingly, it appears that the MA11/TR cells that have grown to sub-confluence (300 h NT MA11/TR) have gained a mesenchymal morphology (fibroblast-like structures) as compared to the MA11 cells (300 h NT

MA11), which seems to grow closer and more dense (detailed images can be seen in archival data set). However, it is difficult to see an obvious difference in morphology one day after seeding out the cells. The MA11/TR cells remained to be PDT-resistant after 20 passages (6 weeks and ≥50 cell cycles) post the last PDT exposure indicating development of acquired and persistent PDT resistance (data not shown).

By using the MTT-assay, a minor development of $TPCS_{2a}$-PDT resistance was observed in the MDA-MB-231 cell line (MDA-MB-231/TR) compared to naïve MDA-MB-231 cells (Fig. 1F). However, the clonogenic assay revealed a 4-fold ($p=0.001$) higher sensitivity of the MDA-MB-231 cells to $TPCS_{2a}$-PDT (at 2 min light exposure) as compared to the $TPCS_{2a}$-PDT-resistant MDA-MB-231/TR cells (Fig. 1G). LD_{90} of MDA-MB-231/TR was almost 2-fold increased compared to that of MDA-MB-231. On the contrary, no induction of $TPCS_{2a}$-PDT resistance in the MCF7/NTR cell line was observed by use of the MTT-assay (Fig. 1F), and no significant differences were found by the clonogenic assay (Fig. 1H).

3.2. Equal uptake and localization of $TPCS_{2a}$ and ROS generation after $TPCS_{2a}$-PDT

PDT, including $TPCS_{2a}$-PDT, induces cell death due to excess generation of cytotoxic ROS concentrations [4]; [17]; [28]. Hence, we assessed if there were any differences in intracellular ROS formation post $TPCS_{2a}$-PDT between the MA11 and MA11/TR cell lines. For both cell lines, ROS-formation increased in a light dose-dependent fashion, however, no difference in ROS-generation between the cell lines was observed 1 hr post treatment (Fig. 2A). In line with this, the expression of the ROS scavenging protein glutathione peroxidase (GPx)1 was found similar in MA11 and MA11/TR cells (data not shown).

$TPCS_{2a}$ is neither a substrate of ABCG2 nor Pgp/MDR1 [21]; [16]. Thus, we hypothesized that the resistance to $TPCS_{2a}$-PDT in the MA11/TR cells could partly be due to a reduced endocytosis or increased exocytosis rate of $TPCS_{2a}$. Flow cytometry was utilized to evaluate difference in intracellular accumulation of photoactive $TPCS_{2a}$ in the MA11 and MA11/TR cell lines. However, no difference in relative $TPCS_{2a}$ fluorescence between the cell lines was observed (Fig. 2B) at the time point relevant to perform light exposure (18 hrs +4 hrs chase in drug free medium).

Intracellular localization and fluorescence signals of $TPCS_{2a}$ at the time corresponding to PDT were by epi-fluorescence microscopy found similar in both MA11 and MA11/TR (Fig. 2C). In both cell lines, $TPCS_{2a}$-fluorescence puncta and co-localization with LTG was detected, indicating localization of $TPCS_{2a}$ in endosomes and lysosomes. Upon $TPCS_{2a}$-PDT, diffuse LTG and $TPCS_{2a}$-fluorescence was observed, demonstrating cytosolic release and similar degree of photochemical destruction of endosomes and lysosomes.

3.3. Cell cycle distribution after $TPCS_{2a}$-PDT in MA11 and MA11/TR cells

We then addressed possible changes in cell cycle distribution between the cell lines after $TPCS_{2a}$-PDT. Twenty hours after treatment, it was found a light-dose dependent increase of G2/M phase accumulation in both MA11 and MA11/TR. However, no significant difference in the cell cycle distribution between the cell lines was observed (Fig. 3A and B).

3.4. Repeated $TPCS_{2a}$-PDTdoes not induce cross-resistance to chemo- or radiotherapy

To evaluate potential development of therapy cross-resistance (chemo- or radiotherapy), MA11 and MA11/TR cells (that had been sub-cultured between 15-23 times) were treated with

increasing concentrations of doxorubicin (Fig. 4A) or ionizing radiation (Fig. 4B). For both treatment options, the cytotoxic response data did not reveal any difference between the cell lines, indicating no cross-resistance to these therapies.

3.5. Apoptosis, necrosis and autophagy responses in MA11 and MA11/TR cells following $TPCS_{2a}$-PDT

Development of PDT-resistance may be manifested by a dysregulation of the mode of death responses, *e.g.* the cancer cells gain cytoprotective pathway(s) that make them less prone to undergo apoptosis [2]. Hence, to assess a potential difference in cytocidal responses we evaluated the degree of apoptosis, necrosis and autophagy between MA11 and MA11/TR post $TPCS_{2a}$-PDT. TUNEL assay combined with PI/TO staining was used to identify the distribution of apoptosis and necrosis, respectively, in the fraction of all dead cells (normalized to 100%) 20 hrs after $TPCS_{2a}$-PDT (Fig. 5A). Non-treated cells displayed a low apoptotic subfraction which was not significantly different between the cell lines. $TPCS_{2a}$-PDT increased the apoptotic subfraction significantly ($p<0.05$) to about 40% in both cell lines. ELISA assay (Fig. 5B and C) was further used to detect key apoptotic proteins after $TPCS_{2a}$-PDT; no significant changes in apoptotic signalling involving p53, caspase-3 or poly ADP ribose polymerase (PARP) were revealed. However, the expression of the Bcl-2-associated death promoter (BAD) was found 2.8-fold higher ($p = 0.022$) in the untreated MA11 cells compared to the MA11/TR cells (Fig. 5B and C). However, upon PDT the MA11/TR cells increased their expression of BAD by a factor of approximately 3 ($p =0.013$), which is about at the same level of total BAD expression in the PDT-treated MA11 cells. No significant difference in p-BAD was observed between the cell lines.

To study the initiation of autophagy, the numbers of cells with LC3 puncta were counted. Within 20 hrs after $TPCS_{2a}$-PDT, approximately 55% (varying from 30 -80% between the individual experiments) of the cells contained more than two LC3 puncta (Fig. 6A) with an average of about 8 puncta per cell (Fig. 6B) in both cell lines. Fluorescence micrographs (Fig. 6C) of untreated MA11 and MA11/TR cells reveal that there is no clear difference in numbers of LC3 puncta, nor diffuse (cytosolic) LC3 signals between the cell lines treated with $TPCS_{2a}$-PDT 20 hrs post light exposure.

The fusion process of the autophagosomes with lysosomes further depends on the conversion of LC3-I to LC3-II. A strong conversion of LC3-I to LC3-II was observed on Western blot analysis in both MA11 and MA11/TR cells 20 hrs post $TPCS_{2a}$-PDT when compared to control cells, indicating the initiation of a fusion response (Fig. 6D). No statistically significant differences of LC3-II signal was found between MA11 and MA11/TR cells. No LC3 conversion could be observed at earlier time points after PDT. Electron microscopy (Fig. 6E) revealed typical dense multivesicular bodies (MVBs) in both MA11 and MA11/TR cells after one and two hours after PDT which were not found in controls. Four hours after $TPCS_{2a}$-PDT most of the vesicles displayed a dilated but still multivesicular morphology, as well as possibly fused MVBs. Twenty hours after $TPCS_{2a}$-PDT most endocytic structures regained dense MVB morphologies. A clear identification of autophagic structures was not possible.

3.6. p38MAPK-mediated death signalling is lost in the $TPCS_{2a}$-PDT-resistant MA11/TR cells

We have previously demonstrated that p38 MAPK induces a death signal after PDT with di-

sulphonated meso-tetraphenylporphyrin ($TPPS_{2a}$), a photosensitizer relevant for *in vitro* PCI [36]. Here we also reveal that $TPCS_{2a}$-PDT of both MA11 and MA11/TR cells strongly enhance the activation of p38 MAPK (phosphorylation on Thr180/Tyr182) immediately (5 min) after light exposure (Fig. 7A). The phosphorylation of p38 MAPK was also found high at 2 hrs and relatively high at 20 hrs post PDT in the resistant MA11/TR cells, compared to the MA11 cells. Hence, $TPCS_{2a}$-PDT induced substantially prolonged p38 MAPK activation in the MA11/TR cells compared to the naïve MA11 cells.

Pre-treatment with the p38 MAPK inhibitor SB203580, revealed a significant increase in MA11 survival upon 1 min $TPCS_{2a}$-PDT ($p<0.05$) (Fig. 7B). The inhibitor was shown to abolish the phosphorylation of the p38 downstream MAPK-activated protein kinase 2 (MK2) on Thr222, indicating decreased activity of p38 MAPK (Fig. 7C). The Thr222 site is reported to be one of the essential phosphorylation sites for MK2's activity [29]. No significant effect on PDT-survival could be detected in MA11/TR cells treated with SB203580 (Fig. 7D). In line with this, minor to no phosphorylation of MK2 could be found in the MA11/TR cells after $TPCS_{2a}$-PDT (Fig. 7C). In contrast to the MA11 cells, no effect on cell survival by the p38 inhibitor SB203580 was observed in the PDT-treated MDA-MB-231 (Fig. 7E) or MCF-7 cells (Fig. 7F), although a similar lack of MK-2 phosphorylation was observed in the MDA-MB-231/TR cells (Fig. 7G).

3.7. Cytoprotective signalling in MA11 and MA11/TR cells after $TPCS_{2a}$-PDT

ELISA analysis of proteins associated with growth and proliferation was carried out 5 min after $TPCS_{2a}$-PDT to determine potential early PDT-induced changes in expression between the MA11 and MA11/TR cells (Fig. 8A and B). Neither phosphorylation of Akt1, ERK1/2 (p44/p42) nor S6 were found different between the cell lines at this time point.

The level of total ERK1/2 was also found lower in the non-treated MA11 cells (about half of what could be found in the non-treated MA11/TR cells at the 20 hours harvest time point) (Fig. 8C). The relative phosphorylation status of ERK1/2 normalized to total ERK1/2 expression and untreated cells, revealed an attenuation of ERK1/2 activity two hours after $TPCS_{2a}$-PDT in both cell lines ($p<0.001$) (Fig. 8D).

The expression of total STAT-3, which phosphorylation is regulated by Janus kinases in response to cytokines and growth factors, was not found significantly affected by $TPCS_{2a}$-PDT at any harvest time point, and did not differ between the cell lines (Fig. 8E). The phosphorylation status and hence activation showed, however, a significant dephosphorylation 5 min after PDT in both cell lines (MA11, $p =0.015$ and MA11/TR, $p<0.001$) (Fig. 8F). Twenty hrs after $TPCS_{2a}$-PDT of the MA11 cells, the phosphorylation level of STAT-3 had returned to that of control cells. In contrast, phosphorylation of STAT-3 in PDT-treated MA11/TR cells was near 2-fold increased ($p =0.009$) compared to untreated MA11/TR control cells.

3.8. PDT-resistant MA11/TR cells over-express EGFR and are sensitive for PCI-based targeting with EGF-saporin

Western blot analyses of cell lysates of untreated naïve MA11 cells revealed an initial low EGFR expression compared to untreated MA11/TR cells harvested 5 min after the PDT time point (Approximately 6-fold lower than the expression found in MA11/TR, $p =0.024$) (Fig. 9A). At the 20 hrs time point, the untreated MA11 cells increased their EGFR expression significantly ($p =0.010$) compared to the 5 min time point, however the EGFR expression was still lower (1.45-fold, $p =0.019$) compared to the untreated MA11/TR cells. A higher expression of EGFR in the MA11/TR cells compared to the MA11 cells was confirmed by ICC (Fig. 9B).

The overexpression of EGFR in the MA11/TR cells made us hypothesize that PCI-based EGFR-targeting could be a rational strategy to eliminate these PDT-resistant cells. Indeed, targeting of EGFR with $TPCS_{2a}$-based PCI of 1 pM EGF-saporin was sufficient to induce a strong cytotoxic response in both MA11 and MA11/TR cells compared to PDT or EGF-saporin alone (Fig. 9C). For MA11/TR cells, PCI of EGF-saporin increased cell killing 2.8-fold over PDT alone at 2.5 min light exposure, compared to 1.9-fold increased cell killing in the MA11 cells at the same light dose.

4. DISCUSSION

PDT can be curative in early stage tumours and some pre-malignant conditions. In contrast, for thick lesions or advanced cancers, recurrence of tumour after PDT is a clinical challenge [4]. The reason for recurrences after PDT is unclear, though limited light penetration in tumour tissue and cytoprotective mechanisms have been reported to play important roles [30] [31]. Hence, repeated PDT has been suggested and shown to improve the clinical outcome in different cancers [32]; [33]; [34] and pre-malignant conditions [35]; [36]. However, several independent laboratories have demonstrated development of *in vitro* PDT-resistance [2]; [11]; [12]; [30], and clinically, cytoprotective signalling including upregulation of phospho-ERK and EGFR in squamous cell carcinoma (SSC) after methyl-δ-aminolevulinic acid (MAL)-PDT [3]. Investigation of cancer cell resistance mechanisms after PDT and repeated PDT is therefore important for the further development and improvement of PDT.

Hence, in this study we aimed to identify mechanisms behind PDT-resistance in human breast cancer cells that had been treated with several ($n \geq 3$) rounds of PDT. We first selected the

ABCG2-overexpressing cell line MA11 and treated the cells with PDT using two different photosensitizers, PhA or $TPCS_{2a}$, having completely different intracellular localization [21] and being either a substrate or a non-substrate of the drug efflux pump ABCG2, respectively. Previously we demonstrated that the MA11 cells are intrinsically resistant to PDT using the photosensitizer PhA [21], which has been shown to be a substrate of the ABCG2 drug efflux pump [19]; [21]. We recently demonstrated that it is possible to overcome the PhA-PDT resistance of the MA11 cells by blocking ABCG2 activity with Fumitremorgin C and the clinically relevant tyrosine kinase inhibitors imatinib and nilotinib [18]. Here we show that the degree of resistance is further enhanced when the MA11 cells are challenged by multiple rounds of PhA-PDT. We found that the PhA-PDT-resistant cells (MA11/PAR) expressed a higher plasma membrane level of ABCG2 than the naïve MA11 cells, demonstrating that repeated PhA-PDT of the MA11 cells results in a PDT-mediated selection of ABCG2-high cells. $TPCS_{2a}$ is not an ABCG2 substrate [21], rendering the MA11 cells sensitive to $TPCS_{2a}$-PDT. Yet, here we show that the MA11 cells acquired PDT-resistance upon challenge with ≥3 rounds of $TPCS_{2a}$-PDT. The $TPCS_{2a}$-PDT resistant cells were designated MA11/TR. In contrast to a recent study by Kralova et al. [37], which demonstrated a shift in the localization of temoporfin (mTHPC or Foscan) to lysosomes in PDT resistant cells, we did not observed any change in the intracellular localization of the $TPCS_{2a}$ between MA11 and MA11/TR cells. Since $TPCS_{2a}$ is under clinical evaluation for the use as a photosensitizer in PCI, we wanted to focus only on this photosensitizer in details. In line with other independent reports [2, 38], we also here observed that PDT-resistant MA11/TR cells have a different morphology than the MA11 naïve and PDT sensitive cells when they reached sub-confluence or confluency. We do not have enough data or mechanistic experiments supporting that the cells have undergone an activation of an EMT program, however,

this should be further elucidated in future studies.

We have previously reported on cross-resistance to $TPPS_{2a}$-and $TPCS_{2a}$-PDT in the doxorubicin-resistant sarcoma cell line MES-SA/Dx5 [16]; [17], which was correlated with ROS scavenging. Surprisingly, the $TPCS_{2a}$-PDT-resistant MA11/TR cells had no significant difference in ROS generation compared to the naïve MA11 cells post $TPCS_{2a}$-PDT. In addition, neither cross-resistance to doxorubicin nor ionizing radiation was established in the MA11/TR cells. In line with this one of the most important antioxidant enzymes in humans, the ROS scavenger GPx1 [17]; [39], was found equally expressed by MA11 and MA11/TR cells (data not shown). Altogether, these findings strongly suggest that the development of $TPCS_{2a}$-PDT-resistance observed in the MA11/TR cells does not involve an enhanced capacity to scavenge ROS.

A strong increase of phosphorylation (at Thr180 and Tyr182) of the stress responsive protein p38 MAPK immediately (~5min) after $TPCS_{2a}$-PDT in both MA11 and MA11/TR was revealed, consistent with our recent reports using other cell lines [17]; [40]; [41]. One of the most striking observations in the present study is the highly increased activation of p38 MAPK after $TPCS_{2a}$-PDT in the MA11/TR cell line. Furthermore, inhibition of p38 MAPK activation with SB203580 did not have any impact on survival of the MA11/TR cells after $TPCS_{2a}$-PDT. However, SB203580 strongly enhanced the viability of PDT-treated MA11 cells indicating that p38 MAPK activation induces death signalling in the PDT-sensitive naïve cells, in agreement with observations in other models [40]. Hence, the present report suggests that the PDT-resistant MA11/TR cells have lost their p38-mediated cell death signalling after $TPCS_{2a}$-PDT, which is most likely the central resistance mechanism observed in these cells. On the contrary, no effect

on survival of p38 inhibition was found in MDA-MB-231 cells, although the resistant MDA-MB-231/TR cells had strongly reduced ability to phosphorylate MK2 in response to $TPCS_{2a}$-PDT. At this stage we cannot explain this observation, however, in light of a recent study by Herranz et al. [42], which identified MK2 as a specific target of mTOR-regulated translation and that we previously demonstrated direct photodamage of mTOR (using another lysosomal localizing photosensitizer $AlPcS_{2a}$), may explain why the specific inhibition of p38 by SB203580 does not influence survival of the MDA-MB-231 cells after $TPCS_{2a}$-PDT. The MCF-7 cells, which intrinsically shows low sensitivity to $TPCS_{2a}$ -PDT was also not affected by SB203580. Our data therefore indicate that breast cancer cells with acquired resistance to $TPCS_{2a}$-PDT have a dysregulated p38 MAPK activity, which has strongly reduced its ability to phosphorylate MK2 in both MA11/TR and MDA-MB-231. However, the implication of the activation of p38 MAPK for death signalling is cell line dependent. Together with p38 MAPK, MK2 is known to be involved in cellular processes including stress and inflammatory responses, cell proliferation and survival [43]. Activation of p38 may in addition cause mitotic arrest [44] which was indeed observed after $TPCS_{2a}$-PDT in the MA11 and MA11/TR cells, however, no difference in cell cycle distribution was observed. Of high relevance to our study is the work of the Gaestel lab, which demonstrated that MK2 knockout mice had enhanced stress resistance and survived bacterial LPS-induced endotoxin shock because of a 90% reduction in the expression of TNF-α [45]. In addition, Köpper *et al.* showed that inhibition or depletion of MK2 protected U2OS sarcoma cells from DNA damage-induced cell death after ultraviolet light or gemcitabine exposure [46]. Based on this and new data revealed in this study, we suggest that loss of MK2 activity protect breast cancer cells from ROS-induced cell death after PDT. To confirm this, further experiments with direct knock out of MK2 in the MA11 cells, should be performed in front of $TPCS_{2a}$-PDT

challenge.

The enhanced proliferation of the MA11/TR cells compared to the MA11 cells, indeed, indicates a dysregulation of proliferation and/or survival signalling in this PDT-resistant cell line. This may be attributed to the strongly enhanced expression of total EGFR and ERK1/2 observed in untreated MA11/TR cells at relative low cell confluence. This is in agreement with a study of Gilaberte *et al.* which recently demonstrated that EGFR is upregulated in relapsed SSC tumours of patients treated with MAL-PDT and in a SSC-13 sub-line that had developed PDT-resistance after multiple treatments with MAL-PDT [3]. Of relevance, some observational clinical case reports have shown that multiple PDT sessions may transform the tumour into a faster growing condition [47]; [48]; [49]. In contrast, PDT-mediated inhibition of total and phosphorylated EGFR expression immediately after treatment has been reported by us and others [50]; [51]; [52] using different cell line models and photosensitizers. Moreover, immunoblotting after $TPCS_{2a}$-PDT revealed that the EGFR downstream proteins ERK1/2, which are protein-serine/threonine kinases that participate in the Ras-Raf-MEK-ERK signal transduction cascade, were dephosphorylated in the MA11 and MA11/TR cells 2 hrs after treatment. The amount of total ERK1/2 was, however, higher in the MA11/TR cells, coinciding with a higher proliferation rate in the MA11/TR cells. Of relevance, p38 MAPK-induced G2/M arrest has been linked to de-phosphorylation of ERK1/2 [53]. The MA11 and MA11/TR cell lines responded, however, similarly to $TPCS_{2a}$-PDT with respect to cell cycle distribution 20 hrs after $TPCS_{2a}$-PDT; both gained a distinct accumulation in G2/M phase, which has also been reported previously by others using different photosensitizers *e.g.* Hypericin, $AlPCS_4$ and $TPPS_4$ where the latter two localize to endosomes and lysosomes [54]; [55]; [56]. Thus, increased EGFR and Erk expression may

play an important role for the increased proliferation rate observed for the $TPCS_{2a}$-PDT resistant MA11/TR cells, and, in addition to the deregulated p38 MAPK signalling pathway, may partly explain the enhanced survival after PDT.

The rupture of endosomal and lysosomal membranes after light activation of PCI-photosensitizers as shown in Fig. 2C, is utilized to enhance the cytosolic delivery of several types of macromolecular drugs (*e.g.* protein-based toxins and targeting toxins) and some chemotherapeutics for cancer therapy [21]; [28]; [57]; [58]; [59]. Regardless of PDT sensitivity, which may vary with accumulation, localization and/or death and survival signalling of treated cancer cells, we have demonstrated that PCI of ribosomal inactivating toxins (*e.g.* saporin and gelonin), of which only 1-10 molecules may be sufficient to kill a cell [60], with or without targeting moieties (*e.g.* growth factors and antibodies), circumvent therapy resistance in a number of cancer types [15]; [16]; [17]. Due to the elevated EGFR expression in the MA11/TR cells, we hypothesized that these cells would be sensitive to PCI of an EGFR-targeting drug. Indeed, PCI of 1 picomolar EGF-saporin decreased viability more in MA11/TR than in MA11 cells when compared to their PDT-sensitivities, demonstrating that PCI of EGF-saporin overcomes the PDT-resistance in the MA11/TR cells. This is consistent with what we have previously observed in other cancer cell lines exhibiting different PDT sensitivities [17]. The PCI effect is dependent both on the degree of target expression and photodamage of the lysosomal membrane. Hence, despite the significant ($p<0.01$) lower PDT effect in the MA11/TR cells, these cells are more sensitive to PCI of EGF-saporin due to a significant ($p<0.02$) higher expression level of EGFR

A $TPCS_{2a}$-PDT-induced de-phosphorylation of STAT-3 was also detected by immunoblotting in

both MA11 and MA11/TR cells at the Tyr705 site. These observations are in line with Liu *et al.*, which reported on reduced STAT-3 and ERK1/2 phosphorylation upon 5-aminolevulinic acid (5-ALA)-PDT [51]. Twenty hours after $TPCS_{2a}$-PDT, the MA11/TR cells regained phosphorylation of STAT-3 exceeding the phosphorylation of untreated cells, also in line with their higher proliferation capacity compared to the naïve MA11 cells after PDT.

Twenty hrs after $TPCS_{2a}$-PDT the total distribution of cells undergoing apoptosis and necrosis was not different between the MA11 and MA11/TR cells. Moreover, ELISA performed immediately after PDT did not reveal any significant changes and differences of cell death or survival signalling responses, except a significant ($p = 0.022$) 3-fold lower expression of the BAD protein, which is a pro-apoptotic member of the Bcl-2 gene family, in the MA11/TR control cells as compared to MA11 cells. However, in the resistant cells, $TPCS_{2a}$-PDT generated a significant 3-fold increase ($p = 0.013$) of BAD to the same level as the treated MA11 cells.
The pro-apoptotic activity of BAD is prevented by phosphorylation of Ser112 by the MAPK pathway [61] and Ser136 by the PI3K-Akt pathway [62]. No significant change in phospho-BAD level was, however, observed. Altogether, we could neither detect any change in degree of apoptosis between the MA11 and the MA11/TR cells after $TPCS_{2a}$-PDT, nor in apoptotic signalling responses post PDT. However, the reduced expression of Bad in the MA11/TR control cells may explain the enhanced viability and proliferation of these cells, and suggests the reduced sensitivity to PDT as compared to the maternal MA11 cells.

$TPCS_{2a}$-PDT in MA11 and MA11/TR cells induced an increase of LC3 puncta and LC3-I to II conversion and this may indicate an autophagy induction. Despite an enlargement of

multivesicular bodies (MVBs) and possibly an increase in MVB fusion profiles at 1- 4 hrs post PDT, there was no clear evidence for an increased number of autophagosomes. However, the accumulation of LC3-II in MA11 and MA11/TR could indicate that the constitutive LC3-II turnover in the endo-/lysosomal pathway is reduced, possibly due to photochemical-induced damage to the membranes of the lysosomes, which was indeed revealed by the LTG micrographs post PDT. Interestingly, the ruptures of lysosomal membranes could indicate that LC3-II containing autophagic membranes are not degraded due to failure to be incorporated in the autolysosomal degradation pathway. However, we cannot rule out the possibility of increased autophagic activity due to the PDT-treatment, but this needs to be studied in more detail.

In summary, here we demonstrate that development and mechanisms of PDT-resistance after repeated cycles of PDT is both dependent on cell line and type of photosensitizer. The p38 MAPK signalling pathway is highly dysregulated in $TPCS_{2a}$-PDT-resistant cells, of which the MA11/TR cells have lost the p38-mediated cell death response after PDT, while PDT-induced death in MDA-MB-231/TR cells is independent of the p38 signalling. MA11/TR cells had a higher basal expression of EGFR and ERK1/2, and a stronger activation of P-STAT-3 upon $TPCS_{2a}$-PDT, which may explain their enhanced proliferation capacity as compared to the naïve MA11 cells. Acquired $TPCS_{2a}$-PDT-resistance did not result in development of cross-resistance to chemo- or radiotherapy, and no difference in mode of death distribution (necrosis, apoptosis or autophagy) after $TPCS_{2a}$-PDT. Finally, $TPCS_{2a}$-PCI-based targeting of EGFR overcome PDT-resistance and PCI will therefore be further evaluated for the treatment of therapy-resistant, aggressive and inoperable cancers.

5. ACKNOWLEDGEMENTS

We thank M.Sc. Idun Dale Rein, Dr. Kirsti Landsverk and Dr. Trond Stokke for helpful advices regarding flow cytometry. We also thank the Norwegian Radium Hospital Research Foundation, South-Eastern Norway Regional Health Authority (Helse Sør-Øst) and the Norwegian Research Council (SFI-CAST) for financial support.

Figure Legends

Fig.1.

Development of PDT-resistance is both photosensitizer and cell line dependent. (A) Cell viability of MA11 and MA11/PAR cells following Pheophorbide A-PDT (PhA concentration: 1 µM) with increasing light dose measured by MTT. PDT-resistance was measured one week after the last (third cycle of PDT and viability by MTT was assessed 24 hrs post light exposure. The data are the mean of triplicates in one individual experiment, which is a representative result out of 4 independent experiments. (Error bars =S.D.). (B) Immunocytochemical staining of ABCG2 in MA11 and MA11/PAR cells. The images are representative micrographs (out of 3 independent experiments) of bulk cells (non-sorted cell population) or side population cells (Hoechst 33342^{low} FACS cells). Green arrows indicate enhanced ABCG2 expression on the plasma membrane of MA11/TR side population cells as compared to MA11 bulk and side population cells. Scale bar: 20 µm. (C) Cellular viability (MTT, 24 hrs post light exposure) of MA11 and MA11/TR cells following $TPCS_{2a}$-PDT (0.5 µg/mL $TPCS_{2a}$) with increasing light doses. The data are the mean of triplicates, which is a representative experiment out of more than three separate experiments (*

= p<0.05, Error bars =S.D.). (D) Percentage cell confluence measured every 3 hrs for 300 hrs after 1 min $TPCS_{2a}$-PDT (0.5 µg/mL $TPCS_{2a}$) of MA11 and MA11/TR by IncuCyte live cell imaging system. The data are the mean of two individual experiments (Error bars =S.D.). (E) Representative images of non-treated (NT) and PDT treated cells 0, 24, 72, 150 and 300 hrs after 1 min $TPCS_{2a}$-PDT from the cell confluence experiment in (D) acquired with IncuCyte. (F) Cellular viability (MTT, assessed 24 hrs post light exposure) of MDA-MB-231 and MDA-MB-231/TR, and MCF-7 and MCF7/NTR (NTR = not $TPCS_{2a}$-PDT resistant after 3 cycles of PDT) following $TPCS_{2a}$-PDT (0.4 µg/mL $TPCS_{2a}$) with increasing light dose. The data are the mean of four individual experiments (Error bars =S.D.). Clonal cell viability (assessed 10-14 days after light exposure) of (G) MDA-MB-231 and MDA MB-231/TR cells, and (H) MCF-7 and MCF-7/NTR cells following $TPCS_{2a}$-PDT with increasing light dose. The data are the mean of three individual experiments (* =p<0.05, Error bars =S.D.).

Fig. 2.

No differences in $TPCS_{2a}$ uptake, localization and PDT-induced endo-/lysosomal destruction and ROS-generation in MA11 and MA11/TR cells. (A) Median DCF fluorescence (ROS formation) 1 hr after 1.5 and 5 min $TPCS_{2a}$-PDT, measured by Flow Cytometry. The data are representative for independent experiments. (B) Median fluorescence of $TPCS_{2a}$ after 18 hrs incubation + 4 hrs chase in drug-free medium, measured by flow cytometry. The data are the mean of three individual experiments normalized to MA11 cells (Error bars =S.D.). (C) Representative epi-fluorescence microscopy images of cells incubated with $TPCS_{2a}$ for 18 hrs and 0.33 µM LysoTracker Green (LTG) for 30 min before (for evaluation of co-localization with $TPCS_{2a}$) or 30 min after 1 min light exposure (PDT, to evaluate lysosomal photodamage). The experiments

were reproduced and fluorescence microscopy images are representative data. Scale bar: 20 µm.

Fig.3.

Cell cycle distribution of MA11 and MA11/TR cells before and after $TPCS_{2a}$-PDT. (A) MA11 and MA11/TR cells are to the same degree arrested in the G2/M cell cycle post $TPCS_{2a}$-PDT (0.5 µg/mL $TPCS_{2a}$ incubation for 18 hrs, prior to wash and 4 hrs chase in drug-free medium and light exposure). Flow cytometry analysis of cell cycle distribution analysis of control cells (NT) and cells harvested 20 hrs after 1 min of $TPCS_{2a}$-PDT. DNA content is based on Hoechst 33258 signal. (B) Average values (%) for each cycle phase. The cell cycles are representative of three individual experiments.

Fig. 4.

$TPCS_{2a}$-resistant MA11/TR cells have neither acquired cross-resistance to chemo- nor radiotherapy. (A) Relative viability/metabolic activity (MTT) following 72 hrs doxorubicin treatment. The data are the mean of three individual experiments (Error bars =S.D.). (B) Clonal cell viability following increasing doses of ionizing radiation. The data are the mean of three individual experiments (Error bars =S.D.).

Fig. 5.

Distribution of dead cells undergoing apoptosis or necrosis. (A) Median distribution of apoptotic and necrotic cells (normalized to total 100%) undergoing apoptosis (measured by TUNEL assay) and necrosis (measured by PI and TO staining) upon 1 and 5 min $TPCS_{2a}$-PDT measured by flow

cytometry. The data are the mean of three individual experiments (Error bars =S.D.). Relative expression, as determined by ELISA, of apoptosis-associated proteins in MA11 (B) and MA11/TR (C) cells harvested 20 hrs after 1.5 min $TPCS_{2a}$-PDT. The data are normalized to total protein content as measured by the DC Protein Assay, and are the mean of three individual experiments (Error bars = S.D.).

Fig.6.

Increased LC3-I to II conversion 20 hrs post $TPCS_{2a}$-PDT does not result in formation of autophagosomes. Percentage of cells with >2 LC3 puncta (A), and the number of LC3 puncta per cell (B) after 1.5 min $TPCS_{2a}$-PDT resulting in 25-35% (MA11) and for 15-20% (MA11/TR) viable cell metabolism (0.35 µg/mL $TPCS_{2a}$). The data are the average of two individual experiments of the mean of 4 x 10^4 cells seeded on 3 cover slips per cell line. (Error bars =S.D.) Significance was assessed by the two-way ANOVA with Bonferroni correction using prism (* =$p<0.001$). Abbreviations in figure: Cntrl = non-treated control; $TPCS_{2a}$ = photosensitizer only; PDT = photosensitizer + light. (C) Representative LC3 puncta fluorescence (green) micrographs of untreated MA11 and MA11/TR cells and cells treated with TPCS2a-PDT 20 hrs post light exposure (same condition as for A and B). Blue fluorescence: nucleus stained with Hoechst 33342. (D) Western blot of LC3-I to –II conversion 20 hrs after 1 min $TPCS_{2a}$-PDT (0.5 µg/mL $TPCS_{2a}$, resulting in approximately the same degree of reduction in viability as in A and B). The blot is representative for more than three individual experiments. Loading was controlled by equal DNA application (measured by DNA absorbance), and Ponceau S. stain of the membranes. N.S.= no statistical difference in LC3 signals between MA11 and MA11/TR cells. (E) Representative electron micrographs of untreated (NT) and PDT treated MA11 and MA11/TR 1,

2, 4 and 20 hrs after 1 min $TPCS_{2a}$-PDT. The micrographs for the 1-2 hrs time-points are representative from at least two individual experiments. Multivescicular bodies (MVBs) are marked with black arrows.

Fig. 7.

$TPCS_{2a}$-PDT resistant breast cancer cells have dysregulated p38MAPK signalling, but loss of its death signalling pathway is cell line dependent. (A) Representative Western blot of phospho-p38 (p-p38) from MA11 and MA11/TR cells from three individual experiments harvested at 5 min, 2 and 20 hrs after 1 min $TPCS_{2a}$-PDT. (B) Cell viability measured by MTT (48 hrs post light exposure) of MA11 cells treated with $TPCS_{2a}$-PDT and 20 μM of the p38 inhibitor SB203580, which was added to the cells 1 hr before light exposure and removed 1.5 hr after $TPCS_{2a}$-PDT. The data are representative of three individual experiments (Error bars = S.D.). Significance was assessed by the paired t-test of the mean from these three experiments (*1 min PDT: $p<0.05$) (C) Western blot of p-MK2 on Thr222 from MA11 and MA11/TR cells two hrs after 1 min $TPCS_{2a}$-PDT with and without combination with 20 μM p38 inhibitor SB203580. The blot is a representative experiment of three individual experiments. (D) MA11/TR viability as in (B). The data are the mean of three individual experiments (Error bars =S.D.). Cell viability measured by MTT of (E) MDA-MB-231, and (F) MCF-7 cells treated with $TPCS_{2a}$-PDT and the combination with 20 μM of the p38 inhibitor SB203580. The data are the mean of three individual experiments (Error bars =S.D.). (G) Western blot of phospho-MK2 (P-MK2) in MDA-MB-231 and MDA-MB-231/TR cells harvested at 2 and 24 hrs after 1 min $TPCS_{2a}$-PDT with the combination of 20 μM p38 inhibitor SB203580. The blot is representative from three individual experiments. All the loadings were controlled by Ponceau S. stains.

Fig. 8.

Enhanced activation of ERK1/2 and STAT-3 post $TPCS_{2a}$-PDT in MA11/TR cells. Relative expression of growth-associated proteins in MA11 (A) and MA11/TR. (B) cells harvested 5 min after 1.5 min $TPCS_{2a}$-PDT. The data are normalized to total protein content as measured by the DC Protein Assay, and are the mean of two individual experiments (Error bars =S.D.). Western blots of (C) ERK1/2, (D) phospho-ERK1/2, (E) STAT-3 and (F) phospho-STAT-3 of cells harvested at increasing time points after 1 min $TPCS_{2a}$-PDT together with untreated control cells (NT). WBs are representative of three individual experiments. Quantification of total proteins were normalized to the NT (20 hrs) sample, and the phosphoproteins to the respective total proteins at each harvest time point. Even protein loading across lanes was visually confirmed by Ponceau S. stain.

Fig.9.

Photochemical internalization of EGF-saporin overcomes PDT-resistance in the EGFR overexpressing MA11/TR cells. (A) Representative Western blot of EGFR of cells harvested at increasing time points after 1 min TPCS2a-PDT (0.5 ug/mL $TPCS_{2a}$) together with untreated control cells (NT). Quantification is based on band densitometry and normalized to the NT sample at the 20 hrs time point. The data are the mean of three individual blots (Error bars = S.D.). Even protein loading across lanes was visually confirmed by Ponceau S. stain. (B) Representative immunocytochemical (ICC) staining of EGFR in MA11 and MA11/TR cells. The nuclei were counter stained with hematoxylin (blue). (C) Assessment of cytotoxic responses

(metabolic activity/viability assessed by MTT) 72 hrs after $TPCS_{2a}$-PCI of 1 pM EGF-saporin versus PDT in MA11 cells and MA11/TR cells ($TPCS_{2a}$ concentration: 0.5 µg/mL). The data points are the average of two independent experiments. A third experiment with higher drug doses gave higher cytotoxic responses however, replicated the same trend. P-values ($p<0.01$) inserted show statistical significant differences in PDT-responses between MA11 and MA11/TR cells. Error bars: S.D.

6. REFERENCES

[1] M.M. Gottesman, Mechanisms of cancer drug resistance, Annu Rev Med 53 (2002) 615-627.
[2] A. Casas, G. Di Venosa, T. Hasan, A. Batlle, Mechanisms of resistance to photodynamic therapy, Curr Med Chem 18(16) (2011) 2486-2515.
[3] Y. Gilaberte, L. Milla, N. Salazar, J. Vera-Alvarez, O. Kourani, A. Damian, V. Rivarola, M.J. Roca, J. Espada, S. González, A. Juarranz, Cellular intrinsic factors involved in the resistance of squamous cell carcinoma to photodynamic therapy, J Invest Dermatol 134(9) (2014) 2428-2437.
[4] P. Agostinis, K. Berg, K.A. Cengel, T.H. Foster, A.W. Girotti, S.O. Gollnick, S.M. Hahn, M.R. Hamblin, A. Juzeniene, D. Kessel, M. Korbelik, J. Moan, P. Mroz, D. Nowis, J. Piette, B.C. Wilson, J. Golab, Photodynamic therapy of cancer: an update, CA Cancer J Clin 61(4) (2011) 250-281.
[5] H.P. Wang, S.Y. Qian, F.Q. Schafer, F.E. Domann, L.W. Oberley, G.R. Buettner, Phospholipid hydroperoxide glutathione peroxidase protects against singlet oxygen-induced cell damage of photodynamic therapy, Free Radic Biol Med 30(8) (2001) 825-835.
[6] Z. Tong, G. Singh, A.J. Rainbow, Sustained activation of the extracellular signal-regulated kinase pathway protects cells from photofrin-mediated photodynamic therapy, Cancer Res 62(19) (2002) 5528-5535.
[7] A. Weyergang, P.K. Selbo, K. Berg, Sustained ERK [corrected] inhibition by EGFR targeting therapies is a predictive factor for synergistic cytotoxicity with PDT as neoadjuvant therapy, Biochim Biophys Acta 1830(3) (2013) 2659-2670.
[8] C. Edmonds, S. Hagan, S.M. Gallagher-Colombo, T.M. Busch, K.A. Cengel, Photodynamic therapy activated signaling from epidermal growth factor receptor and STAT3: Targeting survival pathways to increase PDT efficacy in ovarian and lung cancer, Cancer Biol Ther 13(14) (2012) 1463-1470.
[9] A.C. Moor, Signaling pathways in cell death and survival after photodynamic therapy, J Photochem Photobiol B 57(1) (2000) 1-13.

[10] Z. Assefa, A. Vantieghem, W. Declercq, P. Vandenabeele, J.R. Vandenheede, W. Merlevede, P. de Witte, P. Agostinis, The activation of the c-Jun N-terminal kinase and p38 mitogen-activated protein kinase signaling pathways protects HeLa cells from apoptosis following photodynamic therapy with hypericin, J Biol Chem 274(13) (1999) 8788-8796.
[11] M.C. Luna, C.J. Gomer, Isolation and initial characterization of mouse tumor cells resistant to porphyrin-mediated photodynamic therapy, Cancer Res 51(16) (1991) 4243-4249.
[12] G. Singh, M. Espiritu, X.Y. Shen, J.G. Hanlon, A.J. Rainbow, In vitro induction of PDT resistance in HT29, HT1376 and SK-N-MC cells by various photosensitizers, Photochem Photobiol 73(6) (2001) 651-656.
[13] A.A. Sultan, W. Jerjes, K. Berg, A. Høgset, C.A. Mosse, R. Hamoudi, Z. Hamdoon, C. Simeon, D. Carnell, M. Forster, C. Hopper, Disulfonated tetraphenyl chlorin (TPCS2a)-induced photochemical internalisation of bleomycin in patients with solid malignancies: a phase 1, dose-escalation, first-in-man trial, The Lancet. Oncology 17 (2016) 1217-1229.
[14] P.K. Selbo, A. Weyergang, A. Høgset, O.-J. Norum, M.B. Berstad, M. Vikdal, K. Berg, Photochemical internalization provides time- and space-controlled endolysosomal escape of therapeutic molecules, J Control Release 148(1) (2010) 2-12.
[15] A. Weyergang, M.E.B. Berstad, B. Bull-Hansen, C.E. Olsen, P.K. Selbo, K. Berg, Photochemical activation of drugs for the treatment of therapy-resistant cancers, Photochem Photobiol Sci 14(8) (2015) 1465-1475.
[16] P.K. Selbo, A. Weyergang, A. Bonsted, S.G. Bown, K. Berg, Photochemical internalization of therapeutic macromolecular agents: a novel strategy to kill multidrug-resistant cancer cells, J Pharmacol Exp Ther 319(2) (2006) 604-612.
[17] C.E. Olsen, K. Berg, P.K. Selbo, A. Weyergang, Circumvention of resistance to photodynamic therapy in doxorubicin-resistant sarcoma by photochemical internalization of gelonin, Free Radic Biol Med 65 (2013) 1300-1309.
[18] P.K. Selbo, M. Bostad, C.E. Olsen, V.T. Edwards, A. Høgset, A. Weyergang, K. Berg, Photochemical internalisation, a minimally invasive strategy for light-controlled endosomal escape of cancer stem cell-targeting therapeutics, Photochem. Photobiol. Sci (2015).
[19] R.W. Robey, K. Steadman, O. Polgar, S.E. Bates, ABCG2-mediated transport of photosensitizers: potential impact on photodynamic therapy, Cancer Biol Ther 4(2) (2005) 187-194.
[20] J. Morgan, J.D. Jackson, X. Zheng, S.K. Pandey, R.K. Pandey, Substrate affinity of photosensitizers derived from chlorophyll-a: the ABCG2 transporter affects the phototoxic response of side population stem cell-like cancer cells to photodynamic therapy, Mol Pharm 7(5) (2010) 1789-1804.
[21] P.K. Selbo, A. Weyergang, M.S. Eng, M. Bostad, G.M. Mælandsmo, A. Høgset, K. Berg, Strongly amphiphilic photosensitizers are not substrates of the cancer stem cell marker ABCG2 and provides specific and efficient light-triggered drug delivery of an EGFR-targeted cytotoxic drug, J Control Release 159(2) (2012) 197-203.
[22] A. Weyergang, P.K. Selbo, K. Berg, Photochemically stimulated drug delivery increases the cytotoxicity and specificity of EGF-saporin, J Control Release 111(1-2) (2006) 165-173.

[23] A. Weyergang, P.K. Selbo, K. Berg, Y1068 phosphorylation is the most sensitive target of disulfonated tetraphenylporphyrin-based photodynamic therapy on epidermal growth factor receptor, Biochem Pharmacol 74(2) (2007) 226-235.
[24] C.E. Olsen, K. Berg, P.K. Selbo, A. Weyergang, Circumvention of resistance to photodynamic therapy in doxorubicin-resistant sarcoma by photochemical internalization of gelonin, Free Radic.Biol.Med. 65 (2013) 1300-1309.
[25] A. Weyergang, O. Kaalhus, K. Berg, Photodynamic therapy with an endocytically located photosensitizer cause a rapid activation of the mitogen-activated protein kinases extracellular signal-regulated kinase, p38, and c-Jun NH2 terminal kinase with opposing effects on cell survival, Mol.Cancer Ther. 7(6) (2008) 1740-1750.
[26] Z. Darzynkiewicz, D. Galkowski, H. Zhao, Analysis of apoptosis by cytometry using TUNEL assay, Methods 44(3) (2008) 250-254.
[27] J.W. Jonker, M. Buitelaar, E. Wagenaar, M.A. Van Der Valk, G.L. Scheffer, R.J. Scheper, T. Plosch, F. Kuipers, R.P.J.O. Elferink, H. Rosing, J.H. Beijnen, A.H. Schinkel, The breast cancer resistance protein protects against a major chlorophyll-derived dietary phototoxin and protoporphyria, Proc Natl Acad Sci U S A 99(24) (2002) 15649-15654.
[28] M. Bostad, M. Kausberg, A. Weyergang, C.E. Olsen, K. Berg, A. Høgset, P.K. Selbo, Light-triggered, efficient cytosolic release of IM7-saporin targeting the putative cancer stem cell marker CD44 by photochemical internalization, Mol Pharm 11(8) (2014) 2764-2776.
[29] R. Ben-Levy, I.A. Leighton, Y.N. Doza, P. Attwood, N. Morrice, C.J. Marshall, P. Cohen, Identification of novel phosphorylation sites required for activation of MAPKAP kinase-2, EMBO J 14(23) (1995) 5920-5930.
[30] A. Zamarrón, S.R. Lucena, N. Salazar, F. Sanz-Rodríguez, P. Jaén, Y. Gilaberte, S. González, Á. Juarranz, Isolation and characterization of PDT-resistant cancer cells, Photochem Photobiol Sci. 14 (2015) 1378-1389.
[31] S.R. Lucena, N. Salazar, T. Gracia-Cazana, A. Zamarron, S. Gonzalez, A. Juarranz, Y. Gilaberte, Combined Treatments with Photodynamic Therapy for Non-Melanoma Skin Cancer, Int J Mol Sci 16(10) (2015) 25912-33.
[32] J.C. Haller, F. Cairnduff, G. Slack, J. Schofield, C. Whitehurst, R. Tunstall, S.B. Brown, D.J. Roberts, Routine double treatments of superficial basal cell carcinomas using aminolaevulinic acid-based photodynamic therapy, Br J Dermatol 143(6) (2000) 1270-1275.
[33] C. Morton, M. Horn, J. Leman, B. Tack, C. Bedane, M. Tjioe, S. Ibbotson, A. Khemis, P. Wolf, Comparison of topical methyl aminolevulinate photodynamic therapy with cryotherapy or Fluorouracil for treatment of squamous cell carcinoma in situ: Results of a multicenter randomized trial, Arch Dermatol 142(6) (2006) 729-735.
[34] W. Jerjes, T. Upile, Z. Hamdoon, C. Alexander Mosse, M. Morcos, C. Hopper, Photodynamic therapy outcome for T1/T2 N0 oral squamous cell carcinoma, Lasers Surg Med 43(6) (2011) 463-469.
[35] D.M. Pariser, N.J. Lowe, D.M. Stewart, M.T. Jarratt, A.W. Lucky, R.J. Pariser, P.S. Yamauchi, Photodynamic therapy with topical methyl aminolevulinate for actinic keratosis: results of a prospective randomized multicenter trial, J Am Acad Dermatol 48(2) (2003) 227-232.

[36] A. Salim, J.A. Leman, J.H. McColl, R. Chapman, C.A. Morton, Randomized comparison of photodynamic therapy with topical 5-fluorouracil in Bowen's disease, Br J Dermatol 148(3) (2003) 539-543.
[37] J. Kralova, M. Kolar, M. Kahle, J. Truksa, S. Lettlova, K. Balusikova, P. Bartunek, Glycol porphyrin derivatives and temoporfin elicit resistance to photodynamic therapy by different mechanisms, Sci Rep 7 (2017) 44497.
[38] L.N. Milla, I.S. Cogno, M.E. Rodriguez, F. Sanz-Rodriguez, A. Zamarron, Y. Gilaberte, E. Carrasco, V.A. Rivarola, A. Juarranz, Isolation and characterization of squamous carcinoma cells resistant to photodynamic therapy, J Cell Biochem 112(9) (2011) 2266-78.
[39] H.-C. Lee, D.-W. Kim, K.-Y. Jung, I.-C. Park, M.-J. Park, M.-S. Kim, S.-H. Woo, C.-H. Rhee, H. Yoo, S.-H. Lee, S.-I. Hong, Increased expression of antioxidant enzymes in radioresistant variant from U251 human glioblastoma cell line, Int J Mol Med 13(6) (2004) 883-887.
[40] A. Weyergang, O. Kaalhus, K. Berg, Photodynamic therapy with an endocytically located photosensitizer cause a rapid activation of the mitogen-activated protein kinases extracellular signal-regulated kinase, p38, and c-Jun NH2 terminal kinase with opposing effects on cell survival, Mol Cancer Ther 7(6) (2008) 1740-1750.
[41] L.O. Klotz, C. Fritsch, K. Briviba, N. Tsacmacidis, F. Schliess, H. Sies, Activation of JNK and p38 but not ERK MAP kinases in human skin cells by 5-aminolevulinate-photodynamic therapy, Cancer Res 58(19) (1998) 4297-4300.
[42] N. Herranz, S. Gallage, M. Mellone, T. Wuestefeld, S. Klotz, C.J. Hanley, S. Raguz, J.C. Acosta, A.J. Innes, A. Banito, A. Georgilis, A. Montoya, K. Wolter, G. Dharmalingam, P. Faull, T. Carroll, J.P. Martinez-Barbera, P. Cutillas, F. Reisinger, M. Heikenwalder, R.A. Miller, D. Withers, L. Zender, G.J. Thomas, J. Gil, mTOR regulates MAPKAPK2 translation to control the senescence-associated secretory phenotype, Nat Cell Biol 17(9) (2015) 1205-17.
[43] M. Cargnello, P.P. Roux, Activation and function of the MAPKs and their substrates, the MAPK-activated protein kinases, Microbiol Mol Biol Rev 75(1) (2011) 50-83.
[44] K. Takenaka, T. Moriguchi, E. Nishida, Activation of the protein kinase p38 in the spindle assembly checkpoint and mitotic arrest, Science (New York, N.Y.) 280 (1998) 599-602.
[45] A. Kotlyarov, A. Neininger, C. Schubert, R. Eckert, C. Birchmeier, H.D. Volk, M. Gaestel, MAPKAP kinase 2 is essential for LPS-induced TNF-alpha biosynthesis, Nat Cell Biol 1(2) (1999) 94-97.
[46] F. Köpper, C. Bierwirth, M. Schön, M. Kunze, I. Elvers, D. Kranz, P. Saini, M.B. Menon, D. Walter, C.S. Sørensen, M. Gaestel, T. Helleday, M.P. Schön, M. Dobbelstein, Damage-induced DNA replication stalling relies on MAPK-activated protein kinase 2 activity, Proc Natl Acad Sci U S A 110(42) (2013) 16856-16861.
[47] S. Varma, P.J. Holt, A.V. Anstey, Erythroplasia of queyrat treated by topical aminolaevulinic acid photodynamic therapy: a cautionary tale, Br J Dermatol 142(4) (2000) 825-826.
[48] P. Wolf, R. Fink-Puches, A. Reimann-Weber, H. Kerl, Development of malignant melanoma after repeated topical photodynamic therapy with 5-aminolevulinic acid at the exposed site, Dermatology 194(1) (1997) 53-54.
[49] E. Maydan, P.K. Nootheti, M.P. Goldman, Development of a keratoacanthoma after topical photodynamic therapy with 5-aminolevulinic acid, J Drugs Dermatol 5(8) (2006) 804-806.

[50] A. Weyergang, O. Kaalhus, K. Berg, Photodynamic targeting of EGFR does not predict the treatment outcome in combination with the EGFR tyrosine kinase inhibitor Tyrphostin AG1478, Photochem Photobiol Sci 7(9) (2008) 1032-1040.
[51] W. Liu, A.R. Oseroff, H. Baumann, Photodynamic therapy causes cross-linking of signal transducer and activator of transcription proteins and attenuation of interleukin-6 cytokine responsiveness in epithelial cells, Cancer Res 64(18) (2004) 6579-6587.
[52] N. Ahmad, K. Kalka, H. Mukhtar, In vitro and in vivo inhibition of epidermal growth factor receptor-tyrosine kinase pathway by photodynamic therapy, Oncogene 20(18) (2001) 2314-2317.
[53] M.R. Junttila, S.-P. Li, J. Westermarck, Phosphatase-mediated crosstalk between MAPK signaling pathways in the regulation of cell survival, FASEB J 22(4) (2008) 954-965.
[54] T.G. Gantchev, N. Brasseur, J.E. van Lier, Combination toxicity of etoposide (VP-16) and photosensitisation with a water-soluble aluminium phthalocyanine in K562 human leukaemic cells, Br J Cancer 74(10) (1996) 1570-1577.
[55] D. Grebenová, H. Cajthamlová, K. Holada, J. Marinov, M. Jirsa, Z. Hrkal, Photodynamic effects of meso-tetra (4-sulfonatophenyl)porphine on human leukemia cells HEL and HL60, human lymphocytes and bone marrow progenitor cells, J Photochem Photobiol B 39(3) (1997) 269-278.
[56] A. Vantieghem, Y. Xu, Z. Assefa, J. Piette, J.R. Vandenheede, W. Merlevede, P.A.M. De Witte, P. Agostinis, Phosphorylation of Bcl-2 in G2/M phase-arrested cells following photodynamic therapy with hypericin involves a CDK1-mediated signal and delays the onset of apoptosis, J Biol Chem 277(40) (2002) 37718-37731.
[57] K. Berg, S. Nordstrand, P.K. Selbo, D.T.T. Tran, E. Angell-Petersen, A. Høgset, Disulfonated tetraphenyl chlorin (TPCS2a), a novel photosensitizer developed for clinical utilization of photochemical internalization, Photochem Photobiol Sci 10(10) (2011) 1637-1651.
[58] A. Weyergang, P.K. Selbo, M.E.B. Berstad, M. Bostad, K. Berg, Photochemical internalization of tumor-targeted protein toxins, Lasers Surg Med 43(7) (2011) 721-733.
[59] B. Bull-Hansen, Y. Cao, K. Berg, E. Skarpen, M.G. Rosenblum, A. Weyergang, Photochemical activation of the recombinant HER2-targeted fusion toxin MH3-B1/rGel; Impact of HER2 expression on treatment outcome, J Control Release 182 (2014) 58-66.
[60] K. Eiklid, S. Olsnes, A. Pihl, Entry of lethal doses of abrin, ricin and modeccin into the cytosol of HeLa cells, Exp Cell Res 126(2) (1980) 321-326.
[61] X. Fang, S. Yu, A. Eder, M. Mao, J. Bast, R. C., D. Boyd, G.B. Mills, Regulation of BAD phosphorylation at serine 112 by the Ras-mitogen-activated protein kinase pathway, Oncogene 18(48) (1999) 6635-6640.
[62] S.R. Datta, H. Dudek, X. Tao, S. Masters, H. Fu, Y. Gotoh, M.E. Greenberg, Akt phosphorylation of BAD couples survival signals to the cell-intrinsic death machinery, Cell 91(2) (1997) 231-241.

Fig. 1

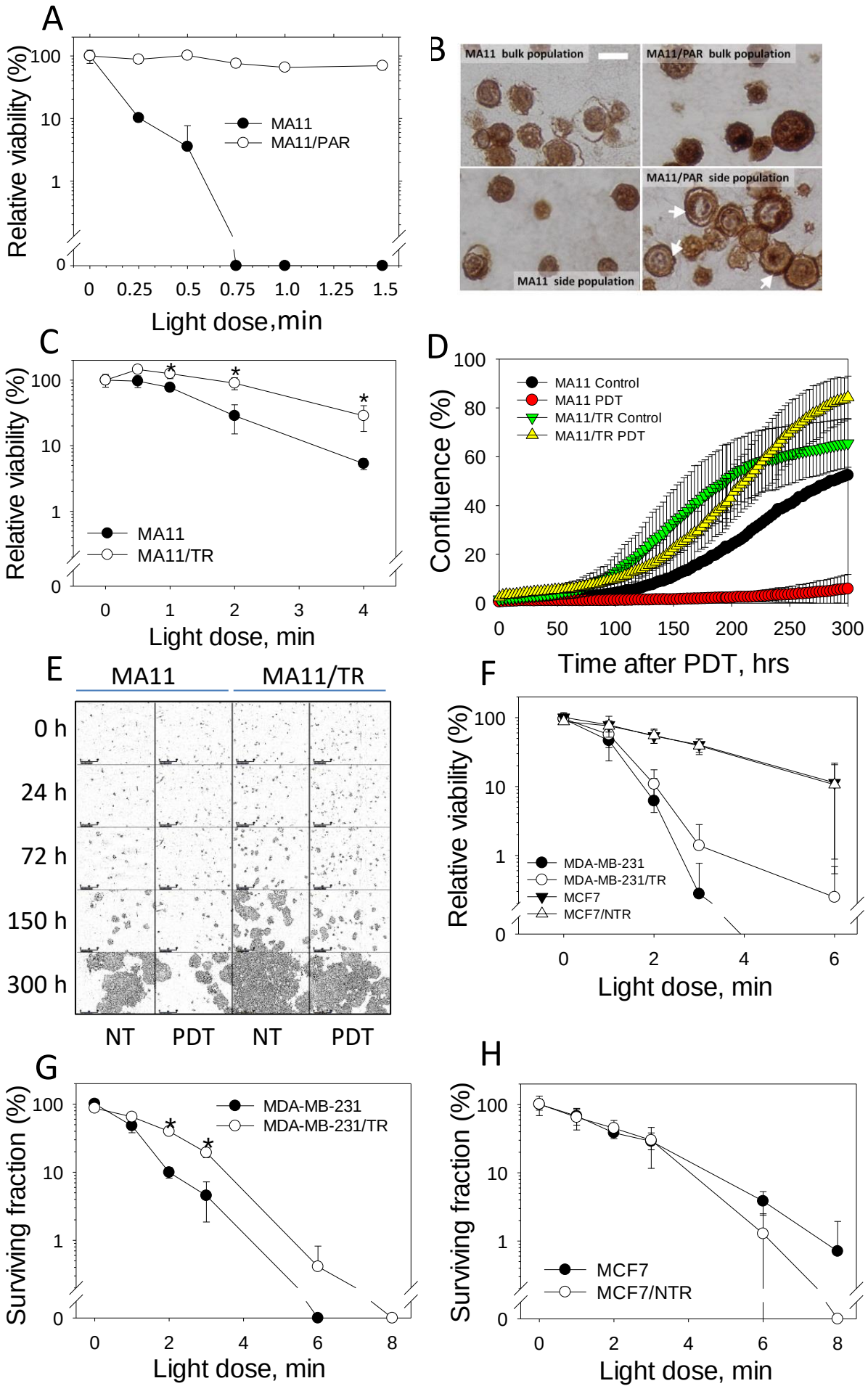
A
Relative viability (%)
MA11
MA11/PAR
Light dose,min
B
MA11 bulk population
MA11/PAR bulk population
MA11 side population
MA11/PAR side population
C
Relative viability (%)
MA11
MA11/TR
Light dose, min
D
Confluence (%)
MA11 Control
MA11 PDT
MA11/TR Control
MA11/TR PDT
Time after PDT, hrs
E
MA11
MA11/TR
0 h
24 h
72 h
150 h
300 h
NT
PDT
NT
PDT
F
Relative viability (%)
MDA-MB-231
MDA-MB-231/TR
MCF7
MCF7/NTR
Light dose, min
G
Surviving fraction (%)
MDA-MB-231
MDA-MB-231/TR
Light dose, min
H
Surviving fraction (%)
MCF7
MCF7/NTR
Light dose, min

Fig. 2

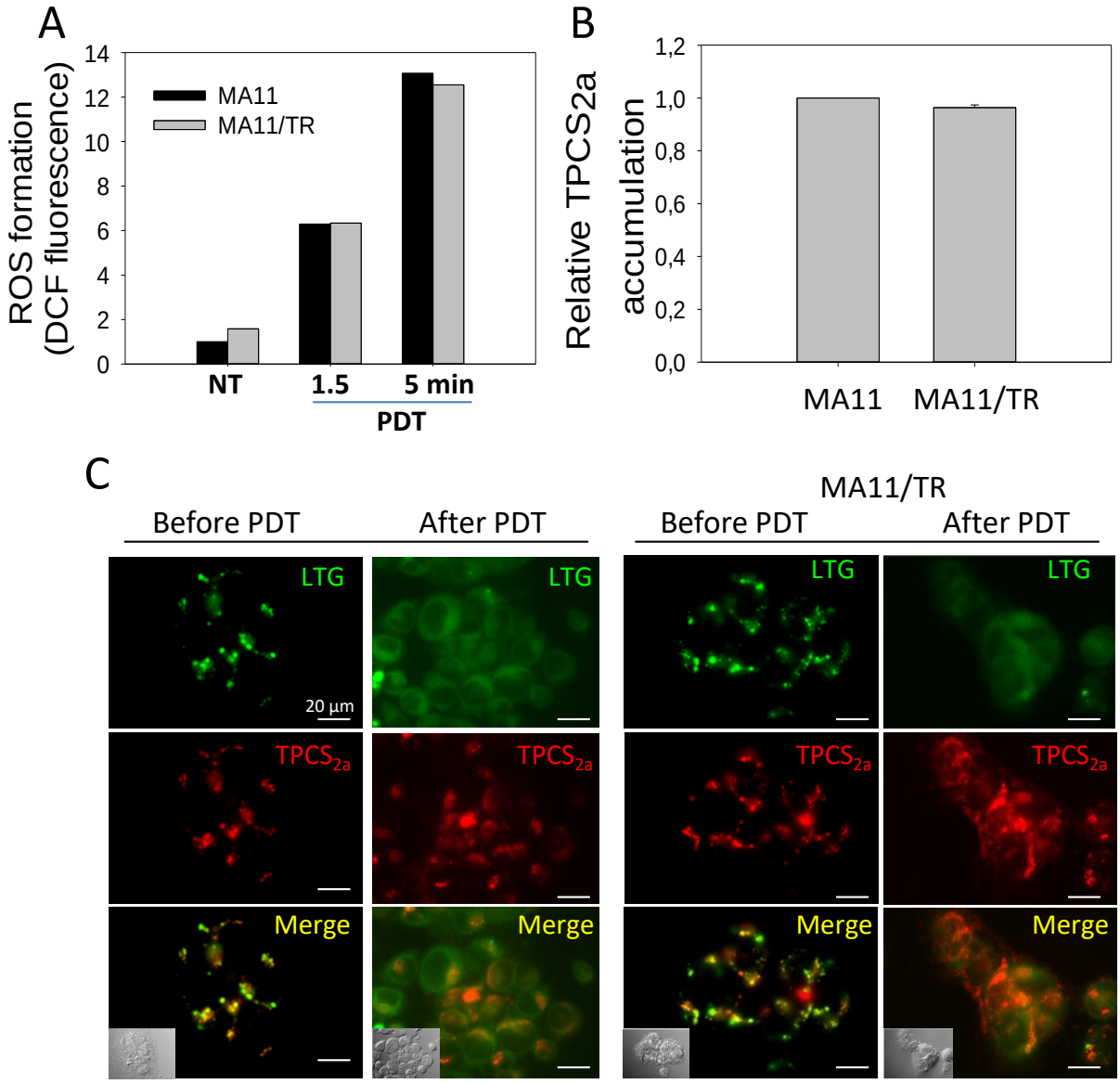
A
ROS formation (DCF fluorescence)
14
12
10
8
6
4
2
0
MA11
MA11/TR
NT
1.5
5 min
PDT
B
Relative TPCS2a accumulation
1,2
1,0
0,8
0,6
0,4
0,2
0,0
MA11
MA11/TR
C
Before PDT
After PDT
MA11/TR
Before PDT
After PDT
LTG
20 µm
TPCS2a
Merge

Fig. 3

A

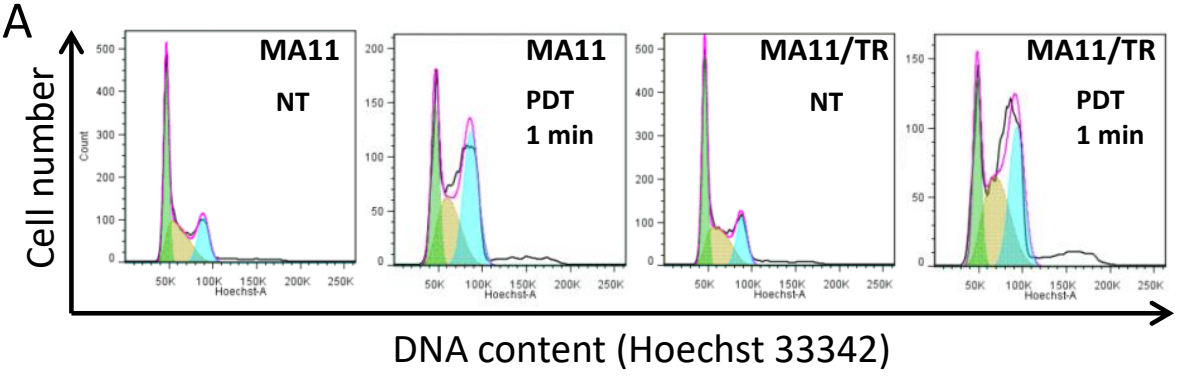

B

	MA11		MA11 PDT		MA11/TR		MA11/TR PDT	
	Average	SE	Average	SE	Average	SE	Average	SE
G1	40,50	1,01	22,10	0,89	38,70	0,96	20,73	0,81
S	34,27	0,88	33,70	3,20	31,63	0,59	38,20	1,02
G2/M	19,67	0,75	37,47	2,15	22,80	1,63	31,70	0,83
SuperG2	4,42	0,62	5,24	0,62	6,08	0,66	6,14	0,47

Fig. 4

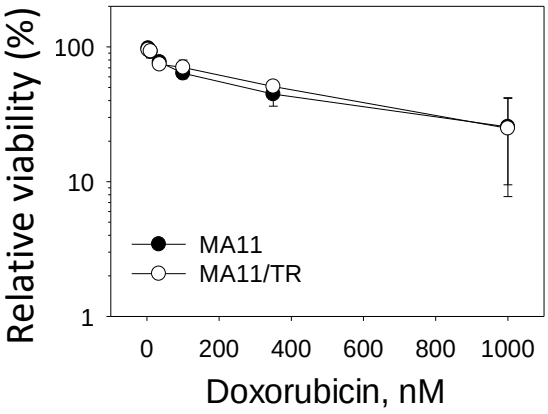
Relative viability (%)
100
10
1
0
200
400
600
800
1000
Doxorubicin, nM
MA11
MA11/TR

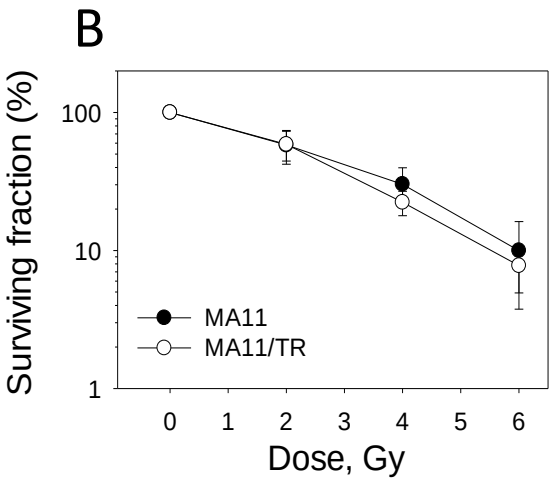
B
Surviving fraction (%)
100
10
1
0
1
2
3
4
5
6
Dose, Gy
MA11
MA11/TR

Fig. 5

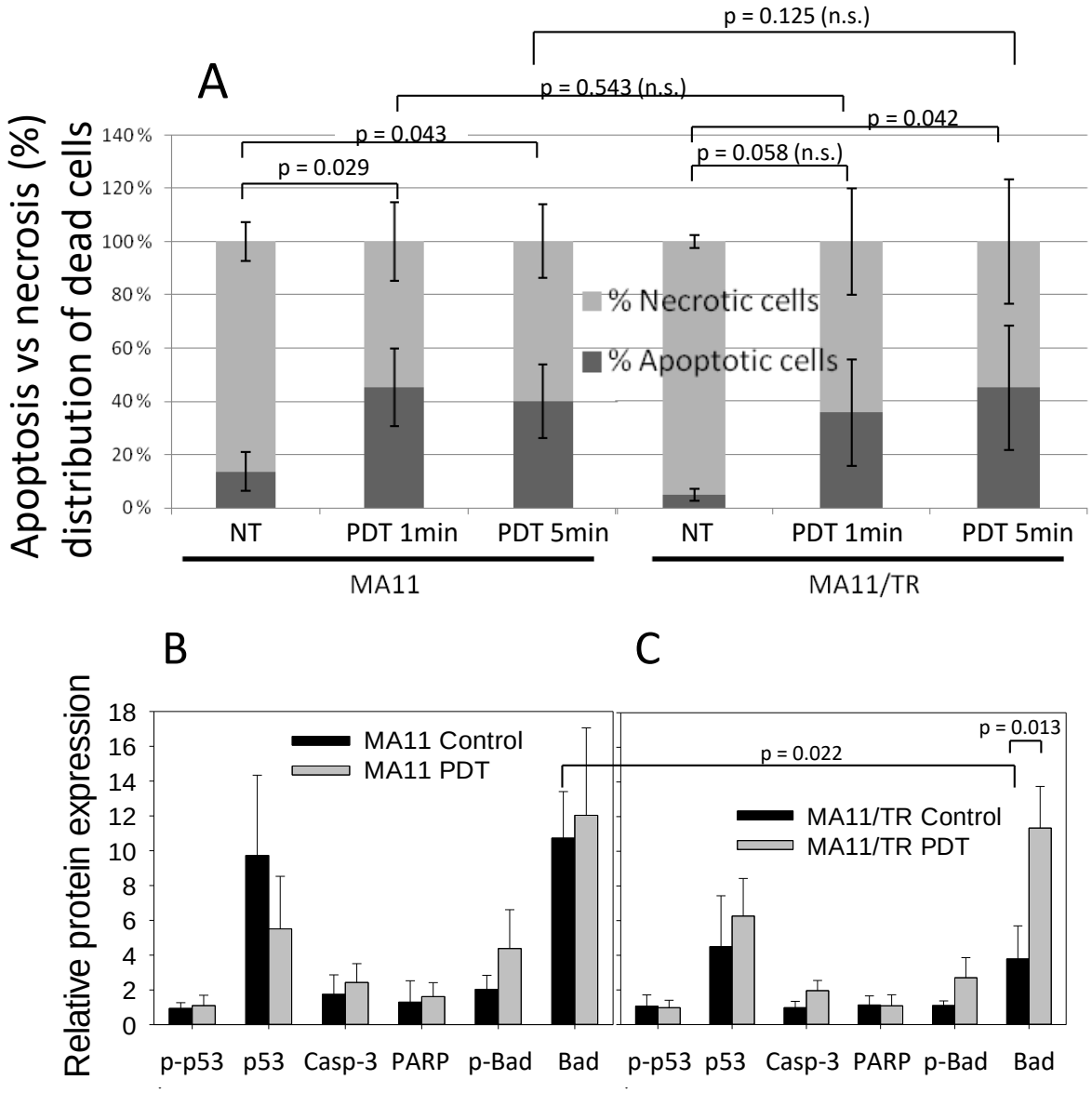
A
Apoptosis vs necrosis (%)
distribution of dead cells
140 %
120 %
100 %
80 %
60 %
40 %
20 %
0 %
p = 0.125 (n.s.)
p = 0.543 (n.s.)
p = 0.042
p = 0.043
p = 0.058 (n.s.)
p = 0.029
% Necrotic cells
% Apoptotic cells
NT
PDT 1min
PDT 5min
NT
PDT 1min
PDT 5min
MA11
MA11/TR
B
C
Relative protein expression
18
16
14
12
10
8
6
4
2
0
MA11 Control
MA11 PDT
p = 0.022
p = 0.013
MA11/TR Control
MA11/TR PDT
p-p53
p53
Casp-3
PARP
p-Bad
Bad
p-p53
p53
Casp-3
PARP
p-Bad
Bad

Fig. 6

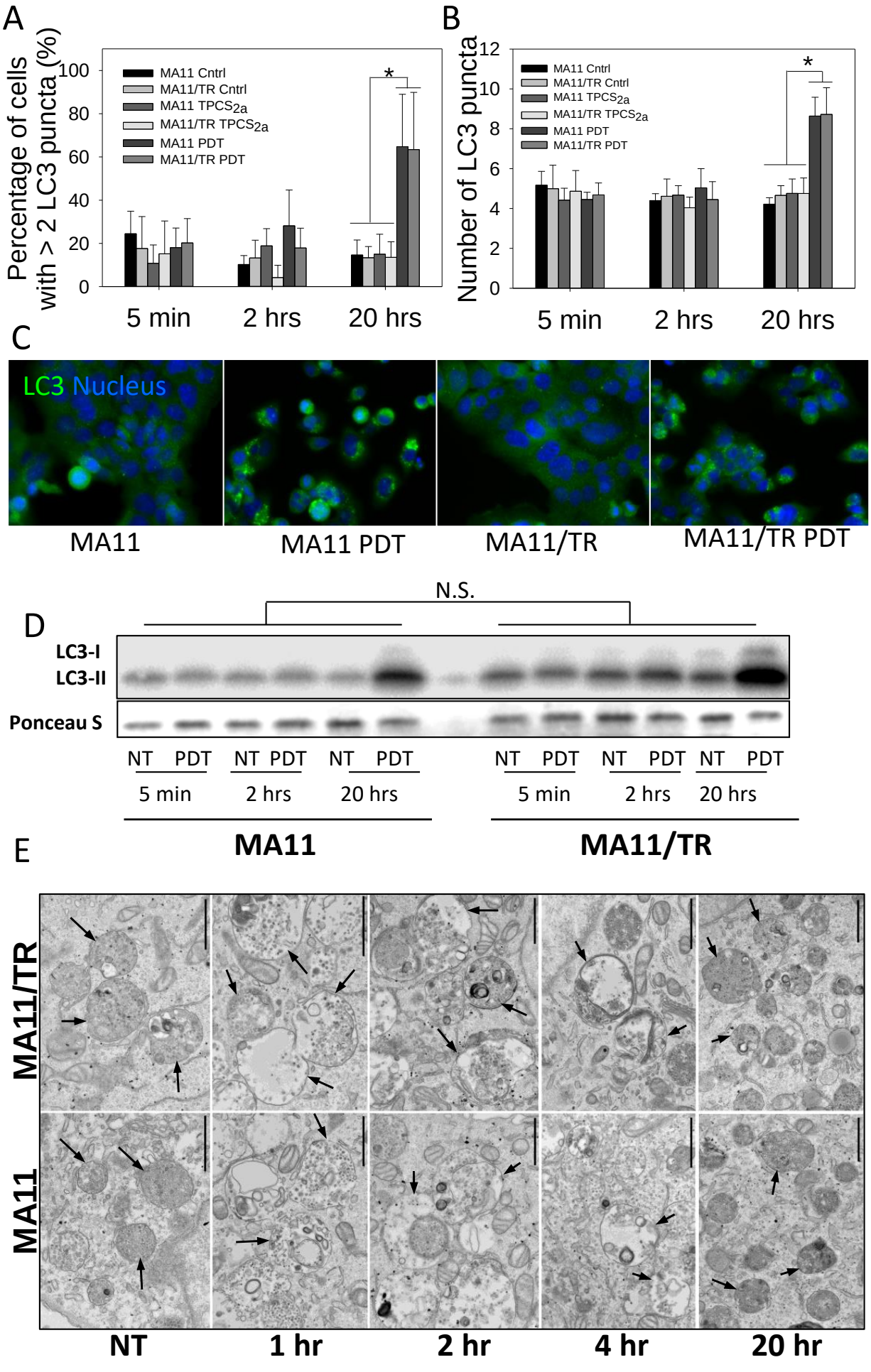
A
Percentage of cells with > 2 LC3 puncta (%)
MA11 Cntrl
MA11/TR Cntrl
MA11 TPCS2a
MA11/TR TPCS2a
MA11 PDT
MA11/TR PDT
*
5 min
2 hrs
20 hrs
B
Number of LC3 puncta
C
LC3 Nucleus
MA11
MA11 PDT
MA11/TR
MA11/TR PDT
D
N.S.
LC3-I
LC3-II
Ponceau S
NT PDT
5 min
2 hrs
20 hrs
MA11
MA11/TR
E
MA11/TR
MA11
NT
1 hr
2 hr
4 hr
20 hr

Fig. 7

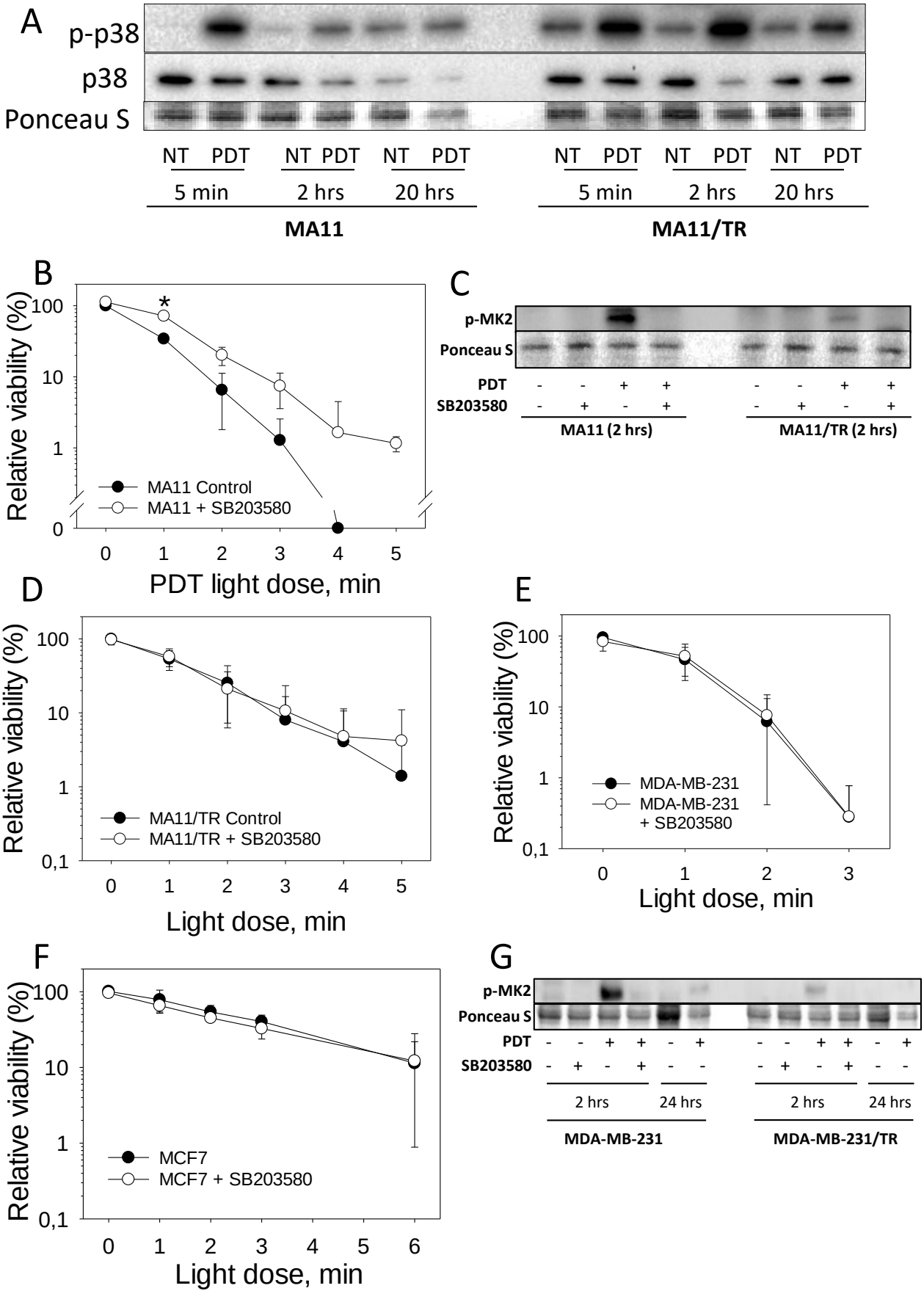
A
p-p38
p38
Ponceau S
NT PDT NT PDT NT PDT NT PDT NT PDT NT PDT
5 min 2 hrs 20 hrs 5 min 2 hrs 20 hrs
MA11
MA11/TR
B
Relative viability (%)
100
10
1
0
*
MA11 Control
MA11 + SB203580
0 1 2 3 4 5
PDT light dose, min
C
p-MK2
Ponceau S
PDT - - + + - - + +
SB203580 - + - + - + - +
MA11 (2 hrs)
MA11/TR (2 hrs)
D
Relative viability (%)
100
10
1
0,1
MA11/TR Control
MA11/TR + SB203580
0 1 2 3 4 5
Light dose, min
E
Relative viability (%)
100
10
1
0,1
MDA-MB-231
MDA-MB-231
+ SB203580
0 1 2 3
Light dose, min
F
Relative viability (%)
100
10
1
0,1
MCF7
MCF7 + SB203580
0 1 2 3 4 5 6
Light dose, min
G
p-MK2
Ponceau S
PDT - - + + - + - - + + - +
SB203580 - + - + - - - + - + - -
2 hrs 24 hrs 2 hrs 24 hrs
MDA-MB-231
MDA-MB-231/TR

Fig. 8

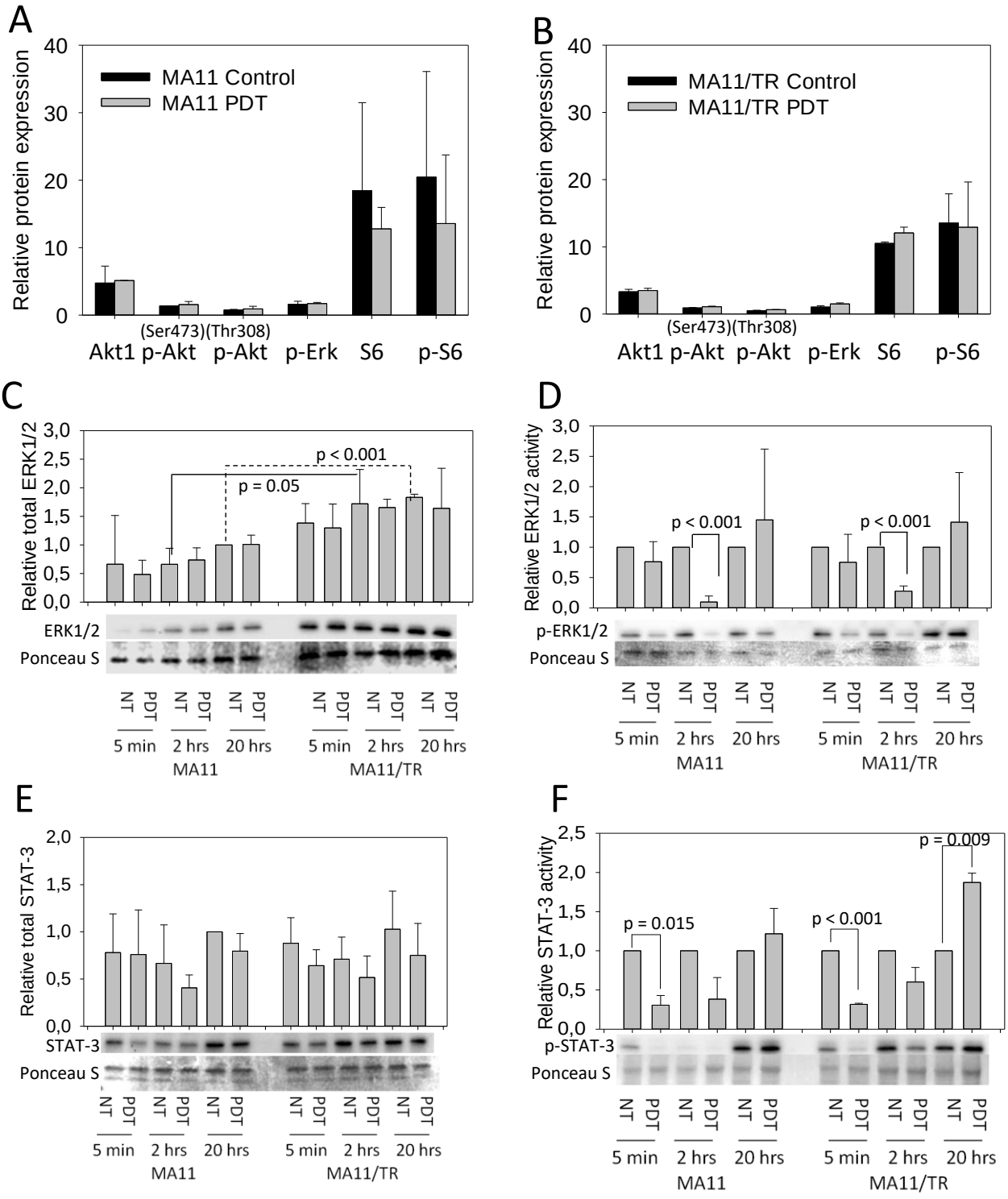
A
Relative protein expression
MA11 Control
MA11 PDT
(Ser473)(Thr308)
Akt1 p-Akt p-Akt p-Erk S6 p-S6
B
MA11/TR Control
MA11/TR PDT
C
Relative total ERK1/2
p < 0.001
p = 0.05
ERK1/2
Ponceau S
NT PDT
5 min 2 hrs 20 hrs
MA11
MA11/TR
D
Relative ERK1/2 activity
p < 0.001
p < 0.001
p-ERK1/2
E
Relative total STAT-3
STAT-3
F
Relative STAT-3 activity
p = 0.015
p < 0.001
p = 0.009
p-STAT-3

Fig. 9

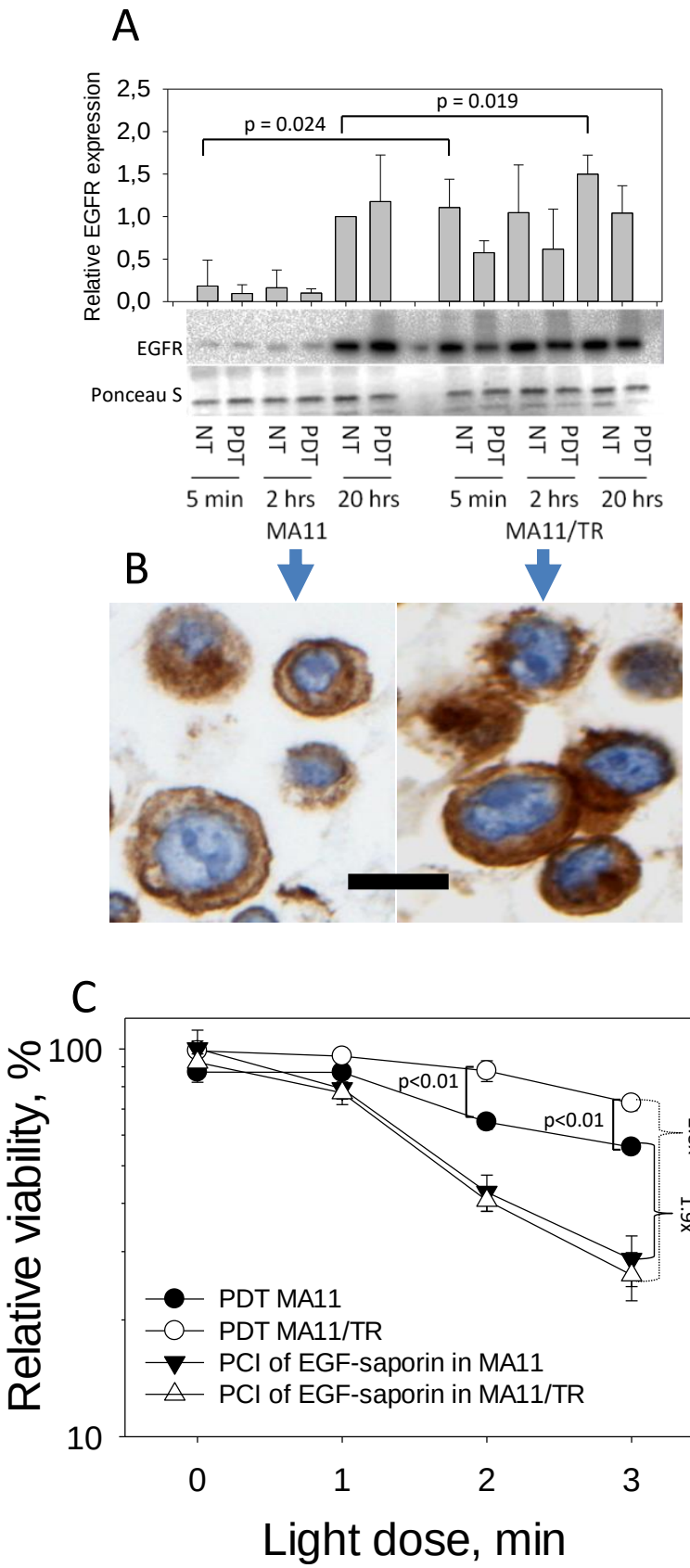
A
Relative EGFR expression
2,5
2,0
1,5
1,0
0,5
0,0
p = 0.024
p = 0.019
EGFR
Ponceau S
NT
PDT
5 min
2 hrs
20 hrs
MA11
MA11/TR
B
C
Relative viability, %
100
10
p<0.01
p<0.01
2.8x
1.9x
PDT MA11
PDT MA11/TR
PCI of EGF-saporin in MA11
PCI of EGF-saporin in MA11/TR
0
1
2
3
Light dose, min

Paper II

Paper III

Paper IV

Impact of Genotypic and Phenotypic Differences in Sarcoma models on the Outcome of Photochemical Internalization (PCI) of Bleomycin

Cathrine Elisabeth Olsen[a], Simen Sellevold[a,b], Theodossis Theodossiou[a], Sebastian Patzke[a], Kristian Berg[a §]

[a]Department of Radiation Biology, Institute for Cancer Research, Oslo University Hospital - Radium Hospital, Montebello, N-0310 Oslo, Norway. [b]Division of Orthopaedic Surgery, Oslo University Hospital, Montebello, N-0310 Oslo, Norway

§ Corresponding author

ABSTRACT

The low curative response to current treatment regimens for most soft tissue sarcomas indicates a strong need for alternative treatment strategies and predictive markers for treatment outcome. PCI (photochemical internalization) is a novel treatment strategy to translocate drugs into cytosol that otherwise would have been degraded in lysosomes. Two highly geno-and phenotypically different uterine and vulvar leiomyosarcoma cell lines, MES-SA and SK-LMS-1, were treated with bleomycin activated by PCI. The MES-SA cells were much more sensitive to PCI of bleomycin than the SK-LMS-1 cells and the treatment induced a 7-8 fold higher increase in DNA double-strand breaks at the same dose of light. A 3-fold higher induction of apoptosis and stronger activation of Bax and p21 was also measured in the *P53WT* MES-SA cells, compared to the *P53mut* SK-LMS-1 cells. The basal formation of reactive oxygen species (ROS) was 3-fold higher in SK-LMS-1 cells than in the MES-SA cells and SK-LMS-1 expressed glutathione peroxidase 1 (GPx1) and more superoxide dismutase 2 (SOD2) than the MES-SA cells. Glutathione depletion with the glutathione synthetase inhibitor buthionine sulfoximine increased the cytotoxic effect of the photochemical treatment (PDT) most strongly in the SK-LMS-1 cells, and reduced PCI-induced H2AX activation in the MES-SA cells, but not in the SK-LMS-1 cells. The results indicate PCI of bleomycin as a potential novel treatment strategy for soft tissue sarcomas, with antioxidant enzymes, in particular GPx1, and the *P53* status as potential predictive markers for response to PCI of bleomycin.

Keywords: photochemical internalization; photodynamic; sarcoma; bleomycin; γH2AX; resistance; reactive oxygen species; glutathione

INTRODUCTION

Soft tissue sarcomas constitute a rare group of cancers among solid cancers. They are generally difficult to treat, and surgery remains the first line treatment, often supplemented by radiation therapy. Surgery does, however, bear the risk of contamination of healthy tissue, leading to cases of tumour recurrence. Radiotherapy improves local control after surgery (1) and chemotherapy increases survival in a metastatic setting (2), but most important are adequate surgical margins. Surgery of high grade sarcomas has often been combined with cytostatics such as doxorubicin and ifosfamide in hope of improving long term survival. The long term results are, however, still not convincing, and adjuvant chemotherapy remains a subject of debate. Thus, there is a need for new treatment strategies to improve the survival rate and reduce the need for debilitating surgery to obtain local control.

Photochemical internalization (PCI) is a novel treatment modality that may be considered for treatment of soft tissue sarcomas. PCI is a technology where a drug accumulated in endocytic vesicles becomes released into cell cytosol due to photodynamic destruction of the endosome membranes. The PCI technology is based on an amphiphilic photosensitizer, such as $TPCS_{2a}$, which localizes to endosomal membranes, and upon light activation at the appropriate wavelength, generates reactive oxygen species (ROS) that rupture the membrane of the endosomes releasing the entrapped drug. A phase I clinical trial, including one sarcoma patient, showed highly promising results, and 13 out of 16 patients showed complete (11) or partial (2) response 28 days after treatment (3). The highly heterogeneous phenotypic and genotypic characteristics of soft tissue sarcomas even within the same subgroup, result in different responses to radio-and chemotherapy (4). It is therefore of great importance to reveal the phenotypic and genotypic characteristics of soft tissue sarcomas that may predict the response to PCI.

Soft tissue sarcomas are classified into over 40 subgroups, according to their histological appearance. With a puresmooth-muscle differentiation, leiomyosarcomas are among the most common soft tissue sarcomas. Leiomyosarcomas are a heterogeneous group of tumours with a range of molecular expression profiles and *P53* status (4). They may arise in any location, but occur most often in the retroperitoneum and pelvis, and in large vessels or extremities (5). The most important prognostic factors are tumour localization and size, and 5 year survival rates,

overall, are 50-60% (2). MES-SA (6) and SK-LMS-1 (7) are two heterogeneous uterine-and vulvar leiomyosar-coma cell lines, respectively, exhibiting dissimilar phenotypic and genotypic characteristics (8). MES-SA cells express p53*WT* , HER2, pAKT, c-Met, but no PTEN or EGFR. In contrast, SK-LMS-1 cells express p53*mut*, do not express HER2, but express PTEN, EGFR, pAKT and c-Met (9-11). On this basis these cell lines appeared ideal to reveal differences in sensitivity to PCI treatment and to initiate studies of predictive markers for treatment response. In this study PCI was utilized to translocate bleomycin into the cells since bleomycin is a poorly internalized chemotherapeutic that has been used in clinical PCI trials. The results indicate that the MES-SA cells are more sensitive to PCI of bleomycin than the SK-LMS-1 and provide insight into the mechanistic causes for this difference in cell sensitivity.

MATERIALS AND METHODS

Cell lines and culturing

The human uterine sarcoma cell line MES-SA (ATTC CRL-1976) and human vulvar leiomyosarcoma cell line SK-LMS-1 (ATCC HTB-88) were obtained from the American Type Culture Collection (LGC Standards AB, Boras, Sweden) and subcultered 2-3 times a week in McCoy's 5a medium (Sigma-Aldrich, St. Louis, MO, USA) and DMEM (Sigma-Aldrich), respectively, supplied with 10% fetal calf serum (FCS; PAA Laboratories, Pasching, Austria), 100 U/mL penicillin (Sigma-Aldrich), and 100 µg/mL streptomycin (Sigma-Aldrich). Detachment of the cells for subcultivation was performed at 37◦C with 0.25% (w/v) trypsin-0.53 mM EDTA solution (Sigma-Aldrich). The cells were kept at 37◦C in a humidified tissue culture incubator with 5% CO2.

Cell growth densities

MES-SA cells ($2x10^5$, $4x10^5$ and $6x10^5$) and SK-LMS-1 cells ($0.75x10^5$, $1.25x10^5$ and $1.75x10^5$) were seeded in 6 well plates. After cellular attachment the plates were analysed in the IncuCyte ZOOM (Essen BioScience, Hertfordshire, UK) by measurement of plate confluence over 90 hrs. Phase contrast high definition images were acquired every 3 hrs. The data were subjected to morphological processing, due to the dissimilar cellular morphology of the two cell lines.

Live cell microscopy

For live cell microscopy cells were seeded (3000 cells/cm^2) in ibiTreat µ-culture 8-well slides (Ibidi, Munich, DE), allowed to attach overnight and imaged using a Cell Observer microscope system (Carl Zeiss; Jena, DE) equipped with a 20x/0.8 PlanApo Phase 2 lens, an AxioCam MRm camera, a temperature controlled XL-chamber, a temperature, humidity and CO_2 controlled stage incubator, a motorized coded X,Y-stage, and a Definite Focus system. Cells were imaged for 20 hrs at 10 min intervals in 2x2-fields with 10% overlap and image tiles aligned using the MosaiX-module (AxioVision 4.2; Carl Zeiss). For documentation of gross growth morphology cells were seeded in 6-well plates (Nunc), grown to near confluence and imaged in 5x5 fields with 10% overlap using a 10x/0.25 Phase 1 N-Achroplan lense. Image tiles were aligned using the MosaiX-module (AxioVision 4.2; Carl Zeiss).

Light source

Illumination of cells was performed by using LumiSource ® (PCI Biotech AS, Lysaker, Norway), a lamp consisting of four 18-W Osram L 18/67 light tubes. The lamp delivers blue light (E*max* =435 nm) with an output of 13.5 mW/cm^2. The irradiance of the lamp varies <10 % across the illumination area (45 x 17 cm).

PDT and PCI treatment

Two hundred thousand cells were allowed to attach in 6-well plates (Nunc) over night, and then incubated with 0.2 μg/mL $TPCS_{2a}$ (PCI Biotech, Lysaker) for 18 hrs. Cells were then washed twice with PBS, and either incubated with 0.3 IU/ml bleomycin (Bleomycin, Baxter AS, Oslo) for 4 hrs prior to illumination. The cells were then illuminated with blue light (435 nm) using the LumiSource ® (PCI Biotech AS) lamp.

Assessment of cell viability

Assessment of cell viability was addressed by clonal cell survival and the MTT assay. Based on plating efficacy, an appropriate number of cells was seeded to obtain approximately 100 colonies in 6-well-plates. Cells were treated as described above, and colonies counted manually after fixation in ethanol and methylene blue staining 10 to 14 days after treatment. The MTT assay was performed by incubation with 0.4 mg/ml MTT (Sigma-Aldrich) for 4 hrs. The medium was then removed, and the formazan crystals were dissolved in DMSO (Sigma-Aldrich). Absorbance was read at 570 nm using a PowerWave XS2 microplate spectrophotometer (BioTek, Winooski, VT, USA).

Intracellular $TPCS_{2a}$ accumulation and ROS formation

For addressing $TPCS_{2a}$ accumulation, $3x10^5$ cells were seeded in 6-well plates, allowed to attach, and incu-bated with 0.2 μg/mL $TPCS_{2a}$ for 18-20 hrs. Then the cells were washed twice in PBS, and incubated in drug free medium for 4 hrs. Cells were analyzed by flow cytometry as described below. Relative ROS formation was addressed by studying the cell permeable agent 2',7'-Dichlorodihydrofluorescin diacetate (DCFH-DA) (Sigma), which upon deacetylation in the cells, converts to non-fluorescent DCFH. DCFH is rapidly oxidized to highly fluorescent DCF by ROS. The fluorescence intensity is proportional to the ROS levels in the cell cytosol. Three hundred thousand cells were seeded in 6-well plates, allowed to attach, and incubated with 0.2

μg/mL $TPCS_{2a}$ for 18-20 hrs. Then the cells were washed twice with PBS, and incubated with 0.3 IU/mL bleomycin or drug free medium for 4 hrs. Immediately after illumination, cells were washed once with PBS, detached with trypsin and resuspended in medium. After 30 min cells were incubated with 0.1 mM DCFH-DA in medium for 1 hr, and analyzed by flow cytometry. Cells were analyzed based on forward and side scattering (area) to gate live cells, and side scatter (area and width) to gate singlets. Fluorescence analyses were performed in LSRII flow cytometers (Becton-Dickinson, San Jose, CA, USA). $TPCS_{2a}$ was excited by either a 405 nm laser (25 mW) or a 407 nm laser (100 mW) and collected through a 660/20 nm emission filter combined with either a 505 nm or 635 nm longpass dichroic filter, respectively. DCF was excited by a 488 nm laser (50 mW), and collected through a 530/30nm or a 525/50 nm emission filter combined with a 505 nm dichroic filter.

Cell protein content

To compare cell protein contents, the DC Protein Assay (BioRad, Hercules, CA, USA) was used as described by the producer. Cell lysates were obtained by lysing $2x10^6$ cells with 100 μl 0.1 M NaOH.

Western blotting

Cells were treated as described above, and harvested at 4 hrs and 20 hrs after treatment by washing the cells with PBS, and placing the plates on ice. Then the cells were lysed with RIPA buffer (added 10 μl/ml Protease Inhibitor Cocktail (Sigma-Aldrich), 10 μl/ml Phosphatase Inhibitor Coctail I and II (Sigma-Aldrich), 10 μl/ml 2 M β-glycerol phosphate, 5 μl/ml 10 mM Na3VO4, 5 μl/ml 200 mM PMSF and 5 μl/ml 200 nM NaF)) or Lane Marker Sample Buffer (Thermo Scientific), sonicated for 10-15 sec and heated (95◦C for 5 min) before the lysates were applied on 4-20% Mini-PROTEAN ® TGX™ 15 well Gels (BioRad) together with Precision Plus Protein Kaleidoscope™ Standard (BioRad) and subjected to sodium dodecyl sulfate-polyacrylamide gel electrophoresis (SDS-PAGE) (200 V, 30 min). Then proteins were blotted (100 V, 2 hrs) onto methanol-activated polyvinylidene difluoride (PVDF) transfer membranes (Amersham Hybond-P, GE Healthcare). The Transblot Turbo system was also used, as recommended by the producer. The membranes were washed in tris-buffered saline with 0.1 % tween 20 (TTBS) and blocked in 5% milk for 1 hr at room temperature. Then, the membranes were washed in TTBS and incubated with antibodies against p21 #sc-397, GPx4 #50497 and SOD2 #*sc*30080 (1:200) (Santa Cruz) or Bax #2772 (Cell Signaling) (1:1000) in 5% bovine serum albumin (BSA), GPx1 #3206 and SOD1 #4266(Cell Signaling) (1:1000) in 5% milk over

night at 4◦C. The membranes were then washed thrice in TTBS and incubated with secondary antibodies against rabbit #7074 (1:1000) or mouse #7076 (1:1000) (Cell Signaling) in 5% milk at room temperature. The membranes were further washed thrice in TTBS before incubation with SuperSignal West Dura Chemiluminescent Substrate (Thermo Scientific) and luminescence measured with ChemiDoc (BioRad). Loading was controlled by anti-γ-tubulin antibody; clone GTU-88 #*T* 6557 (Sigma-Aldrich) or incubating the membranes with Ponceau S. Stain (Sigma-Aldrich).

Cell cycle analysis, assessment of H2AX phosphorylation and apoptosis (TUNEL assay)

After treatment, cells were detached with trypsin, washed in PBS, and resuspended in 500 µL ice cold methanol and stored at -20◦C. Methanol fixed cells were washed once with PBS, and added 35 µL TdT reaction mix (3.5 µL TdT Reaction Buffer, 2.1 µL 25 mM CoCl2, 0.35 µL Biotin-16-dUTP, 0.35 µL 10 mM DTT, 0.14 µL TdT enzyme, 28.58 µL ddH2O) (Roche) and incubated for 30 min at 37◦C. Then the cells were washed once with PBS, and incubated with 50 µL of primary antibody mix (mouse α-γH2AX 1:500 (Millipore) in 5% milk in PBS) for 30 min at room temperature. Then the cells were washed once with PBS, and incubated with 50 µl secondary antibody mix (goat α-rabbit-PE 1:50 (Invitrogen), rabbit α-mouse-FITC (Dako) and streptavidin-Cy5 1:400 (GE Healthcare) in 5% milk in PBS) for 30 min at room temperature. Then the cells were washed once with PBS and resuspended in 500 µL Hoechst 33258 (1.5 µg/mL) in PBS, and incubated overnight at 4◦C. Analysis was performed in an LSRII (Becton-Dickinson, San Jose, CA, USA). PE, FITC and Cy5 were excited by 561 nm (40 mW), 488 nm (50 mW) and 640 nm (40 mW) lasers, and collected through 582/15 nm, 525/50 nm and 670/14 nm emission filters, the former combined with 570 nm and 505 nm longpass dichroic filters, respectively. Single cells were gated either based on side scatter (area and width) or on side scatter (area) and Hoechst (width). Cell cycle analysis was performed by FlowJo Software (Tree Star Inc, Ashland, Oregon, U.S.A.) on Hoechst 33258-stained cells, based on Hoechst area, and analyzed by fitting the Dean-Jett-Fox model to define cell cycle distribution.

Metabolic analysis

Fifteen thousand cells were inoculated onto special 96 well plates for the XF^{e}96 Seahorse metabolic analyzer. The cells were incubated overnight in their normal media at 37◦C, 5% CO2 humidified atmosphere. One hour prior to the experiments, the cells were placed on Seahorse Assay media supplemented either with 2 mM pyruvate, 10 mM glucose and 2 mM L-glutamine or 2 mM L-glutamine but no pyruvate and glucose. The cells were incubated for 1 hr in a 37◦C

humidified atmosphere (non CO_2) and then assayed for their oxygen consumption rate (OCR) and lactate induced extracellular acidification rate (ECAR) as per standard XF^e96 protocols. The cells were assayed in four conditions: I) basal, II) injection of 1 μM oligomycin, III) injection of 1 μM FCCP, and IV) 1 μM Antramycin-A and Rotenone. These conditions are described by XF^e96 manufacturers as the mitostress assay.

Statistical evaluations of data

To evaluate significance the t-test (student's t-test) was used if not otherwise stated. The cell cycle distributions were statistically analyzed by two-tailed paired t-tests. Results were considered significant when $p<0.05$. The statistical analyses were performed by the software SigmaPlot 12.5 (Systat Software, Inc., San Jose, CA, USA)

RESULTS

Different cell growth patterns between uterine and vulvar leiomyosarcomas, but no difference in growth rates

Cell growth assessed by the IncuCyte ZOOM is shown in Fig. 1, and revealed insignificant overall growth rate differences between the cell lines. The calculated doubling times were 31.3±1.2 (S.D.) and 32.2±1.4 (S.D.) hrs for the MES-SA and SK-LMS-1 cells, respectively. The cell density curves were used to calculate the appropriate number of cells to seed in each experiment, based on the experiment duration and plate type, to maintain optimal growth conditions. Live cell microscopy showed, however, phenotypic differences in growth pattern, migration and the formation and appearance of colonies of the two cell lines (Fig. 1C and D, and Suppl. Video 1). The MES-SA cells appear round, only rarely found with pseudopods and express low mobility and form dense colonies. In contrast, the SK-LMS-1 cell appear flat with long pseudopods and high mobility. Accordingly, the MES-SA and SK-LMS-1 cells form dense and scattered colonies, respectively.

Insignificant differences in sensitivity to bleomycin

Therapeutic effects of increasing doses of bleomycin were addressed by clonal cell viability, as described in Material and Methods (Fig. 2A). The cells were treated with bleomycin for 4 hrs. The clonal cell viability decreased with increasing doses of bleomycin for both cell lines. The LD_{50} values were found similar (2.75 IU/ml) for both cell lines as calculated by the exponential decay formulas.

PCI increases the therapeutic effect of bleomycin

Studies on response to $TPCS_{2a}$ and light (photodynamic therapy (PDT)) showed that the $TPCS_{2a}$-treated MES-SA cells were slightly more sensitive to light than the SK-LMS-1 cells (Fig. 2B). In both cell lines PCI of bleomycin reduced the cell viability in a synergistic manner (Fig. 2C and D). However, the MES-SA cells were found more sensitive to increasing doses of bleomycin in cells treated with PCI than the SK-LMS-1 cells.

PCI of bleomycin increases DNA double strand breaks

Bleomycin exerts cytotoxic effects by induction of DNA strand breaks, including double-strand breaks (12). A major increase in DNA double strand breaks addressed by measurements of γH2AX was found when MES-SA cells were treated with PCI of bleomycin (Fig. 3). The γH2AX staining was increased more than 20-fold 1 hr after PCI of bleomycin, while only a 3-4

fold increase was seen in the SK-LMS-1 cells. In both cell lines bleomycin alone or PDT induced no increase in γH2AX staining. The analyses of γH2AX staining by flow cytometry were confirmed by fluorescence microscopy which showed that the staining was nuclear and appeared almost homogenous in the PCI of bleomycin treated MES-SA cells and less intense and more punctuate in the SK-LMS-1 cells (Fig. 4).

The γH2AX staining of untreated G2/M phase cells was approximately 2-fold higher than in G1 cells of both cell lines, reflecting the doubling of the DNA content of cells in G2/M phase (Fig. 3C and D). However, the γH2AX staining was similarly strong in both cell cycle phases 1 hr after PCI of bleomycin. The γH2AX staining was found decreasing with time after treatment in both cell lines, but was still high 44 hrs after treatment in MES-SA cells (Fig. 3A and B). The repair kinetics appear similar after high (300 sec) and low doses (90 sec) of light, indicating that the repair mechanisms are not influenced by the photochemical treatment (data not shown). Interestingly, the γH2AX staining appeared to decline slightly faster in G1 cells than in the G2/M cell population in both cell lines (Fig. 3C and D). Twenty hours after PCI of bleomycin treatment of MES-SA cells the γH2AX staining in G1 cells had declined to 17.7±11.2% (n=5) of that at 1 hr after treatment while in the G2/M population γH2AX declined to 30± 8.0% (n=5). The difference in rate of reduction of γH2AX staining had a one-tailed p-value =0.0381, and a two-tailed p-value =0.0763.
The untreated SK-LMS-1 cells exhibited a 3-4-fold higher γH2AX staining than the MES-SA cells (Fig. 3). This is, however, partly reflecting the approximately 2-fold higher DNA content in the SK-LMS-1 cells (data not shown).

The differences in cellular response to PDT and PCI of bleomycin as described above may be due to differences in cellular uptake of photosensitizer, differences in rate of ROS formation, cellular protection mechanisms against ROS or differences in expression of oncogenic signals. The following are attempts to reveal the mechanistic parameters of importance for the differences in response to PDT and PCI of bleomycin between MES-SA and SK-LMS-1 cells.

Cellular uptake of $TPCS_{2a}$

Studies of $TPCS_{2a}$ accumulation, at a time point corresponding to the time of light exposure of $TPCS_{2a}$ -sensitized cells, revealed that the SK-LMS-1 cells accumulated more photosensitizer than the MES-SA cells (Fig. 5A). The median fluorescence after subtracting the background fluorescence, in the SK-LMS-1 cells was found to be 3.3±0.15(S.E.)-fold higher than in the MES-SA cells. However, the SK-LMS-1 cells are larger than the MES-SA cells. The protein

content was 3.7±0.28(S.E.)-fold higher per cell in SK-LMS-1 cells (data not shown). Thus, the accumulation of $TPCS_{2a}$ was 12% lower per cell volume in the SK-LMS-1 cells than in the MES-SA cells.

ROS generation in MES-SA and SK-LMS-1 cells after treatment

ROS formation was studied after the various treatments (Fig. 5B and C). In both cell lines all photochemical treatments induced detectable increases in ROS. The increase in ROS-formation after normalization to the control levels was higher per cell in the MES-SA cells than in the SK-LMS-1 cells (B). The increase in ROS-formation was close to proportional to the light doses in the MES-SA cells, while doubling of the light dose caused only an approximately 60% increase in ROS formation in the SK-LMS-1 cells. Treatment of PCI of bleomycin did not induce any additional ROS formation compared to PDT.

The ROS assay is based on flow cytometric single cell analyses. ROS formation in untreated cells was 12.5-fold ±6.5 (S.E.) higher in SK-LMS-1 cells than in the MES-SA cells. Taking into account the absolute relative formation of ROS per mg protein it appears that the generation of ROS is 3.3-fold higher in untreated SK-LMS-1 cells than in the MES-SA cells (Fig. 5C), and the total ROS formation in the PDT/PCI of bleomycin treated cells is approximately twice as high in the SK-LMS-1 cells as in the MES-SA cells (range 1.8-2.6-fold).

SK-LMS-1 cells exhibit higher expression levels of superoxide dismutase and glutathione peroxidase than MES-SA cells

The enzymes superoxide dismutase (SOD) and glutathione peroxidase (GPx) are essential in detoxification of ROS generated by the cells and by treatment-induced ROS. The basal levels of mitochondrial SOD2 generally involved in catalysing the dismutation of superoxide radical into H2O2, was found to be more strongly expressed in the SK-LMS-1 cell line compared to MES-SA cells, while cytosolic and peroxisomal SOD1 was found equally expressed in both cell lines (Fig. 6A). Cytosolic GPx1 was found expressed only in the SK-LMS-1 cell line, while GPx4 hardly was detectable in either of the cell lines.

The impact of GSH on cell survival and double-strand breaks after PDT and PCI of bleomycin

Glutathione (GSH) is a strong antioxidant as well as substrate for GPx enzymes. Measurements of the basal levels of GSH showed an approximately 50% higher level in MES-SA cells than in the SK-LMS-1 cells (Fig. 6B). Treatment with L-Buthionine-S,R-Sulfoximine (BSO), which is an inhibitor of γ-glutamylcystein synthetase, lead to a ≥80% decreased GSH level in both cell lines after treatment with 50 μM BSO for 24 hrs (Fig. 6B). BSO induced an

incubation time-dependent toxicity that excluded utilization of the clonogenicity assay. The highest non-toxic concentration of BSO was initially determined (72 hrs treatment at 50 μM for MES-SA and 100 μM for SK-LMS-1) by the MTT assay (Fig. 6C and D). Both cell lines were found more sensitive to PDT in the presence of BSO, but the effect appeared much stronger in the SK-LMS-1 cells (Fig. 6E and F). The cytotoxicity of PCI of bleomycin is usually analyzed by clonogenic cell viability assay due to the slow response to bleomycin. Three days of incubation was found too short to detect a significant synergistic effect of PCI of bleomycin in the MTT assay and the impact of BSO on the cytotoxicity of PCI of bleomycin could therefore not be detected.

GSH and GPx activities have been shown to influence chromosomal DNA damage and repair in cells treated with ionizing radiation and bleomycin (13, 14). In MES-SA cells treated with PCI of bleomycin the γH2AX staining was lowered by 46% (0.54±0.24) as seen by a slightly reduced peak value and a longer tail towards low γH2AX staining by pretreatment with BSO, while BSO treatment had no apparent effect in the SK-LMS-1 cells (0.98±0.25 of that in the absence of BSO, Fig. 7). BSO had no detectable effect on γH2AX staining in either cell line treated with bleomycin only or PDT.

Treatment-induced effects on cell cycle regulations and induction of apoptosis

The cell cycle distribution in response to PDT and PCI of bleomycin was studied by flow cytometry of Hoechst stained methanol fixed cells. A two-fold increase of MES-SA cells in G2/M phase was seen 20 hrs after treatment with PCI and PDT with 150 sec of light ($p < 0.03$, Fig. 8). Concurrently, PDT reduced the fraction of cells in S phase by almost 50% ($p=0,064$) and less by means of PCI (PDT vs PCI, $p < 0,05$). In SK-LMS-1 cells subjected to PDT the G2/M fraction was lower by 40 % compared to untreated control cells 20 hrs after treatment ($p < 0.01$), while after PCI of bleomycin the cell cycle distribution was only slightly modified with a 25% increase in the G2M phase ($p = 0.06$). Bleomycin treatment resulted in no statistically significant effect in either cell line.

MES-SA cells express wild type p53 while p53 is mutated in SK-LMS-1 cells (11, 15). This difference may influence on the cell cycle regulation and induction of apoptosis. Apoptosis, addressed by identification of DNA fragmentation (TUNEL assay,) showed that neither PDT nor PCI of bleomycin induced apoptosis 1 hr after treatment. Twenty hours after PDT and PCI of bleomycin, apoptosis appeared in both cell lines (Fig. 9A and B). There were no differences in the apoptotic fraction between the cells treated with PDT and PCI of bleomycin, but the

apoptotic fraction was 3-fold higher in MES-SA cells than in SK-LMS-1 cells. Additionally, when PDT and PCI of bleomycin light doses were increased (from 150 sec to 300 sec of light) in the MES-SA cell line, an increase in DNA fragmentation with time was observed (data not shown). The highest doses tested at the latest time points after treatment revealed approximately 30% apoptosis (300 sec of light, 44 hrs after irradiation, data not shown) in the MES-SA cell line.

The apoptotic fraction did not change between 20 and 44 hrs after illumination (Fig. 9B). In the procedure for analysis of apoptosis, floating cells are collected together with the cells bound to the substratum. It has previously been shown that apoptotic cells floating in the medium after PDT with a structurally similar photosensitizer ($TPPS_{2a}$) remain detectable in the medium for more than 60 hrs after illumination (16). In accordance with the cell line differences in induction of apoptosis after PCI, Bax was induced 20 hrs after illumination in the MES-SA cells, but not in the SK-LMS-1 cells (Fig. 9C). Activation of the p53 downstream protein p21 was also seen after PCI of bleomycin, but only in the MES-SA cells, in accordance with the p53 status. However, no activation of Bax or p21 was seen after PDT in either cell line.

Metabolic activity characteristics of MES-SA and SK-LMS-1 cells

The reduced dependency on oxidative phosphorylation and enhanced use of glycolysis have been described as characteristic for cancer cells (17). Recent studies indicate that increased utilization of glycolysis correlates not only with survival benefits in a hypoxic environment but also increased drug resistance (18). Addressing the mitochondrial respiration showed that the SK-LMS-1 cells consumed oxygen at approximately the same rate (OCR/min) as the MES-SA cells when corrected for the difference in cell protein (3.7 : 1) (Fig. 10A). When removing the glucose and pyruvate from the media, the basal respiration levels slightly increased for both cell lines, but the maximum respiration capacity upon FCCP administration remained the same (Fig. 10B).

When, however, the glycolytic profiles of the two cell lines were assessed, MES-SA cells were found to demon-strate an approximately 2.5-fold higher glycolytic activity (ECAR/min) than SK-LMS-1 cells when corrected for cell volume (Fig. 10C). ATP synthase inhibition, by adding 1 μM oligomycin, only slightly increased the glycolytic activity in both cell lines, without much affecting the ratio of the respective activities before oligomycin administration. When removing glucose and pyruvate from the medium, the glycolytic activity in the cell two lines was in general lowered (Fig. 10D), with the MES-SA cells being mostly affected by the glucose and

pyruvate absence. This resulted in a profound decrease of the gap between the glycolytic activities of the two cell lines.

DISCUSSION

In the present study the two pheno- and genotypically diverging soft tissue sarcoma cell lines MES-SA and SK-LMS-1 have been evaluated for treatment response to PCI of bleomycin. The MES-SA cells were found slightly more sensitive to PDT and substantially more sensitive to PCI of bleomycin than the SK-LMS-1 cells. The cell line difference in treatment response is related to the observation that PCI of bleomycin induced more double-strand breaks and apoptosis in MES-SA cells than in SK-LMS-1 cells. The GSH-based protection mechanisms appear also to be involved in the sensitivity to PCI of bleomycin and PDT.

The induction of DNA double strand breaks as measured by phosphorylation of the histone H2AX (γH2AX) was seen in both cell lines after PCI of bleomycin although much stronger, *e.g.* 7-8-fold at 150 sec of light, in the MES-SA cells than in the SK-LMS-1 cells. Bleomycin alone induced hardly any double-strand breaks, confirming that PCI induces the translocation and activation of bleomycin in the nucleus. The biological consequences of the double-strand breaks are the main cause of the bleomycin- and ionizing radiation-induced tumour necrosis (19). The difference in PCI of bleomycin-induced cytotoxicity between the two evaluated cell lines may therefore to a high extent be related to the formation of double strand breaks and/or differences in the efficiency of the corresponding repair mechanisms.

Bleomycin is regarded as a radiomimetic and the effects on cells by bleomycin and ionizing radiation are highly similar. Glutathione is a radioprotector and depletion of glutathione by inhibiting the enzyme γ-glutamylcysteine synthetase with BSO increases cellular radiosensitivity and increases the formation of radiation-induced chromosomal aberrations (20). This is in contrast to the attenuation of H2AX activation found after PCI of bleomycin in BSO treated MES-SA cells. However, it has been reported that glutathione can reactivate oxidized bleomycin so that it can undergo repeated cycles of chromosome cleavage (21, 22). It was unfortunately not possible to evaluate the impact of glutathione depletion on the cytotoxicity induced by PCI of bleomycin. The importance of glutathione to protect against ROS, mainly singlet oxygen, induced by the photochemical treatment was, however, substantial and in accordance with previous reports (23). The stronger sensitizing effect of BSO in the SK-LMS-1 than the MES-SA cells correlates well with the expression of GPx1 only found in the SK-LMS-1 cells. The sensitizing effect of BSO in the MES-SA cells may be due to a direct antioxidant effect of glutathione or the conjugation of glutathione to photooxidized biomolecules by glutathione-S-transferase followed by detoxification through expulsion from the cells (24). Altogether, these

results indicate that glutathione is an important factor in cellular response to PDT and PCI of bleomycin.

The basal level of double-strand breaks is higher by a factor of 2 corrected for the amount of DNA per cell, in the SK-LMS-1 than in the MES-SA cells. Darzynkiewicz and coworkers have shown that ROS generated by metabolic activity may lead to formation of double-strand breaks, indicating a higher rate of basal ROS formation in the SK-LMS-1 than in the MES-SA cells (25, 26). This is also in accordance with the 3-fold higher ROS formation detected in untreated SK-LMS-1 cells than in the MES-SA cells. The elevated ROS formation observed in cancer cells is largely due to a defective mitochondrial electron transport chain (27) leading to activation of antioxidant enzymes such as SOD and GPx (28). The SK-LMS-1, but not the MES-SA, cells express GPx1 and SOD2 while both cell lines express SOD1 and almost no GPx4. It is thus tempting to speculate that an elevated rate of ROS formation stimulates expression of GPx1 and SOD2 in the SK-LMS-1 cells. The expression of GPx1 and SOD2 is expected to provide improved protection against ROS generating treatment modalities such as PDT, bleomycin and PCI of bleomycin.

PCI of bleomcyin induced a more than 20-fold increase in γH2AX staining in the MES-SA cells compared to the 3-fold increase in SK-LMS-1 cells. GPx1, that was found expressed in SK-LMS-1 cells, has been shown to be located in cytosol and the mitochondria, but also in the nucleus (29). In contrast, SOD2, that also was found mainly expressed in the SK-LMS-1 cells, has not been found to be located in the nucleus and is expected to influence on the dismutation of O·- to H_2O_2 in the mitochondria, but is not likely to be involved in quenching bleomycin-induced double-strand breaks. Thus, the dissimilar expression of GPx1 and inverse correlation with double-strand breaks may indicate that GPx1 attenuates the level of double-strand breaks. This is in accordance with the reduced γH2AX staining of bleomycin-treated colon cancer cells pretreated with selenium, enhancing GPx1 activity 5-8 fold (14). However, GPx1 transfection of GPx1-negative MCF-7 cells enhanced γH2AX staining after bleomycin treatment and reduced the cytotoxicity while the selenium pretreatment had no effect on survival of the colon cancer cells (14). The influence of GPx1 on H2AX activation and cell survival is therefore not fully understood.

The repair kinetics of DNA double-strand breaks appeared to not depend on the light dose used in PCI of bleomycin-treatment. However, the results indicate that the repair in G1 phase of the cell cycle is faster than in the G2/M phase. The repair of double-strand breaks in G1 is based

on non-homologues end joining (NHEJ), while the repair in S and G2/M phase is based on homologues recombination (HR) (30). The current results thus indicate that double-strand breaks induced in G1 are more rapidly repaired by the NHEJ mechanism than cells in later stages of the cell cycle. Studies based on knock-out mutant cells with defective NHEJ repair mechanisms become hypersensitive to ionizing radiation when treated in G1 (31, 32). Similarly, HR knock-out cells become hypersensitive when treated in the S-G2/M phase (31). Dysfunctional DNA repair mechanisms may influence sensitivity to PCI of bleomycin and contribute to predict treatment response. *E.g.* deficiency in DNA-PK, a downstream kinase in the repair of double-strand breaks by the NHEJ pathway, influences sensitivity to ionizing radiation (33, 34). Similar results have not been reported after treatment with bleomycin.

MES-SA cells are known to express wild type p53. The p53 downstream proteins p21 and Bax were not activated by PDT in the MES-SA cells, but strongly activated by PCI of bleomycin. Interestingly, PDT induced a similar induction of apoptosis as PCI of bleomycin without induction of Bax, indicating that the pathways for induction of apoptosis by PDT and bleomycin are different. Bleomycin alone has previously been shown to induce Bax and reduce Bcl-2 expression, induce cytochrome C release and caspase 8/9/3 activation (35). PDT has also been shown to induce apoptosis, which includes enhanced Bax expression (36) utilizing non-lysosomal photosensitizers (37). However, lysosomal rupture by PDT with the photosensitizer Pc13 was followed by mitochondrial disruption, cytochrome C release and caspase activation, but did not increase Bax expression. Instead Bax was shown to translocate from cytosol to the mitochondria (38). Similarly, Bax was found to be translocated from cytosol to mitochondria without a concomitant enhanced expression of Bax in ASTC-a-1 lung adenocarcinoma cells treated with the lysosomally located photosensitizer NPe6 and light (39). Thus, current literature indicates that PDT based on lysosomally located photosensitizers induces release of cathepsins into the cytosol causing cleavage of Bid to t-Bid. This further causes mitochondrial release of cytochrome C supported by translocation (but not enhanced expression) of Bax to the mitochondria (40, 41).

The activation of apoptosis in MES-SA cells and to a much lower extent in SK-LMS-1 cells is expected to be related to p53 status and may contribute to the higher sensitivity of MES-SA cells to PCI of bleomcyin than the SK-LMS-1 cells. However, the fraction of cells entering apoptosis as measured by the TUNEL assay is relatively low. The induction of apoptosis by lysosomally located photosensitizers appears generally less pronounced than with photosensitizers located in other compartments and may instead induce a stonger autophagic response (37). As pointed out

above, the release of cathepsins into the cytosol is regarded as the main apoptosis pathway after PDT with lysosomally located photosensitizers (40, 41). The expression of cathepsin activity after such PDT has, however, been shown to be relatively low due to cytosolic cathepsin inhibitors (stefins), high sensitivity of cathepsins to PDT and only partial rupture of the lysosomal fraction (42). Without these protection mechanisms the PCI technology would not have been able to rupture endocytic vesicles without inducing complete cell death.

The similar levels of apoptosis induction after PDT and PCI up to 44 hrs after treatment may indicate that activation of bleomcyin by PCI does not result in an increased induction of apoptosis. However, our experience with PCI-induced bleomcyin activation shows that the cytotoxic effects of bleomycin are relatively slow. This is seen by the need for clonogenicity assays to reveal the full treatment effect of PCI of bleomycin as compared to PDT. Viability assays such as MTT performed 2 days after light exposure reveal little or no effect of the PCI-activated bleomycin. This is also in accordance with the lack of enhanced ROS formation in PCI of bleomycin-treated cells as compared to the PDT response despite the well documented ROS formation by bleomycin treatment (12). Therefore, we cannot rule out that bleomycin-induced apoptosis is a significant downstream cause of the strong cytotoxic effect of PCI of bleomycin in MES-SA cells initiated by DNA double-strand breaks.

The loss of p53 has been postulated to lead to a metabolic switch, also named the Warburg effect, as p53 is thought to suppress glycolytic activity and promote oxidative phosphorylation (43). In this respect it was expected that the glycolytic activity would dominate in the SK-LMS-1 cells, but surprisingly the glycolytic activity was found highest in the MES-SA cells. The glycolytic activity was however almost non-responsive to the respiratory inhibitor oligomycin meaning that during oligomycin inhibition the cells' ATP requirements were met by glycolysis. Given the fact that the two cell lines exhibited similar OCR profiles, the MES-SA cells appear to express a profile closer to Warburg metabolism than the SK-LMS-1 cells. It should be pointed out that the Warburg effect correlates with drug resistance and should be taken into account when searching for predictive markers for treatment response (43).

In conclusion, the uterine MES-SA cells responded slightly more to PDT than the vulvar soft tissue sarcoma SK-LMS-1 cells. In contrast, the MES-SA cells were substantially more sensitive than the SK-LMS-1 cells to PCI of bleomycin which correlates well with the 7-8-fold higher rate of double-strand breaks formation as measured by γH2AX staining. One may hypothesize that SK-LMS-1 have more leaky mitochondria since express a similar respiratory activity, but a 3 –

fold higher rate of ROS formation, resulting in increased expression of GPx1 and SOD2. The expression of these antioxidant enzymes correlates with the attenuated induction of double-strand breaks in the SK-LMS-1 as well as the strongly enhanced PDT sensitivity in glutathione depleted cells. Expression of GPx1 and the P53 status should be considered as predicitive markers of response to PCI of bleomycin.

ACKNOWLEDGEMENTS

The project was supported by South-Eastern Norway Regional Health Authority (C.E.O), The Norwegian Cancer Society (S.P.), European Commission MSCA IF (T.A.T), The Norwegian Radium Hospital Research Foundation (S.S) and Simon Fougner Hartmanns Familiefond. We would like to thank Dr. Kirsti Landsverk, Dr. Trond Stokke and M.Sc. Idun Dale Rein of the Core Facility for Flow Cytometry for excellent help and discussion. We would also thank Ellen Skarpen for useful interpretation of initial microscopy data, Roman Generalov for initial bleomycin dose-response experiments, and Ane Sofie Viset Fremstedal for contribution to PCI experiments, Western blot preparation and analysis, and flow cytometry sample preparation.

FIGURE LEGENDS

Fig. 1

Cell confluence in percent at increasing time after seeding of 200 000, 400 000 and 600 000 cells (MES-SA, Fig. A) and 75 000, 125 000 and 175 000 cells in 6-well plates (SK-LMS-1, Fig. B). Cell confluence was calculated from images obtained by the IncuCyte ZOOM (Essen BioScience) from 16 individual areas in the wells every 3 hrs (Error bars =S.D.). Representative images of live MES-SA (C) and SK-LMS-1 (D) cells obtained by live cell Microscopy in 1 µ-Slide 8 well ibiTreat Microscopy Chambers.

Fig. 2

Clonal cell viability of MES-SA and SK-LMS-1 cells treated with bleomycin and PCI of bleomycin: (A) Cell treated with increasing concentrations of bleomycin for 4 hrs. The curves are fit to exponential decay curves for MES-SA cells following the equation $f(x) = 22 \times e^{-4.2x} + 57 \times e^{-0.23x} + 22 \times e^{-0.059x}$ ($r^2 = 0.998$) and for the SK-LMS-1 cells following $f(x) = 86 \times e^{-0.92x} + 14 \times e^{-0.040x}$ ($r^2 = 0.998$) where x is the bleomycin dose; (B) The cells were treated with PDT, bleomycin (0.3 IU/ml) or PCI of bleomycin with 90 or 180 sec of light as indicated on the figure and described in the Materials & Methods; (C) and (D) MES-SA and SK-LMS-1 cells were treated with PDT and PCI with increasing doses of bleomycin and light as indicated in the figure. All the other experiments with bleomycin are based on using 0.3 IU/ml bleomycin and are therefore indicated with a thickened line. The data are the mean of 3 individual experiments. Error bars =S.E.

Fig. 3

H2AX activation by PCI of bleomycin: Median γH2AX was analyzed in untreated (NT) cells and cells treated with either 0.3 IU/ml bleomycin (BLM) for 4 hrs, $TPCS_{2a}$ without light (PS) for 18 hrs, PS+BLM without light, 150 sec PDT and PCI of 0.3IU/ml bleomycin (MES-SA (A) and SK-LMS-1 (B)). Cells were harvested 1 and 20 hrs (and MES-SA 44 hrs) after PDT/PCI. The data are the average of one (PS and PS+BLM) and at least four individual PDT/PCI experiments, and are normalized to the median of NT cells at each harvest time point (Error bars =S.E.). PS and PS+BLM were not measured at the 44 hrs timepoint. Merged representative flow cytometry dot plots of γH2AX vs Hoechst staining are also shown for the 1 hr time point, with separate histograms of Hoechst A and γH2AX staining.

γH2AX status of G1 and G2/M cells 1 and 20 hrs (and MES-SA 44 hrs) after PCI of

bleomycin and 150 sec light in MES-SA (C) and SK-LMS-1 (D) cells, representative from the data in (A) and (B).

Fig. 4

γH2AX staining of MES-SA and SK-LMS-1 cells treated with PCI of bleomycin: Epi-fluorescence microscopy images of untreated (NT) cells and cells harvested 1 hr after 150 sec PCI, subsequently subjected to methanol-fixation. DAPI shows nuclear staining, FITC shows γH2AX-staining, DIC shows phase contrast, while Merge shows the overlayed DAPI-and FITC-micrographs. The experiment was performed once to confirm the localization of the γH2AX staining.

Fig. 5

(A) Relative $TPCS_{2a}$ accumulation at the time point for PDT/PCI. The data are representative from three individual experiments. (B) Relative ROS generation per cell after treatment as indicated in the figure. The data are the mean of three individual experiments normalized to untreated (NT) cells of both cell lines. (C) Absolute relative ROS generation per mg cell protein normalized to the untreated (NT) MES-SA cells. (Error bars =S.E.).

Fig. 6

(A) Western blots of SOD1, SOD2, GPx1 and GPx4 with respective γ-tubulin blots in SK-LMS-1 (SK) and MES-SA (M) cells. (B) GSH content (nmol) per μg cell protein in untreated cells (NT) and cells treated with 50 and 500 μM BSO for 20 hrs. The data are the mean of two individual experiments (Error bars =S.E.). (C) and (D) MTT of MES-SA and SK-LMS-1 cells subjected to 24, 48 and 72 hrs incubation with increasing concentrations of BSO. The data are the triplicates from one experiment (Error bars =S.D.). (E) and (F) MTT of MES-SA and SK-LMS-1 cells 48 hrs after PDT with and without co-incubation with 50 μM and 100 μM BSO, respectively. The data are triplicates from a representative experiment out of three and two individual experiments, respectively. (Error bars =S.D.).

Fig. 7

Representative dot plots of γH2AX vs Hoechst staining in untreated cells (NT) and cells treated with bleomycin (BLM), 150 sec PDT or 150 sec PCI of bleomycin, with and without the combination of 50 or 100 μM BSO present throughout the experiment. Cells fixed in methanol 1 hr after PDT/PCI. The data is one representative experiment out of three or more individual experiments.

Fig. 8

Cell cycle of non-apoptotic cells harvested 20 hrs after bleomycin (BLM), PDT or PCI exposed to 150 sec of light. The figures in (A) are representative for responses to treatments as indicated in the figure. In (B) the cell cycle distribution in controls and treated cells are shown based on analyses as described in Materials & Methods. Bars, SD (n=5 for MES-SA cells, n=4 for SK-LMS-1 cells.

Fig. 9

Induction of apoptosis after PDT and PCI treatment: (A) Dot plot of cells stained by the TUNEL-assay, indicating apoptosis, based on flow cytometry of untreated (NT) cells and cells treated as in Fig. 8. The data is representative from 4 and 5 individual experiments. (B) The quantification of apoptotis as in (A), after treatments as indicated in the figure. Error bars =S.E. PS and PS +BLM without light were not measured at the 44 hrs timepoint. (C) Western blots of Bax and p21 measured 20 hrs and 4 hrs, respectively, after 90 and 150 sec PDT or PCI, representative of three individual experiments.

Fig. 10

Metabolic characterization of MES-SA and SK-LMS-1 cells: Relative oxygen consumption rate per minute (OCR/min) per cell and relative extracellular acidification rate (ECAR/min) per 15 000 cells seeded in 96 well plates, measured by the SeaHorse XF^{e} Analyzer with (A and C) and without (B and D) the presence of glucose and pyruvate in the media. (A and C) is the average of the means from four individual experiments (Error bars =S.E.). (B and D) is the average of the means from two independent experiments (Error bars =S.E.). The arrows show the addition of 1 μM oligomycin, 1 μM FCCP and 1 μM antimycin A and 1 μM rotenone. The scales have been adjusted to provide a direct correlation of the metabolic activity per mg of cell protein.

Suppl.video

Live MES-SA and SK-LMS-1 cells imaged every 10th min in a time course of 23 hrs. The images are combined showing approx 45 min time-duration per sec video.

REFERENCES

1. Casali PG, Blay J-Y, of experts ECEUROBONETCP. Soft tissue sarcomas: ESMO Clinical Practice Guidelines for diagnosis, treatment and follow-up. Annals of oncology : official journal of the European Society for Medical Oncology. 2010;21 Suppl 5:v198-v203.
2. Stiller CA, Trama A, Serraino D, Rossi S, Navarro C, Chirlaque MD, et al. Descriptive epidemiology of sarcomas in Europe: report from the RARECARE project. European journal of cancer (Oxford, England : 1990). 2013;49:684-95.
3. Sultan AA, Jerjes W, Berg K, Høgset A, Mosse CA, Hamoudi R, et al. Disulfonated tetraphenyl chlorin (TPCS2a)-induced photochemical internalisation of bleomycin in patients with solid malignancies: a phase 1, dose-escalation, first-in-man trial. The Lancet Oncology. 2016;17:1217-29.
4. Beck AH, Lee C-H, Witten DM, Gleason BC, Edris B, Espinosa I, et al. Discovery of molecular subtypes in leiomyosarcoma through integrative molecular profiling. Oncogene. 2010;29:845-54.
5. WHO Classification of Tumours of Soft Tissue and Bone. Fletcher CD, Bridge JA, Hogendoorn PCW, Mertens F, editors: International Agency for Research on Cancer, Lyon; 2013.
6. Harker WG, MacKintosh FR, Sikic BI. Development and characterization of a human sarcoma cell line, MES-SA, sensitive to multiple drugs. Cancer research. 1983;43:4943-50.
7. Fogh J, Fogh JM, Orfeo T. One hundred and twenty-seven cultured human tumor cell lines producing tumors in nude mice. Journal of the National Cancer Institute. 1977;59:221-6.
8. Sciacca L, Mineo R, Pandini G, Murabito A, Vigneri R, Belfiore A. In IGF-I receptor-deficient leiomyosarcoma cells autocrine IGF-II induces cell invasion and protection from apoptosis via the insulin receptor isoform A. Oncogene. 2002;21:8240-50.
9. Zhu Q-S, Ren W, Korchin B, Lahat G, Dicker A, Lu Y, et al. Soft tissue sarcoma cells are highly sensitive to AKT blockade: a role for p53-independent up-regulation of GADD45 alpha. Cancer research. 2008;68:2895-903.
10. Murphy JD, Spalding AC, Somnay YR, Markwart S, Ray ME, Hamstra DA. Inhibition of mTOR radiosensitizes soft tissue sarcoma and tumor vasculature. Clinical cancer research : an official journal of the American Association for Cancer Research. 2009;15:589-96.
11. Fröhlich LF, Mrakovcic M, Smole C, Zatloukal K. Molecular mechanism leading to SAHA-induced autophagy in tumor cells: evidence for a p53-dependent pathway. Cancer cell international. 2016;16:68.
12. Chen J, Stubbe J. Bleomycins: towards better therapeutics. Nature reviews Cancer. 2005;5:102-12.
13. Mira A, Gili JA, Lopez-Larraza DM. The influence of nonprotein thiols on DNA damage induced by bleomycin in single human cells. Journal of environmental pathology, toxicology and oncology : official organ of the International Society for Environmental Toxicology and Cancer. 2013;32:219-28.
14. Jerome-Morais A, Bera S, Rachidi W, Gann PH, Diamond AM. The effects of selenium and the GPx-1 selenoprotein on the phosphorylation of H2AX. Biochimica et biophysica acta. 2013;1830:3399-406.
15. Bache M, Oehlmann S, Meye A, Bartel F, Kappler M, Würl P, et al. Radiosensitization in sarcoma cell lines with a p53 missense mutation correlates with prevention of irradiation G2/M arrest but not with induction of apoptosis. Oncology reports. 2001;8:1007-11.
16. Noodt BB, Berg K, Stokke T, Peng Q, Nesland JM. Different apoptotic pathways are induced from various intracellular sites by tetraphenylporphyrins and light. British journal of cancer. 1999;79:72-81.
17. Warburg O, Wind F, Negelein E. The metabolism of tumors in the body. J Gen Physiol.

1927;8(6):519-30.
18. Bhattacharya B, Mohd Omar MF, Soong R. The Warburg effect and drug resistance. British journal of pharmacology. 2016;173:970-9.
19. Iliakis G. The role of DNA double strand breaks in ionizing radiation-induced killing of eukaryotic cells. BioEssays : news and reviews in molecular, cellular and developmental biology. 1991;13:641-8.
20. Dutta A, Chakraborty A, Saha A, Ray S, Chatterjee A. Interaction of radiation- and bleomycin-induced lesions and influence of glutathione level on the interaction. Mutagenesis. 2005;20:329-35.
21. Ghoshal N, Sharma S, Banerjee A, Kurkalang S, Raghavan SC, Chatterjee A. Influence of reduced glutathione on end-joining of DNA double-strand breaks: Cytogenetical and molecular approach. Mutation research. 2017;795:1-9.
22. Chatterjee A, Jacob-Raman M, Mohapatra B. Potentiation of bleomycin-induced chromosome aberrations by the radioprotector reduced glutathione. Mutation research. 1989;214:207-13.
23. Miller AC, Henderson BW. The influence of cellular glutathione content on cell survival following photodynamic treatment in vitro. Radiation research. 1986;107:83-94.
24. Theodossiou TA, Olsen CE, Jonsson M, Kubin A, Hothersall JS, Berg K. The diverse roles of glutathione-associated cell resistance against hypericin photodynamic therapy. Redox biology. 2017;12:191-7.
25. Tanaka T, Halicka HD, Huang X, Traganos F, Darzynkiewicz Z. Constitutive histone H2AX phosphorylation and ATM activation, the reporters of DNA damage by endogenous oxidants. Cell cycle (Georgetown, Tex). 2006;5:1940-5.
26. Huang X, Tanaka T, Kurose A, Traganos F, Darzynkiewicz Z. Constitutive histone H2AX phosphorylation on Ser-139 in cells untreated by genotoxic agents is cell-cycle phase specific and attenuated by scavenging reactive oxygen species. International journal of oncology. 2006;29:495-501.
27. Papa L, Manfredi G, Germain D. SOD1, an unexpected novel target for cancer therapy. Genes & cancer. 2014;5:15-21.
28. van Gisbergen MW, Voets AM, Starmans MHW, de Coo IFM, Yadak R, Hoffmann RF, et al. How do changes in the mtDNA and mitochondrial dysfunction influence cancer and cancer therapy? Challenges, opportunities and models. Mutation research Reviews in mutation research. 2015;764:16-30.
29. Miranda SG, Wang YJ, Purdie NG, Osborne VR, Coomber BL, Cant JP. Selenomethionine stimulates expression of glutathione peroxidase 1 and 3 and growth of bovine mammary epithelial cells in primary culture. Journal of dairy science. 2009;92:2670-83.
30. Branzei D, Foiani M. Regulation of DNA repair throughout the cell cycle. Nature reviews Molecular cell biology. 2008;9:297-308.
31. Takata M, Sasaki MS, Sonoda E, Morrison C, Hashimoto M, Utsumi H, et al. Homologous recombination and non-homologous end-joining pathways of DNA double-strand break repair have overlapping roles in the maintenance of chromosomal integrity in vertebrate cells. The EMBO journal. 1998;17:5497-508.
32. Lee SE, Mitchell RA, Cheng A, Hendrickson EA. Evidence for DNA-PK-dependent and -independent DNA double-strand break repair pathways in mammalian cells as a function of the cell cycle. Molecular and cellular biology. 1997;17:1425-33.
33. Wang J, Hu L, Allalunis-Turner MJ, Day RS, Deen DF. Radiation-induced damage in two human glioma cell lines as measured by the nucleoid assay. Anticancer research. 1997;17:4615-8.
34. Peddi P, Loftin CW, Dickey JS, Hair JM, Burns KJ, Aziz K, et al. DNA-PKcs deficiency leads to persistence of oxidatively induced clustered DNA lesions in human tumor cells. Free Radical Biology and Medicine. 2010;48(10):1435-43.

35. Kucuksayan E, Cort A, Timur M, Ozdemir E, Yucel SG, Ozben T. N -acetyl- L -cysteine inhibits bleomycin induced apoptosis in malignant testicular germ cell tumors. Journal of Cellular Biochemistry. 2013;114(7):1685-94.
36. Guo Q, Dong B, Nan F, Guan D, Zhang Y. 5-Aminolevulinic acid photodynamic therapy in human cervical cancer via the activation of microRNA-143 and suppression of the Bcl-2/Bax signaling pathway. Molecular Medicine Reports. 2016.
37. Reiners JJ, Agostinis P, Berg K, Oleinick NL, Kessel D. Assessing autophagy in the context of photodynamic therapy. Autophagy. 2010;6:7-18.
38. Marino J, Vior MCG, Furmento VA, Blank VC, Awruch J, Roguin LP. Lysosomal and mitochondrial permeabilization mediates zinc(II) cationic phthalocyanine phototoxicity. The International Journal of Biochemistry & Cell Biology. 2013;45(11):2553-62.
39. Liu L, Zhang Z, Xing D. Cell death via mitochondrial apoptotic pathway due to activation of Bax by lysosomal photodamage. Free Radical Biology and Medicine. 2011;51(1):53-68.
40. Caruso JA. Differential Susceptibilities of Murine Hepatoma 1c1c7 and Tao Cells to the Lysosomal Photosensitizer NPe6: Influence of Aryl Hydrocarbon Receptor on Lysosomal Fragility and Protease Contents. Molecular Pharmacology. 2004;65(4):1016-28.
41. Jr JJR, Caruso JA, Mathieu P, Chelladurai B, Yin X-M, Kessel D. Release of cytochrome c and activation of pro-caspase-9 following lysosomal photodamage involves bid cleavage. Cell Death and Differentiation. 2002;9(9):934-44.
42. Berg K, Moan J. Lysosomes as photochemical targets. International journal of cancer. 1994;59:814-22.
43. Levine AJ, Puzio-Kuter AM. The Control of the Metabolic Switch in Cancers by Oncogenes and Tumor Suppressor Genes. Science. 2010;330(6009):1340-4.

Fig 1

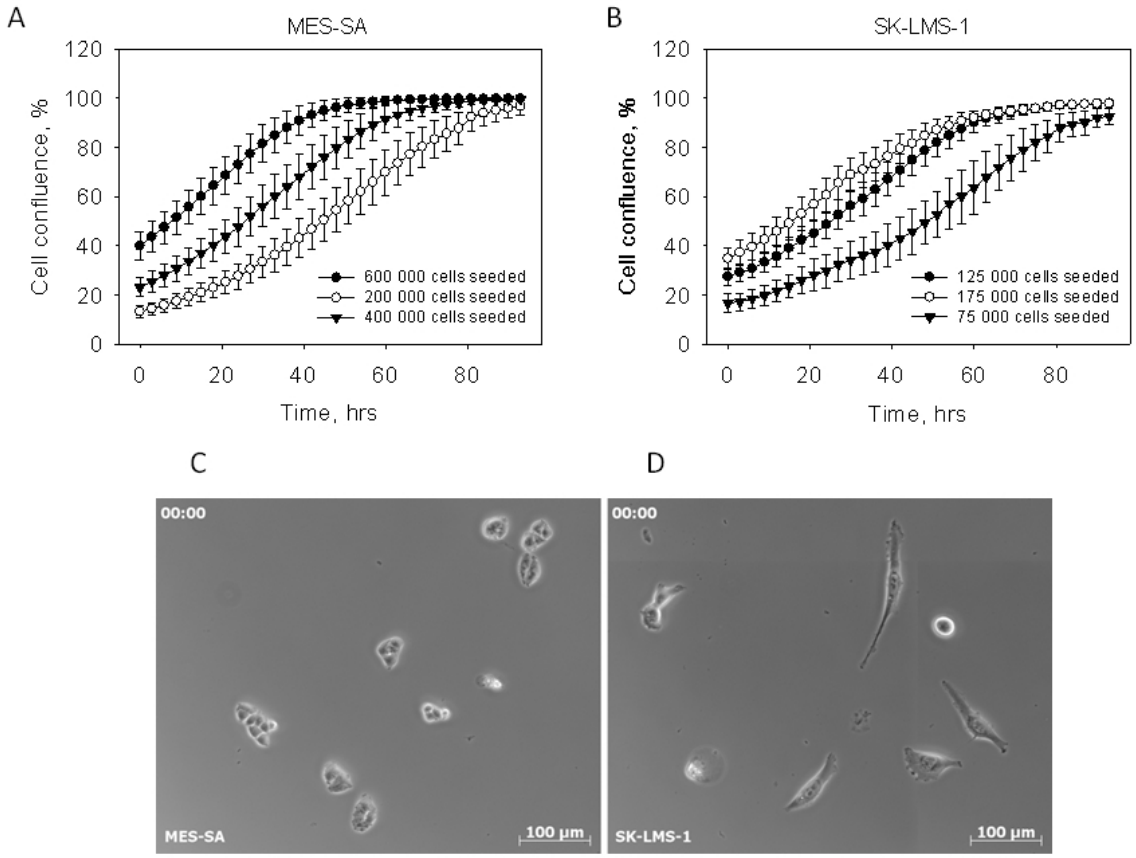
A
MES-SA
Cell confluence, %
120
100
80
60
40
20
0
0
20
40
60
80
Time, hrs
600 000 cells seeded
200 000 cells seeded
400 000 cells seeded
B
SK-LMS-1
Cell confluence, %
120
100
80
60
40
20
0
0
20
40
60
80
Time, hrs
125 000 cells seeded
175 000 cells seeded
75 000 cells seeded
C
00:00
MES-SA
100 µm
D
00:00
SK-LMS-1
100 µm

Fig 2

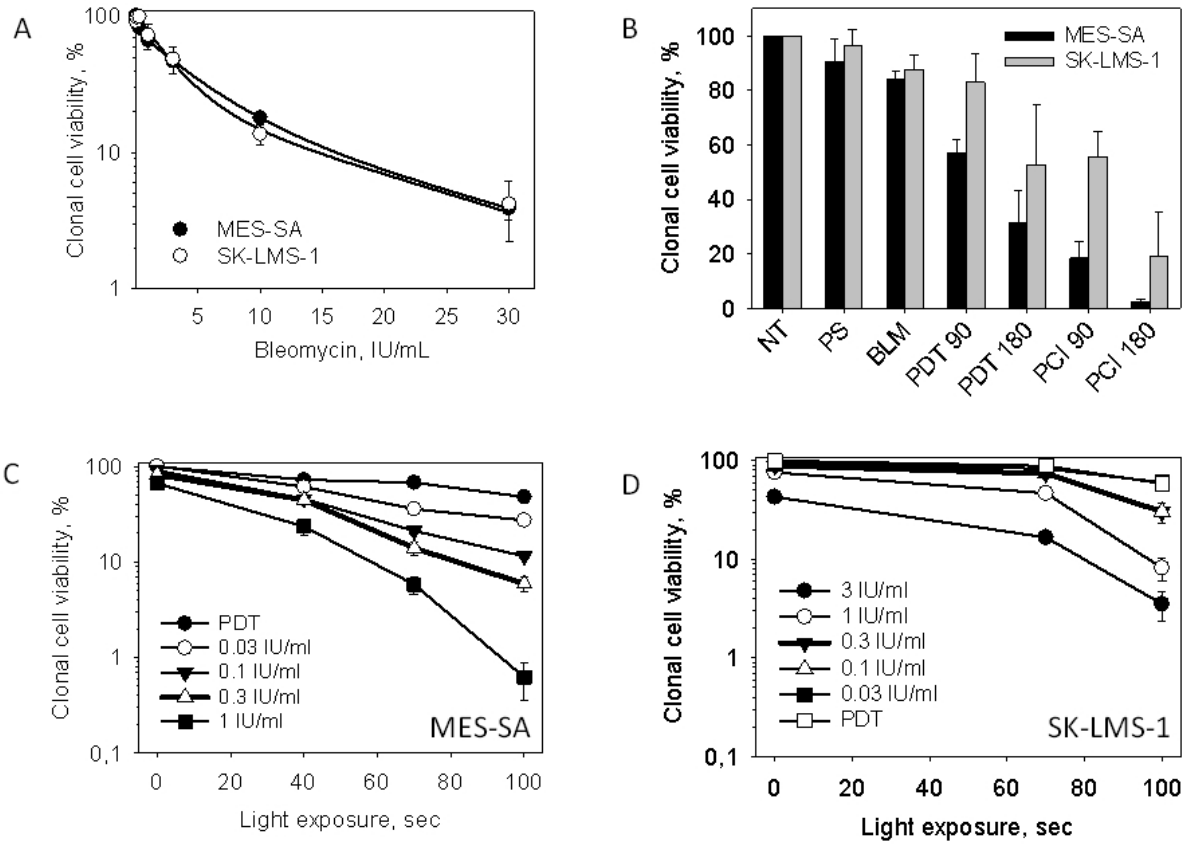
A
Clonal cell viability, %
100
10
1
MES-SA
SK-LMS-1
5
10
15
20
25
30
Bleomycin, IU/mL
B
Clonal cell viability, %
MES-SA
SK-LMS-1
NT
PS
BLM
PDT 90
PDT 180
PCI 90
PCI 180
C
Clonal cell viability, %
PDT
0.03 IU/ml
0.1 IU/ml
0.3 IU/ml
1 IU/ml
MES-SA
Light exposure, sec
D
Clonal cell viability, %
3 IU/ml
1 IU/ml
0.3 IU/ml
0.1 IU/ml
0.03 IU/ml
PDT
SK-LMS-1
Light exposure, sec

Fig 3

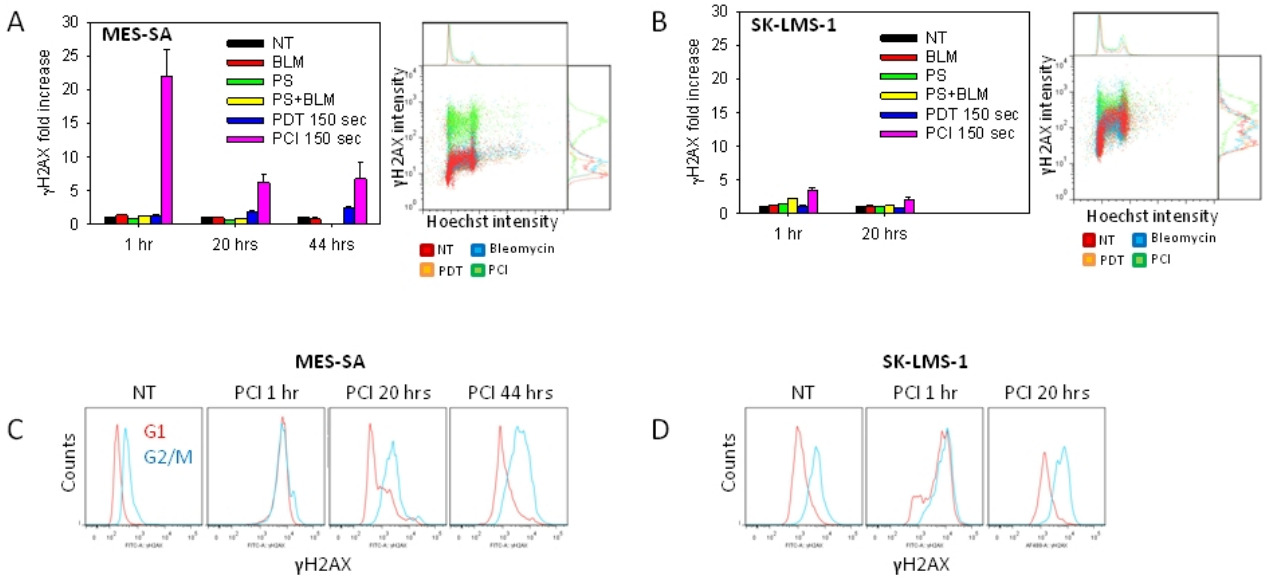
A
MES-SA
γH2AX fold increase
NT
BLM
PS
PS+BLM
PDT 150 sec
PCI 150 sec
1 hr
20 hrs
44 hrs
γH2AX intensity
Hoechst intensity
NT
Bleomycin
PDT
PCI
B
SK-LMS-1
γH2AX fold increase
NT
BLM
PS
PS+BLM
PDT 150 sec
PCI 150 sec
1 hr
20 hrs
γH2AX intensity
Hoechst intensity
NT
Bleomycin
PDT
PCI
C
MES-SA
NT
PCI 1 hr
PCI 20 hrs
PCI 44 hrs
Counts
G1
G2/M
γH2AX
D
SK-LMS-1
NT
PCI 1 hr
PCI 20 hrs
Counts
γH2AX

Fig. 4

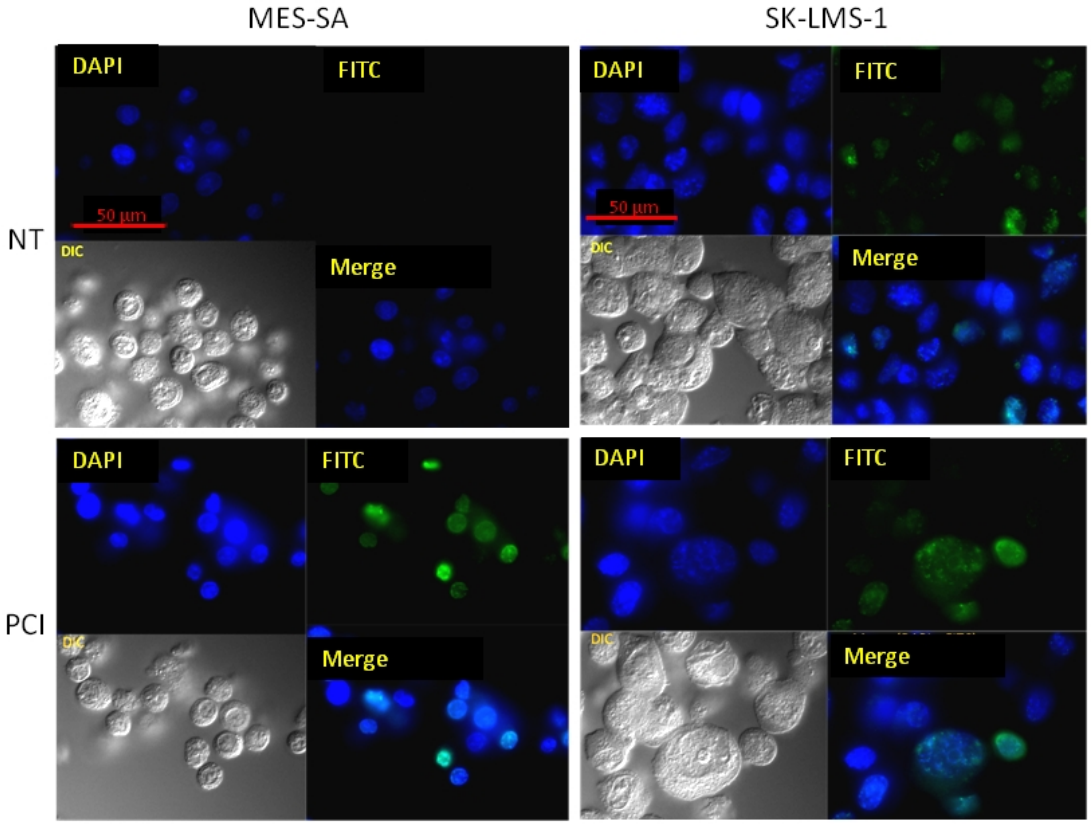

Fig 5

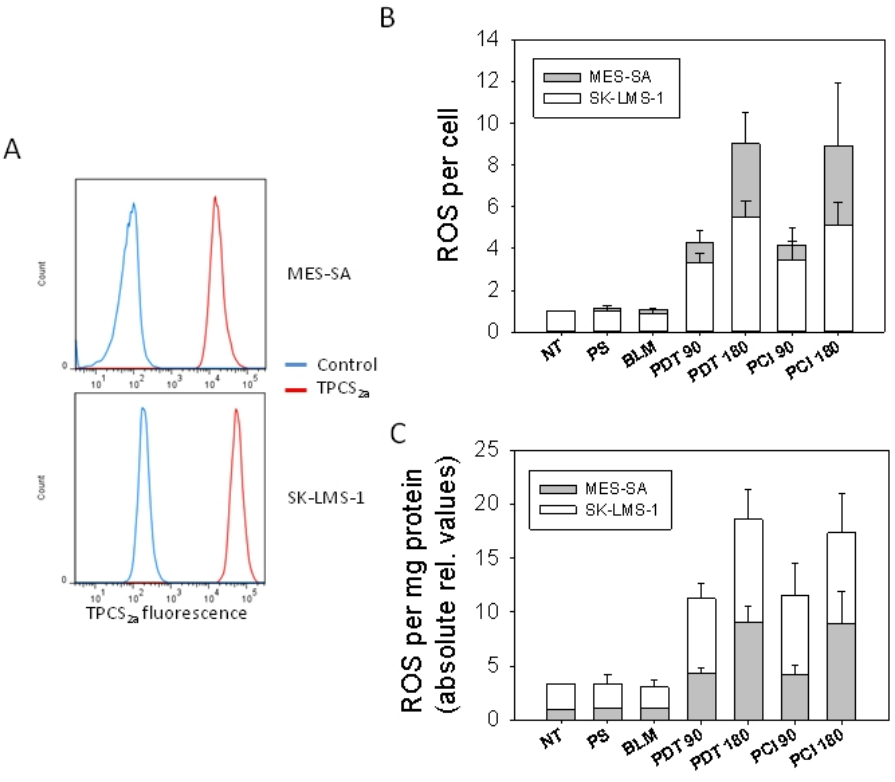
A
MES-SA
SK-LMS-1
Control
TPCS2a
Count
TPCS2a fluorescence
B
ROS per cell
MES-SA
SK-LMS-1
NT
PS
BLM
PDT 90
PDT 180
PCI 90
PCI 180
C
ROS per mg protein
(absolute rel. values)

Fig 6

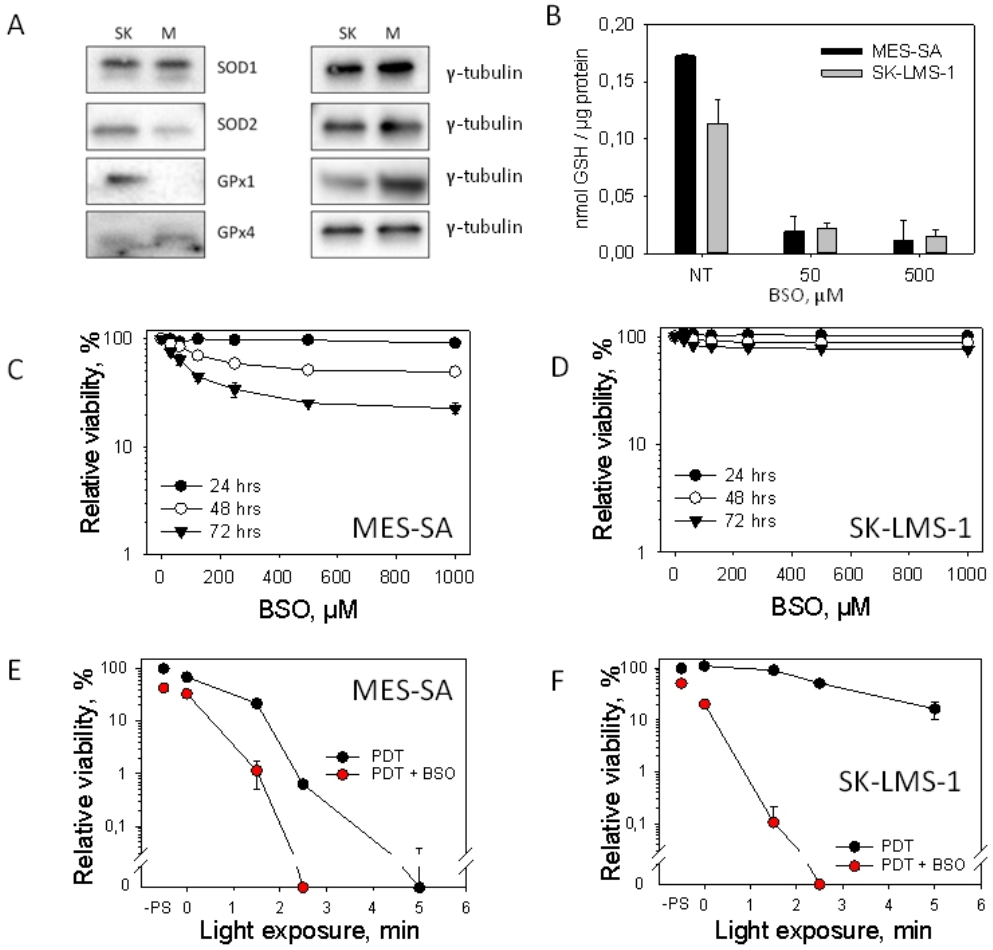
A
SK
M
SOD1
SOD2
GPx1
GPx4
γ-tubulin
B
nmol GSH / µg protein
MES-SA
SK-LMS-1
NT
50
500
BSO, µM
C
Relative viability, %
24 hrs
48 hrs
72 hrs
MES-SA
BSO, µM
D
SK-LMS-1
E
PDT
PDT + BSO
Light exposure, min
F

Fig 7

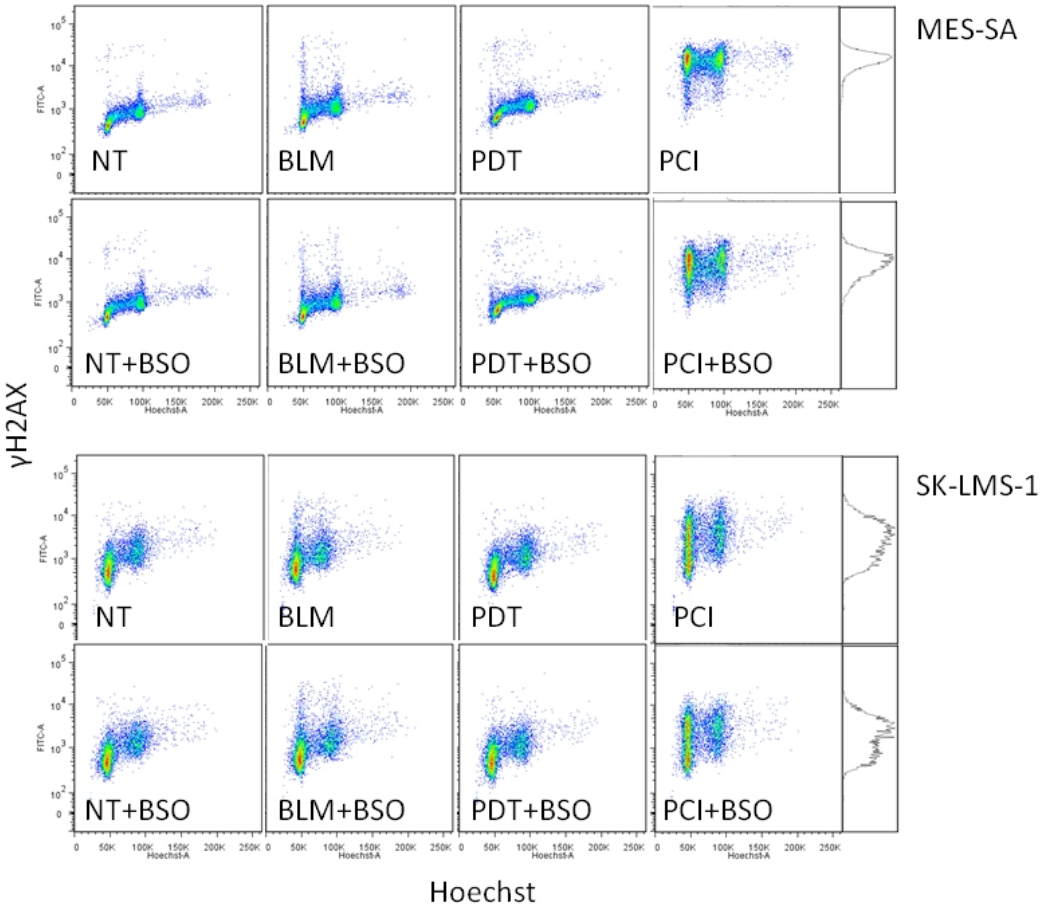
MES-SA
SK-LMS-1
NT
BLM
PDT
PCI
NT+BSO
BLM+BSO
PDT+BSO
PCI+BSO
γH2AX
Hoechst

Fig.8

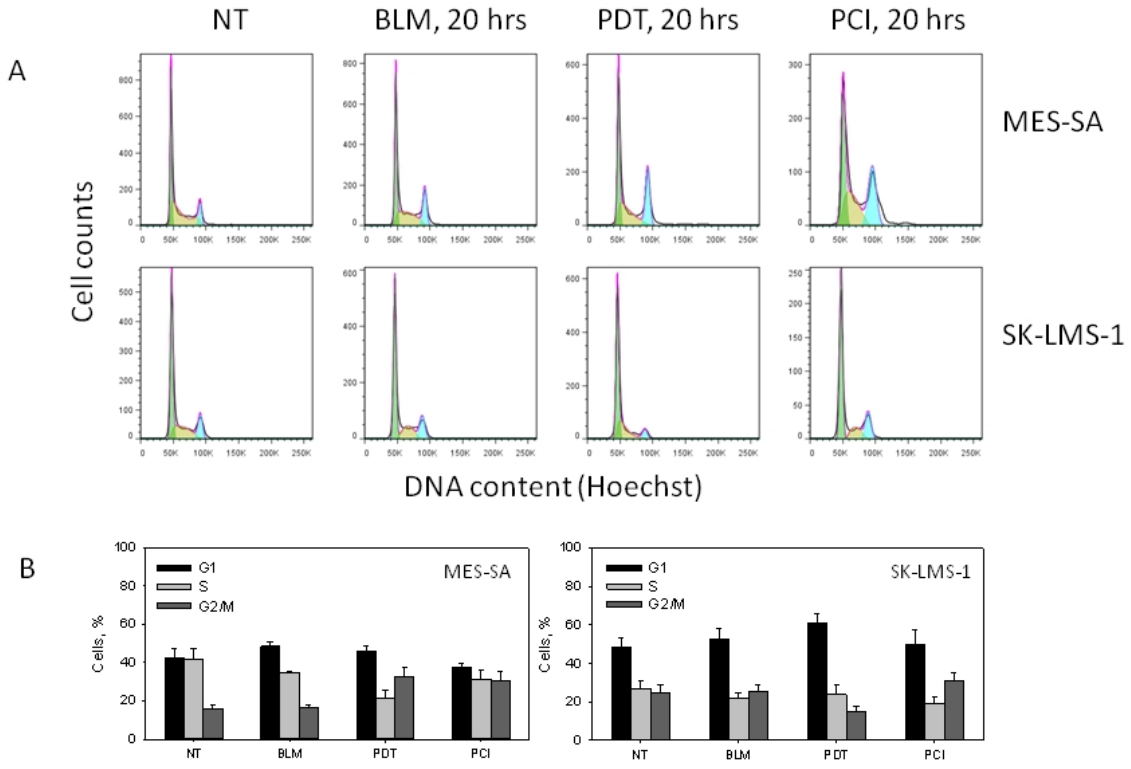
A
NT
BLM, 20 hrs
PDT, 20 hrs
PCI, 20 hrs
MES-SA
SK-LMS-1
Cell counts
DNA content (Hoechst)
B
G1
S
G2/M
MES-SA
SK-LMS-1
Cells, %
NT
BLM
PDT
PCI

Fig. 9

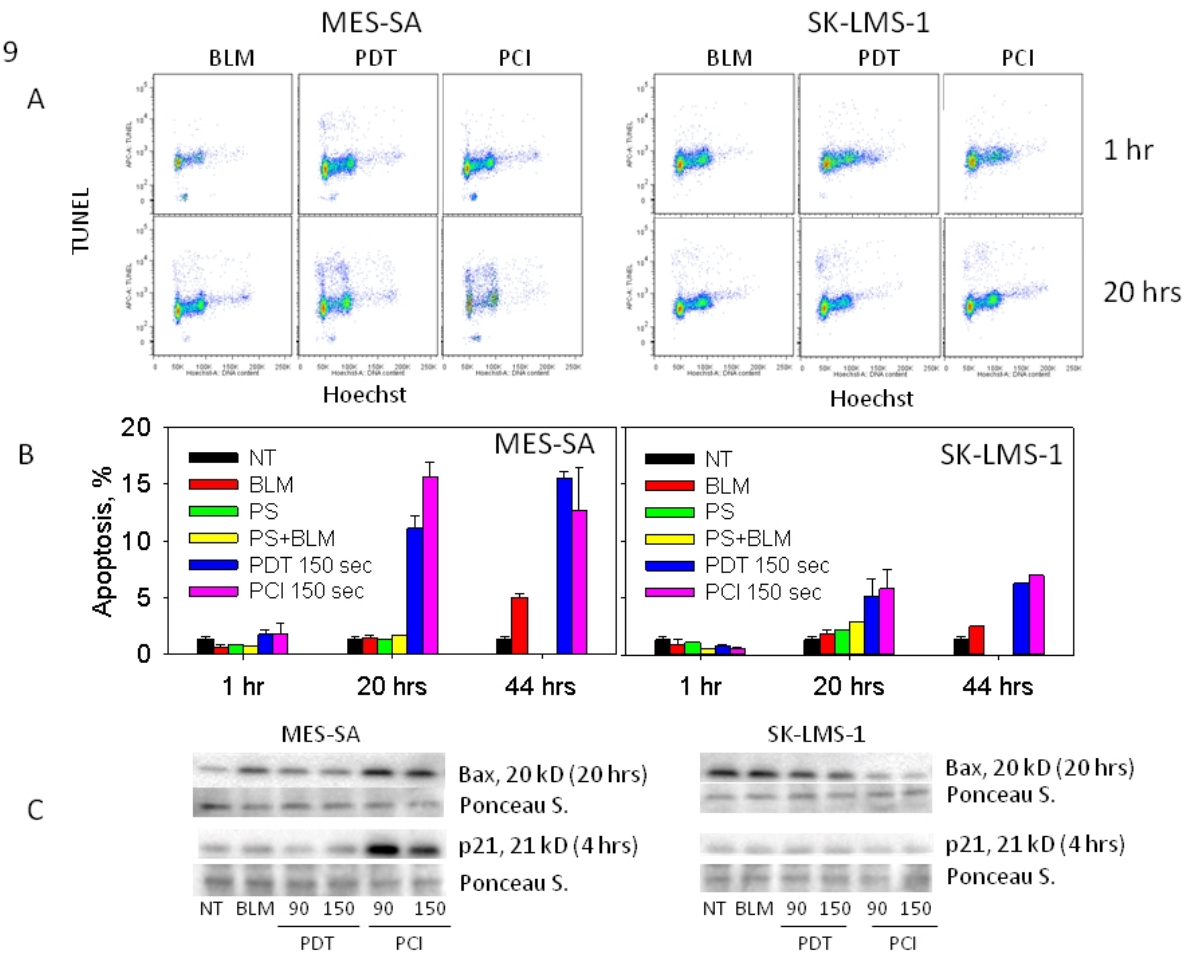
A
MES-SA
SK-LMS-1
BLM
PDT
PCI
TUNEL
Hoechst
1 hr
20 hrs
B
Apoptosis, %
NT
BLM
PS
PS+BLM
PDT 150 sec
PCI 150 sec
1 hr
20 hrs
44 hrs
C
Bax, 20 kD (20 hrs)
Ponceau S.
p21, 21 kD (4 hrs)
NT BLM 90 150 90 150
PDT
PCI

Fig. 10

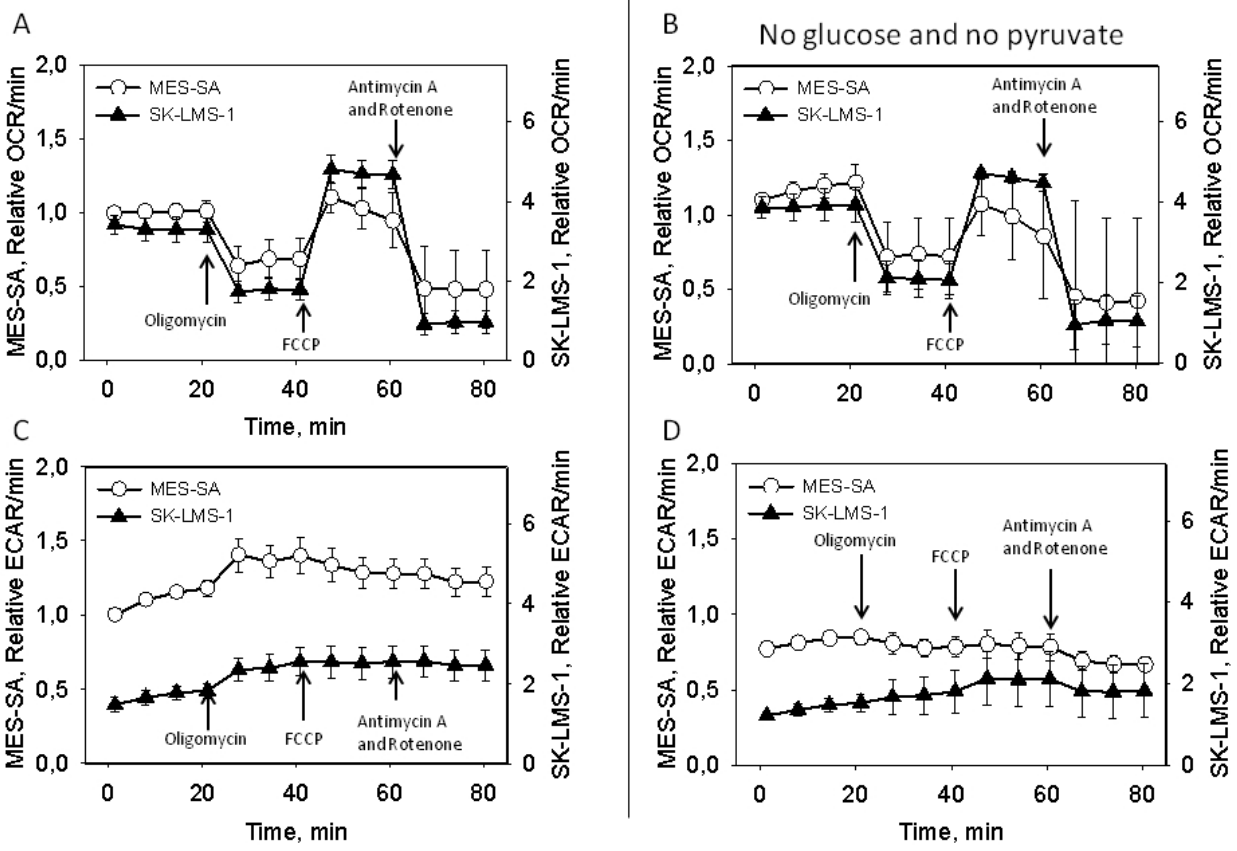
A
B
No glucose and no pyruvate
C
D
MES-SA
SK-LMS-1
Antimycin A and Rotenone
Oligomycin
FCCP
MES-SA, Relative OCR/min
SK-LMS-1, Relative OCR/min
MES-SA, Relative ECAR/min
SK-LMS-1, Relative ECAR/min
Time, min
0,0
0,5
1,0
1,5
2,0
0
2
4
6
0
20
40
60
80

Paper V

Paper VI